Ludwig-Maximilians-Universität München

Mechanisms of myeloid cell recruitment and biomarker potential in interstitial lung diseases

Flavia Regina Greiffo

Ludwig-Maximilians-Universität München

From the Comprehensive Pneumology Center (CPC)/ Institute for Lung Biology and Disease and Ludwig-Maximilians University Munich

Internal directors: Dr. rer. nat Antje Brand, PD. Dr. med. Anne Hilgendorff, Dr. vet.med. Ali Önder Yildirim

Mechanisms of myeloid cell recruitment and biomarker potential in interstitial lung diseases

Dissertation presented for holding the title of Doctor of Philosophy (Ph.D.) at the Medical Faculty of Ludwig-Maximilians University Munich

Presented by

Flavia Regina Greiffo

from Joinville, Santa Catarina, Brazil

Munich, 2019

With the approval of the Medical Faculty of the Ludwig-Maximilians University Munich

Evaluators:

Supervisor: PD. Dr. med. Anne Hilgendorff

Second evaluator: Prof. Dr. Oliver Söhnlein

Dean: Prof. Dr. dent. med. Reinhard Hickel

Date of oral defense: 13-Nov-2019

Table of content

Abbreviations

A

AKAP13	A-kinase anchoring protein 13
ALAT	Latin American Thoracic Association
APC	Antigen presenting cells
ATI	Alveolar type I
ATII	Alveolar type II
ATP	Adenosine triphosphate
ATS	American Thoracic Society
α-SMA	alpha smooth muscle actin

B

BAL	Bronchoalveolar lavage
BSA	Bovine serum albumine

C

CCL18	Chemokine ligand 18
CCL2	Chemokine ligand 2
CCR2	Chemokine receptor 2
CD	Cluster of differentiation
CFSE	Carboxyfluorescein succinimidyl ester
CHI3L1	Chitinase-3-like protein 1
CK18	Cytokeratin 18
cMoP	Common monocyte progenitor
COPD	Chronic obstructive pulmonary disease
CSF1R	Colony-stimulating factor 1 receptor
CTD	Connective-tissue diseases
CTGF	Connective tissue growth factor
CTNNA	Catenin alpha-E
CX3CL1	CX3C chemokine ligand 1
CX3CR1	CX3C chemokine receptor 1
CXCL	CXC chemokine ligand

D

DAMP	Damage-associated molecules patterns
DLCO	Diffusing lung capacity of carbon monoxide
DLPD	Diffuse lung parenchymal diseases
DMEN	Dulbecco's modified eagle medium

DNA	Deoxyribonucleic acid
DPP9	Dipeptidyl Peptidase 9
DSP	Desmoplakin
E	
ECM	Extracellular matrix
ELMO	Engulfment cell motility
ERS	European Respiratory Society
F	
FGF	Fibroblast growth factor
FLT3	FMS-like tyrosine kinase
FVC	Forced vital capacity
G	
GM-CSF	Granulocyte/macrophage colony stimulator factor
GMP	Granulocyte-macrophage receptor
H	
HLA	Human leukocyte antigen
HP	Hypersensitivity pneumonitis
HRCT	High-resolution computational tomography
HSC	Hematopoietic stem cells
HSP70	Heat shock protein 70
I	
ICAM	Intracellular adhesion molecule
IL	Interleukin
ILD	Interstitial lung diseases
IPF	Idiopathic pulmonary fibrosis
J	
JRS	Japanese Respiratory Society
K	
KL6	Krebs von den Lungen-6
M	
M-CSF	Macrophage colony stimulator factor
MDP	Macrophage and dendritic cell progenitor

MDSC	Myeloid-derived suppressor cells
MFI	Mean fluorescence intensity
MMP	Matrix metalloproteinases
MUC1	Mucin 1
MUC5B	Mucin 5B

N

NSIP	Non-specific interstitial pneumonia

O

OTU	Operational taxonomic unit

P

PARC	Pulmonary and activation-regulated chemokine
PARN	Poly(A)-specific ribonuclease
PBMC	Peripheral blood mononuclear cells
PBS	Phosphate buffer saline
PDFG	Platelet-derived growth factor
PF	Pulmonary fibrosis
PFT	Pulmonary function test

R

RNA	Ribonucleic acid
ROR1	Receptor tyrosine kinase-like orphan receptor 1
ROS	Reactive oxygen species
RTEL1	Regulator of telomere elongation helicase 1

S

SCF	Stem cell factor
SEMA7A	Semaphorin 7A
SFTPA2	Surfactant protein A2
SFTPC	Surfactant protein C
SSP	Phosphoprotein

T

TERC	Telomerase RNA Component
TERT	Telomerase reverse transcriptase
TGF-ß	Transforming growth factor beta
Th	T helper
TLC	Total lung capacity
TLR	Toll-like receptor

TNF-α	Tumor necrosis factor alpha
TOLLIP	Toll-interacting protein
Tregs	T regulatory cells

Summary

Interstitial lung diseases (ILDs) are fibrotic disorders with chronic inflammation and fibrinogenesis leading to lung scaring and lung function decline. Ultimately, progressive pulmonary fibrosis results in altered pulmonary physiology, abnormal gas exchange, and organ failure. ILDs include known causes and idiopathic causes, as it is the case of idiopathic pulmonary fibrosis (IPF) and non-specific interstitial pneumonia (NSIP). The most detrimental type of ILD is IPF in which anti-fibrotic drugs (nintedanib and pirfenidone) only decrease disease progression. For other ILD types, corticoid treatment helps to decrease exacerbation. Currently, clinical trials are evaluating the applicability of anti-fibrotic drugs for treating non-IPF ILDs. Therefore, mechanistic insights and in-depth cell characterization during tissue injury and remodeling in ILD are of great interest in the respiratory medical field.

Circulating immune cell populations have been suggested to play a critical role in ILDs. For instance, mononuclear phagocytes are involved in the initiation, repair and regeneration of pulmonary fibrosis. Moreover, the close interaction between circulating and lung tissue-resident immune cells is critical to contribute to tissue homeostasis or lead to disease. However, precise myeloid phenotypes (e.g. myeloid-derived suppressor cells and monocytes) and their mechanisms of recruitment in ILDs have not yet been explored.

In the first results chapter of this thesis, myeloid-derived suppressor cells (MDSC) abundance and function were investigated for the first time in IPF patients. For that, peripheral blood of 170 patients including IPF, non-IPF ILD, chronic obstructive pulmonary diseases (COPD) and controls were collected to characterize and quantify MDSC by flow cytometry. Circulating MDSC in IPF and non-IPF ILD were increased when compared with control. Moreover, cross sectional and longitudinal analysis of the abundance of MDSC inversely correlated with pulmonary function test in IPF only. IPF patients with high number of MDSC showed downregulation of co-stimulatory T cells signals quantified by qRT-PCR. Furthermore, MDSC were able to suppress lymphocytes $CD4^+$ and $CD8^+$ cells proliferation in vitro. Last, CD33 CD11b

double positive cells, suggestive of MDSC, were found in neighboring fibrotic niches of the IPF lungs. Taking together, these results show that MDSC are potential biomarker for IPF and are suppressing T cell responses.

In the second results chapter, we aimed at analyzing monocyte phenotype and recruitment from the blood to the lung tissue in ILD. Importantly, CX3CR1 expression on immune cells has been demonstrated to increase fibrosis features. For that, flow cytometry analysis of circulating monocytes was performed in 105 subjects (83 ILD, and 22 controls). Monocyte localization and abundance in the lung was assessed by immunofluorescence and flow cytometry analysis. For receptor-ligand function and transmigration pattern, monocytes were isolated from blood and cultured either alone or with endothelial cells. Here, we showed that classical monocytes (CM) were increased, while non-classical monocytes (NCM) were decreased in ILD: NSIP, hypersensitivity pneumonitis (HP) and connective tissue disease associated with ILD (CTD-ILD) compared with controls. Monocytes abundance positively correlated with lung function. Fractalkine levels, the ligand of CX3CR1, were higher in lung tissue than in plasma in ILD and also co-localized with bronchial ciliated cells. Fractalkine enhanced endothelial transmigration of NCM in ILD only. Flow cytometry and immunofluorescence staining showed increased NCM in ILD. NCM-derived cells in the ILD lungs co-stained with CX3CR1, M2-like and phagocytic markers. In summary, we show that epithelial-derived fractalkine drives the migration of NCM-CX3CR1 which provides an interstitial scavenger and phagocytic myeloid cells population in fibrotic ILD lungs.

1. Introduction

1.1 Interstitial lung diseases

Interstitial lung diseases (ILDs) are also called diffuse lung parenchymal diseases (DLPD) or pulmonary fibrosis (PF). According to the American Thoracic Society (ATS) and European Respiratory Society (ERS) statements, ILD/DPLD/PF describes a large group of lung parenchymal diseases characterized by multiple alterations in lung physiology (Travis et al., 2013). ILD patients show impaired gas exchange, excessive and progressive accumulation of extracellular matrix (ECM), as well as high influx of inflammatory cells (Travis et al., 2013).

ILDs are categorized according to their cause (figure 1). The known causes of ILD are drug toxicity, connective tissue diseases, environmental exposures, and genetics. ILD with no previous cause or association are classified as idiopathic. ILD can also be classified as granulomatous diseases, in these cases patients display higher susceptibility to infections (Fischer & du Bois, 2012).

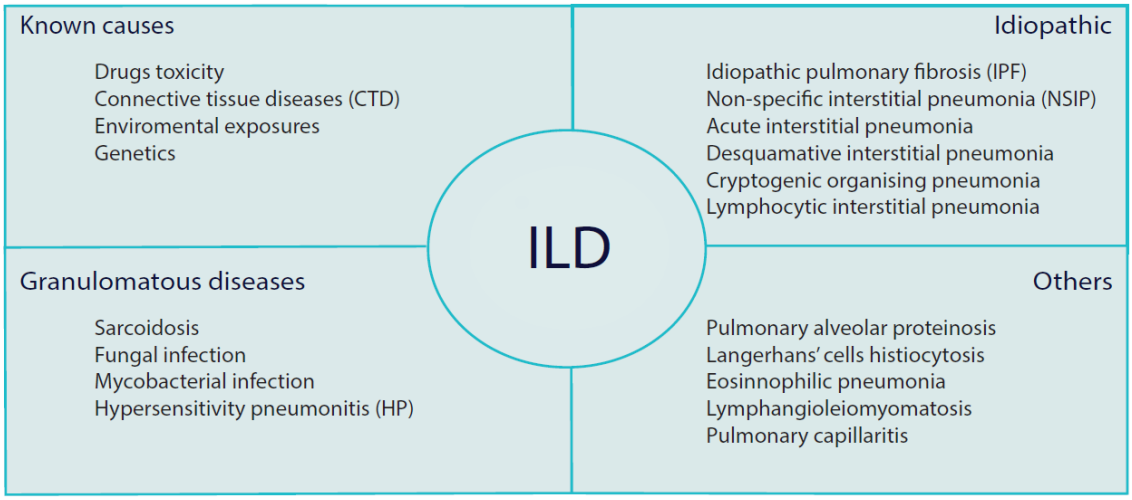

Figure 1. ILD categorization is divided in four different groups according to etiology: 1) known causes, 2) idiopathic, 3) granulomatous, 4) others (adapted from (Fischer & du Bois, 2012)).

1.2 Epidemiology, complications and mortality in ILDs

ILDs cases are internationally widespread. Idiopathic interstitial pneumonias (IIP) includes idiopathic pulmonary fibrosis (IPF) which is the most common and harmful IIP (Cottin et al., 2019) (Raghu et al., 2011). However, other ILDs: non-specific interstitial pneumonia (NSIP). hypersensitivity pneumonitis (HP), connective-tissue diseases (CTD) and Sarcoidosis have shown high complication and mortality risk due pulmonary fibrosis as well (Wells et al., 2018).

1.2.1 Idiopathic ILDs

Idiopathic interstitial pneumonias (IIP) are a classification of ILDs with unknown etiology, such as IPF and NSIP (Travis et al., 2013). IPF is the most detrimental type of ILD, with 3-5 years of median survival. Approximately 10-20% of IPF patients are admitted in hospitals with acute exacerbation per year. Most of the IPF patients with exacerbations die from acute respiratory failure. IPF cases have been reported to be more frequent in Europe and North America than South America and Asia (Raghu et al., 2018). In the United States, the prevalence of IPF is estimated to range from 10 to 60 cases per 100,000 among adults over the age of 65 years old (Lederer & Martinez, 2018). In Europe, the incidence of IPF is increasing to rates around 3-9 per 100,000 per year (Hutchinson, Fogarty, Hubbard, & McKeever, 2015). IPF cases are more common in men than women (Ley & Collard, 2013). In contrary to IPF, most of the patients diagnosed with idiopathic fibrotic-NSIP are non-smokers and middle-aged women and 46% of NSIP cases are reported in Asian countries. Moreover, NSIP survival rate is 82.3% after 5 years and 73.2% after 10 years. (Travis et al., 2008).

1.2.2 Known causes of ILDs

ILD is an important clinical manifestation in CTD. CTD-ILD includes scleroderma, rheumatoid arthritis, Sjögren's syndrome and polymyositis/dermatomyositis. Cohorts from United States and Europe have shown that CTD-ILD is reported in 70% of the

scleroderma cases, 10-20% rheumatoid arthritis, 9-24% Sjögren's syndrome and 20-70% in myositis (S. C. Mathai & Danoff, 2016). The median survival of CTD-ILD patients (scleroderma and Sjörgren) is 5-8 years (Vij & Strek, 2013). Generally, CTD-ILD is diagnosed in adults at age of 40 representing a worse prognosis than IPF when adjusted by age (Kocheril et al., 2005).

1.2.3 Granulomatous ILDs

HP incidence in the United States is more common in women who are 65 years old. The yearly prevalence rate of HP is approximately 11 per 100,000 adults (65 years old or older), in which 20-29% reported cases of HP-ILD. When HP is associated to ILD, mortality rate increases up to 10%. In 4 years (between 2004 and 2008), mortality rate of HP patients was 72% and HP-ILD was 80%. Thus, after 8 years following-up the same cohort, mortality rate was 58% for HP and 71% for HP-ILD. These data showed that older age and male gender were associated with higher mortality (Fernandez Perez et al., 2018). In Europe and South America (Brazil), HP is estimated to represent the most predominant ILD after IPF, with prevalence of 4 to 15% and 15%, respectively (Thomeer, Costabe, Rizzato, Poletti, & Demedts, 2001) (Riario Sforza & Marinou, 2017). Last, sarcoidosis has been observed mostly in young adults (men and women), 20 to 39 years old. In Europe, sarcoidosis incidence has been reported in 5 to 40 per 100,000 adults (Iannuzzi, Rybicki, & Teirstein, 2007). Scandinavian countries are the greater contributors to Sarcoidosis cases in Europe. In Sweden, in 2003 till 2012, the yearly records of sarcoidosis cases are 11.5 per 100,000 people (Arkema, Grunewald, Kullberg, Eklund, & Askling, 2016).

1.3 Pathophysiology of ILDs

The alterations in lung physiology that occurred in ILD are due to acute or chronic injuries from unique or continued exposures, which can be air-borne and blood-borne resulting in pulmonary fibrosis. The faster progression and detrimental pathophysiology of IPF resulted in more studies to characterize the disease.

Pathogenic mechanisms include cell-cell interactions of many different cell types, mainly epithelial cells, myofibroblasts, and immune cells (Bagnato & Harari, 2015). Furthermore, gene mutations and polymorphisms, microbiota, proteins interactions, and growth factors affect the lung epithelium and ECM (Wuyts et al., 2013). Animal and in vitro models, such as bleomycin, silica, asbestos and fluorescein isothiocyanate (FITC), TGF-β-induced fibrosis explore the pathophysiology of lung fibrosis (Q. Xu, Norman, Shrivastav, Lucio-Cazana, & Kopp, 2007) (Moore et al., 2013).

1.3.1 Idiopathic ILDs

Molecular and cellular mechanisms are important regulators of disease status and progression in idiopathic ILDs. Indeed, IPF and NSIP are characterized by accumulation of fibroblasts and myofibroblasts differentiation, epithelial cells dysfunction, and immune cells dysregulation leading to ECM deposition (Ley, Brown, & Collard, 2014) (Fischer et al., 2015).

The initiation of IPF is a result of excessive lung tissue repair in response to wound healing process (Thannickal, Zhou, Gaggar, & Duncan, 2014). Genetic changes can contribute to the development of IPF. For example, genetic variations in the telomere length, TERT, TERC, PARN, and RTEL1 are associated with an increased IPF risk (Armanios et al., 2007). Moreover, other gene polymorphism, as in MUC5B (rs35705950) closely related to IPF susceptibility (Seibold et al., 2011) (Peljto et al., 2013). IPF patients with the MUC5B promoter polymorphism present a milder disease course, and improved survival (Seibold et al., 2011). IPF has also been shown to be associated with variations in DSK, AKAP13, CTNNA, and DPP9, genes related to cell adhesion and cell structure (Fingerlin et al., 2013) (Lederer & Martinez, 2018). Importantly, MUC5B polymorphism has been shown to correlate with variations in DSK and AKAP13 (Allen et al., 2017).

Injury factors, such as virus, cigarette smoke, exposure to radiation or drugs might be potential triggers to repetitive alveolar epithelial cell injury that leads to ECM deposition by myofibroblasts (Wuyts et al., 2013). In IPF lungs, alveolar type I (ATI)

and alveolar type II (ATII) cells are phenotypically altered. ATI and ATII apoptosis, stress and senescence lead to fibrotic scarring (Martinez et al., 2017). In IPF, hyperplasia of ATII cells and disruption of the alveolar epithelium within fibroblastic foci and loss of acinar architecture are important histopathology features of lung tissue damage (Gross & Hunninghake, 2001) (figure 2). Furthermore, IPF is characterized by increased bronchial basal cells and ATII migration and proliferation affecting tissue regenerative capacity. ATII apoptosis and senescence have been shown to contribute to increased secretion of pro-inflammatory cytokines, such as transforming growth factor beta (TGF-β), tumor necrosis factor alpha (TNF-α) and matrix metalloproteinases (including MMP-1, MMP-2, MMP-7, MMP-19) (Yu et al., 2012) (Martinez et al., 2017).

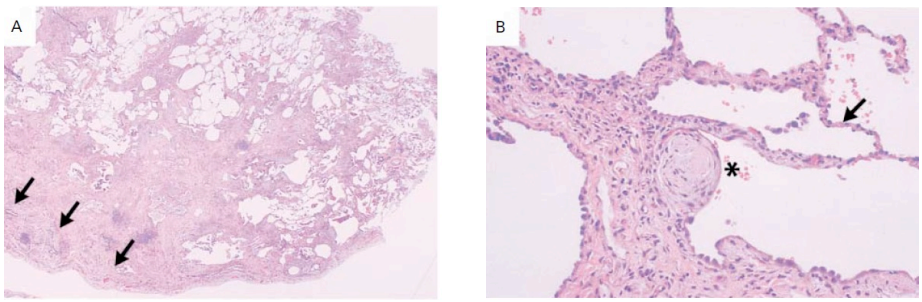

Figure 2. IPF lung sections: hematoxylin-and-eosin (HE) staining of an open-lung biopsy specimen from a patient presenting with progressive dyspnea and diffuse parenchymal infiltrates. (A) Fibrosis in sub pleura indicated with black arrows, collapse and obliteration of alveolar air spaces. Magnification 15x. (B) Fibroblast focus indicated with asterisk and nodule of spindle cells arranging extracellular matrix deposition. Magnification 150x (adapted from (Gross & Hunninghake, 2001)).

The injury of lung epithelium in IPF promotes migration, proliferation and activation of fibroblast and myofibroblast. Fibroblasts are activated by growth factors, such as fibroblast growth factor (FGF) and TGF-β that secrete ECM components increasing matrix stiffness (Wynn, 2008). IPF myofibroblasts are known to express and activate the levels of TGF-β by integrin pulling forces, increasing matrix stiffness. TGF-β expression has been shown to be an important regulator of pro-fibrotic surface markers (e.g PDGFRα, ROR1, SEMA7A) and transmembrane receptor (e.g. integrin

alpha (v) beta 6) in lung myofibroblasts (Heinzelmann et al., 2016) (Horan et al., 2008). ECM in the lung is primarily consisted of collagen type I and IV, elastins and laminins (Booth et al., 2012). Additionally, fibronectin and glycosaminoglycans maintain lung cell polarity and survival (Booth et al., 2012). In this line, stiffer ECM and myofibroblast activation alter mechanical properties of the lung (White, 2015). Moreover, stiffer and pre-stained ECM, as well as, myofibroblast activation and ECM deposition leads to MMP secretion which in a feedback loop mechanism delays repair processes in IPF lungs (Parker et al., 2014).

IPF pathophysiology is mediated by several alterations including the immune system. In IPF, the immune system contributes with a repetitive failure of pathogen response mechanisms which impact ECM deposition (Desai, Winkler, Minasyan, & Herzog, 2018). T helper (e.g. Th2, Th17) cells promote fibrosis by suppressing the immune system and increasing myofibroblast proliferation (Barron & Wynn, 2011). Moreover, macrophages can enhance the production and secretion of pro-fibrotic mediators, such as TGF-ß and platelet-derived growth factor (PDGF) (Kolahian, Fernandez, Eickelberg, & Hartl, 2016). Neutrophils are known to produce MMP (i.e. MMP-9) (Ikezoe et al., 2014) and TGF-ß activating myofibroblast and promoting ECM deposition (Kolahian et al., 2016). Additionally, B cells accumulation have been shown to be associated with IPF manifestation and disease outcome (Xue et al., 2013).

Another form of idiopathic ILD is NSIP. NSIP may be idiopathic or secondary to toxins and CTD. NSIP pathophysiology is characterized by a constant infiltration of immune cells to the lung interstitium and lymphocytes to the alveolar space, as well as fibroblast within a variable collagen deposition (Jegal et al., 2005). NSIP pattern shows diffuse injury of the alveolar walls and parenchyma. However, different from IPF, NSIP fibrosis pattern is usually not distributed in the periphery (Smith, 2016) (figure 3). According to the histological features, NSIP can be divided in NSIP (inflammation and/or inflammation with fibrosis) and fibrotic-NSIP (mainly fibrosis) (Travis et al., 2013).

In NSIP, epithelial cell injury and repair failure, accumulation of fibroblast and myofibroblast differentiation, and dysregulation of immune cells in the lungs leads to collagen and ECM deposition (W. Xu et al., 2014). Different from IPF, NSIP does not have presence of fibroblast foci (Raghu et al., 2018). NSIP and IPF are both associated with variations in the telomere length TERT, TERC, and surfactant protein C (SFTPC) (Borie et al., 2016) (Nogee et al., 2001).

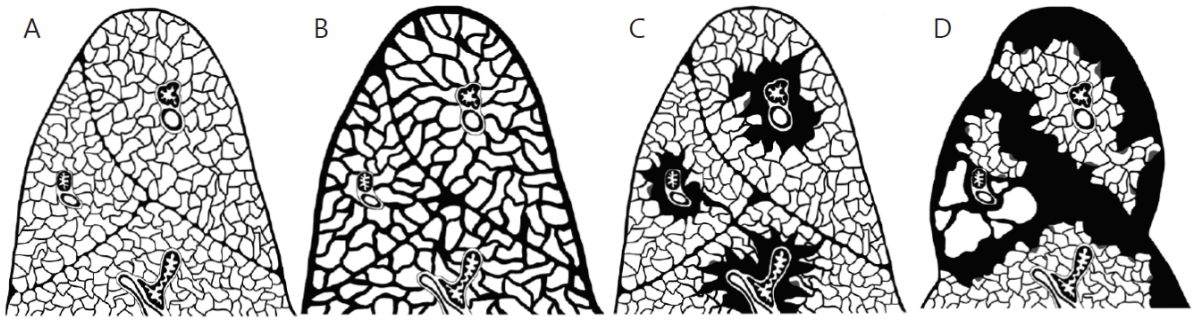

Figure 3. Schematic representation of histopathologic differences in healthy, NSIP and IPF lungs: (A) represents a healthy lung with thin alveolar and pleura components; Bronchovascular bundles are located in the center of the lobules. (B) Represents a NSIP lung with increase of thickness in the parenchyma and alveolar walls thickening. Despite of a diffuse lung alteration (C) Fibrotic-NSIP lung shows the airway centered in the extracellular matrix deposition and scattered fibroblast foci. (D) IPF lung is represented by irregular fibrosis with complete disruption of alveolar walls and considered distribution of fibroblast foci (adapted from (Smith, 2016)).

1.3.2 Known causes of ILDs

Pulmonary fibrosis in CTD-ILD is characterized by a multi-compartmental disease manifestation with the presence of several concurrent impairment of lung function. The common underlying mechanisms of CTD-ILD in scleroderma, rheumatoid arthritis (RA), and Sjögren's syndrome are immune-mediated lung damage (Fischer et al., 2015).

The scleroderma lung study shows that at the time of diagnosis there is no difference in dyspnea and lung function between cutaneous-limited and diffuse scleroderma patients. However, after 1 year, diffuse-scleroderma patients show increased HRCT-scored fibrosis, worse functional activity and quality of life, when compared with cutaneous-limited scleroderma patients (Clements et al., 2007). In RA-ILD, the lung phenotype is characterized by inflammation of the pleura including pleura thickening and effusions, as well as epithelium and endothelium injury (Shaw, Collins, Ho, & Raghu, 2015). The Sjörgen's syndrome-ILD manifestations include diffuse lymphocytic infiltration in the airways, bronchial hyperresponsiveness, bronchiectasis, bronchiolitis or recurrent respiratory infections (Flament et al., 2016). In general, the histopathology feature in CTD-ILD is represented by large lymphoid follicles surrounding the bronchiole similarly with NSIP pattern (Fischer et al., 2015).

1.3.3 Granulomatous ILDs

In HP, mononuclear cells (lymphocytes, monocytes and activated macrophages) infiltration to the alveolar and interstitium compartments is a characteristic disease pathophysiology feature (Salvaggio & deShazo, 1986). HP is characterized by antigen presentation and developed sensitization disease with humoral and cellular immune response (Bourke et al., 2001). In susceptible individuals, exposure to e.g. contaminated forced-air systems, birds (mainly budgerigar fanciers and pigeon fanciers), mold, dust, and occupational antigens result in HP. Genetic mutation in human leukocyte antigen (HLA) gene has been shown to contribute to the development of HP (Selman, Pardo, & King, 2012). Repetitive inflammation due to antigen presentation results in lung structure damage and fibrosis. In cases of chronic HP, the pathological hallmarks are the presence of center lobular fibrosis and peribronchiolar fibrosis, often associated with fibroblast foci which can mimic IPF (Salisbury et al., 2017).

In sarcoidosis, the lungs are affected by a high infiltration of phagocytes and antigen presenting cells (APC) into the parenchyma and alveolar spaces. In sarcoidosis, HLA class II molecules and T cell receptors are important players during antigen and

bacterial infections. Along the same line, susceptibility to sarcoidosis may be a result of HLA polymorphism (Costabel & Hunninghake, 1999). Formation and accumulation of granulomas are fundamental abnormalities of sarcoidosis (Iannuzzi et al., 2007). The granuloma is a result of lymphocytes $CD4^+$ cells mediating macrophage recruitment and activation (Rosen, 2007). Due to the lung injury differences, this thesis focuses in IPF, NSIP, HP and CTD-ILD.

1.4 Clinical features of ILDs

ILD patients present as first symptoms dyspnea and cough (often dry) that can be associated with fever, fatigue and weight loss. In IPF, it is common to present bibasilar inspiratory crackles and finger clubbing (Raghu et al., 2011). ILD are fibrotic diseases characterized by a restrictive alteration type in the pulmonary function test (PFT) (Alhamad, Lynch, & Martinez, 2001). Abnormal PFT in ILD are defined as 15% decline in the absolute values of diffuse lung capacity for carbon monoxide (DLCO), 10% decline in forced vital capacity (FVC) and total lung capacity (TLC) (Raghu et al., 2011).

Radiological approach gives a great support to the clinical diagnostics in ILD. Chest HRCT is crucial during ILD characterization depicting the reticular changes in the lung. The regions with low density, the so-called mosaic attenuation, are indicative of fibrosis (Martinez et al., 2017). The specific localization of tissue injury, bilateral, peripheral, basal distribution can be used to diagnose the precise type of ILD. However, HRCT does not always show a clear ILD pattern. In these cases, lung biopsy is required for a precise diagnosis and classification. Lung biopsy is a high risk procedure in which age, disease severity and comorbidities challenge its benefit/risk balance (Cottin, 2016). Therefore, less invasive procedures are greater contributors to investigate the molecular and cellular components involved in the pathophysiology.

Molecular biomarkers and blood immunophenotyping help ILD management. Clinically, molecular biomarkers in ILD can elucidate disease predisposition, pathogenesis, mechanisms, as well as progression. Biomarkers are measured in

body fluids, such as blood/serum, and bronchoalveolar lavage (BAL). Molecular biomarkers show to be involved in different mechanisms of lung injury. Biomarkers related to the epithelial cell injury are surfactant proteins (especially SPC, and SPA2), Krebs von den Lungen-6 (KL6)/ mucin1 (MUC1), mucin 5B (MUC5B), telomerases (especially TERT and TERC) and cytokeratin 18 (cCK18) (Camelo, Dunmore, Sleeman, & Clarke, 2014). Biomarkers related to the immune dysregulation are toll-like receptor 3 (TLR3), ELMO domain containing 2 (ELMOD2), toll-interacting protein (TOLLIP) and α-defenins (Ley et al., 2014). Importantly, specific biomarkers involved in the macrophage activation are CC chemokine ligand 18 (CCL18)/ PARC and YKL40 (Guiot, Moermans, Henket, Corhay, & Louis, 2017). Biomarkers of the adaptive immune system are represented by heat shock protein 70 (HSP70), CXC motif chemokine (CXCL13), T cells subsets and T regulatory cells (Tregs) (Sellares et al., 2018) (Vuga et al., 2014). Last, extracellular matrix deposition biomarkers are MMPs, phosphoprotein 1 (SSP1 or OPN), periostin and circulating fibrocytes (Ley et al., 2014). Although, all those biomarkers show to be associated with pulmonary fibrosis diagnosis, prognosis, and/or mortality, there is no clear available biomarker for clinical practice yet (Guiot et al., 2017). Importantly, the serum biomarkers: MMP7, SPD, CCL18 and KL6 are not recommended for distinguishing IPF from non-IPF ILDs (Raghu et al., 2018). In a more comprehensive and integrated manner, systems medicine helps to characterize ILD, as well as to find and understand therapeutic approaches (Greiffo, Eickelberg, & Fernandez, 2017) (Appendix). High-throughput omics technologies are an advantage tool to ILD. For instance, transcriptomics (i.e. MMP7) (Zuo et al., 2002) and genetics (i.e. MUC5B) (Seibold et al., 2011) studies show association with lung fibrosis progression and survival, respectively.

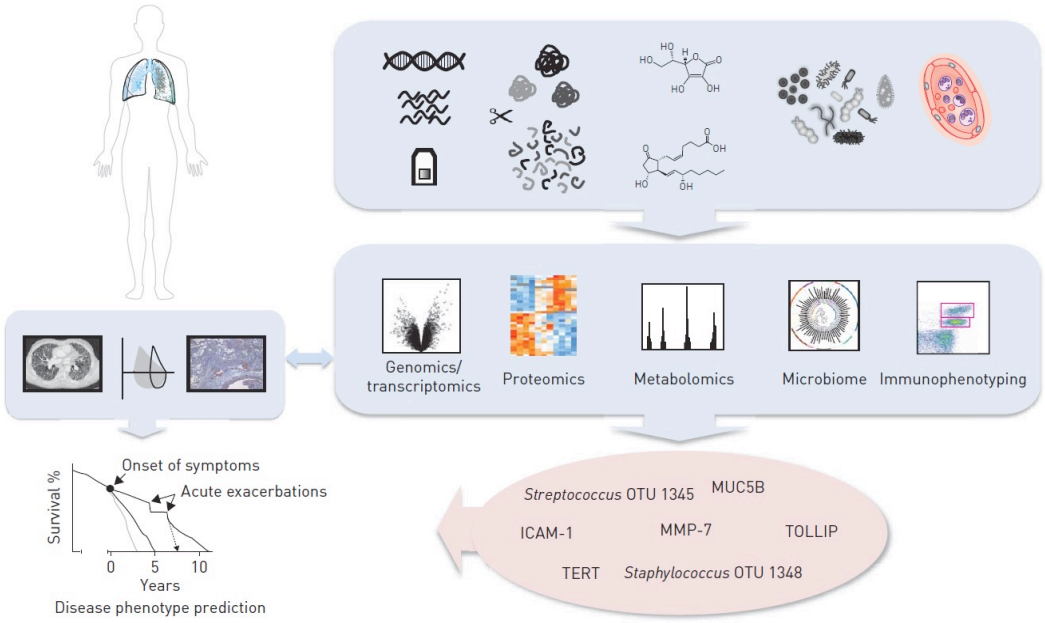

Figure 5. Systems medicine approaches applied to ILD: RNA, DNA, proteins, metabolites, microbiome and circulating cells are integrated in the omics technologies to future clinical applicability (Greiffo et al., 2017).

1.5 Diagnosis of ILDs

The diagnosis of ILDs starts with a comprehensive history, physical examination (especially chest auscultation, and detection of inspiratory crackles), physiological test (e.g. PFT) and laboratory tests. First, known causes of ILD are identified, such as HP or CTD-ILD. HRCT helps to better identify the ILD-related patterns. In NSIP and HP, HRCT shows profuse nodules. In IPF, HRCT reveals characteristically reticular changes associated with traction bronchiectasis and honey combing. Honeycombing is defined as “sub pleural cystic airspaces with well-defined walls” (Raghu et al., 2018) (Martinez et al., 2017) (figure 4). When the HRCT is inconclusive, guidelines recommend open lung biopsy to help characterization of definitive patterns e.g. proliferative fibroblast and myofibroblast (fibroblast foci) in the lung parenchyma, distortion of the lung architecture and detection of honeycombing (Martinez et al., 2017) (figure 4). The histopathological patters of ILD are acute lung injury, fibrosis, cellular infiltrates, airspace filling, nodules, minimal changes (e.g. edema, pulmonary emboli, bronchiolitis) (Leslie, 2009).

Moreover, patient's gender (G), age (A) and lung physiology (P) data (GAP index) can predict mortality of IPF patients. The GAP assessment has been developed as a prognostic estimation. GAP identifies three stages: 1 year mortality of 6% to stage 1, 16% to stage 2 and 39% to stage 3 (Ley et al., 2012).

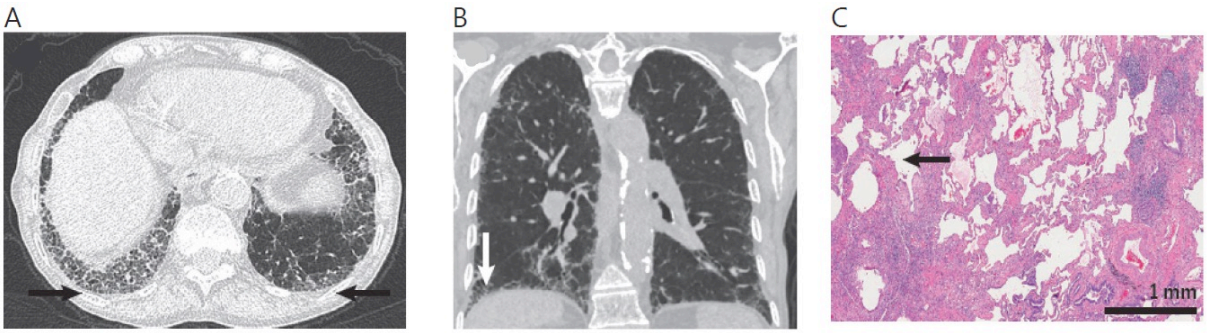

Figure 4. Honeycombing revealed by HRCT and histology. (A) HRCT shows the lung lower zones and (B) sagittal plane of lungs from a woman diagnosed with IPF. Black and white arrows show honeycomb areas. (C) High-power H&E staining of IPF lung shows the micro-honeycombing areas indicated with black arrows (adapted from (Martinez et al., 2017)).

1.6 Treatment for ILDs

The treatment for ILDs is limited to ameliorate symptoms and minimize lung injury. In the past years, nintedanib and pirfenidone are recommended as anti-fibrotic drugs for IPF patients (Raghu et al., 2011). Both treatments show decrease disease progression by improving survival and declining FVC by approximately 50% over 1 year of disease course (Raghu et al., 2011). The drug mechanism of nintedanib is designed to inhibit tyrosine kinase activity and of pirfenidone is designed to inhibit TGF-ß production. Nintedanib and pirfenidone have shown to decrease the number of respiratory exacerbations, hospitalizations and mortality rate of IPF (Richeldi et al., 2014) (King et al., 2014). According to the latest guideline from the American Thoracic Society, European Respiratory Society, Japanese Respiratory Society and Latin American Thoracic Association (ATS/ERS/JRS/ALAT), IPF patients may not be treated with corticosteroids (i.e. prednisone), mucolytic drugs (i.e. N-acetyl cysteine),

anticoagulant medications (i.e. warfarin) and blood vessels constrictors (i.e. endothelin receptor antagonist, ambrisentan) because these drugs showed low confidence in the estimated anti-fibrotic effect for IPF patients (Raghu et al., 2015).

Although pro-fibrotic therapies show to slow-down disease progression, the currently treatment of non-IPF ILD includes oral steroids (e.g. prednisone) and immunosuppressor (e.g. mycophenolate, azathioprine, cyclophosphamide) (Behr et al., 2017). The treatment of pulmonary fibrosis with oral steroid and/or immunosuppressor aims to decrease inflammation and suppress immune system over activity. However, in severe cases of ILDs those medicaments are not enough to control and decrease the disease progression (Raghu et al., 2011). Moreover, not all ILD patients respond to steroid treatments which show urgent need new strategies to treat non-IPF ILD (Behr et al., 2017).

Furthermore, non-pharmacologic treatment has been strongly recommended in the clinical practice. In this line, oxygen therapy and pulmonary rehabilitation decrease dyspnea (Raghu et al., 2011) and improve exercise capacity, as well as patients' quality of life (Dowman et al., 2017). Last, lung transplantation is recommended when patients in palliative treatment do not respond well and fibrosis is severe, however, median survival of lung transplantation is approximately 5 years (Chambers et al., 2017). Altogether, more research towards treatment for ILD investigating molecular mechanisms or finding potential biomarkers is needed.

1.7 Myeloid cells in ILDs

Myeloid cells are originated from the hematopoietic stem cells niche and classified as common myeloid progenitor cells. Monocytes, macrophages, granulocytes, and myeloid-derived suppressor cells (MDSC) are originated from myeloid progenitor cells niche. Myeloid cells play an important role in organism protection under pathological conditions. Under homeostasis, myeloid cells are crucial in the initiation, perpetuation or inhibition of the adaptive immune system (Engblom, Pfirschke, & Pittet, 2016).

In pulmonary fibrosis, damage-associated molecules patterns (DAMP) are involved in tissue destruction and activation of myeloid and epithelial cells. DAMP signaling, such as TLR-2, IL-33, uric acid, ATP and TGF-ß, increase inflammation and fibrosis, as well as myeloid cells recruitment to the site of injury (Ellson, Dunmore, Hogaboam, Sleeman, & Murray, 2014). Simultaneously, blood clotting damages the vessels and affect tissue resident cells increasing the infiltration of myeloid cells to the lungs. In the inflammatory phase of ILD, monocytes and neutrophils phagocyte microorganisms and debris, and prevent the perpetuation of injury (Wynn, 2011). After this acute inflammatory phase, pro-repair cytokines (i.e. TGF-ß and IL-10) and M2-like macrophages activate myofibroblasts leading to ECM deposition and scar tissue formation (Wynn, 2011). Importantly, any dysregulation in the tissue regeneration phase can result in fibrosis. The repetitive damage process results in the accumulation of myeloid cells in the fibroblast foci and decreases the adaptive immune cell response, such as T cell activation and proliferation (Wynn, 2011) (Florez-Sampedro, Song, & Melgert, 2018).

Myeloid cells display high plasticity which is induced by tissue environment. During ILD, myeloid derived cells are differentiated and activated in response to injury and surrounding matrix. Wound healing induces M2-like macrophages to increase the proliferation of fibroblasts-like cells (Bonnans, Chou, & Werb, 2014). Moreover, myeloid derived cells phenotype is critical to drive lung remodeling. Characterizing the immune cells phenotype is one step-forward to determine cell maturation and function in the site of injury (Tosh & Slack, 2002).

1.7.1 Myeloid-derived suppressor cells (MDSC) in ILDs

Myeloid-derived suppressor cells (MDSC) are a heterogeneous population of immature myeloid cells and leukocyte lineage (Talmadge & Gabrilovich, 2013). MDSC have two subsets, monocytic MDSC (M-MDSC) and granulocytic MDSC (G-MDSC). MDSC are classified by negative expression of various myeloid origin cells including CD3, CD16, CD19, CD20 and CD56. M-MDSC are defined as Lineage$^-$

HLA-DR$^-$ CD33$^+$ CD11b$^+$ and CD14$^+$ cells, and G-MDSC as Lineage$^-$ HLA-DR$^-$ CD33$^+$ CD11b$^+$ CD66b$^+$ cells (Talmadge & Gabrilovich, 2013) (Damuzzo et al., 2015).

MDSC accumulation has been reported to be common in many chronic diseases and pathological conditions, such as lung cancer, transplantation, infection and autoimmunity (figure 6) (Gabrilovich & Nagaraj, 2009). For instance, in non-small cell lung cancer, patients with higher number of circulatory MDSC showed poorer survival or worse response to treatment (Feng et al., 2012). In chronic lung inflammation (i.e. tuberculosis (TB) and *Pseudomonas aeruginosa* infection) MDSC inhibited immune surveillance (du Plessis et al., 2013) (Rieber et al., 2013). Moreover, higher number of MDSC decreased numbers of Tregs and T cells in COPD patients (Kalathil et al., 2014). It is known that MDSC function is linked to the suppressor capabilities and T cell response contributing to tumor-immune cell evasion (Talmadge & Gabrilovich, 2013).

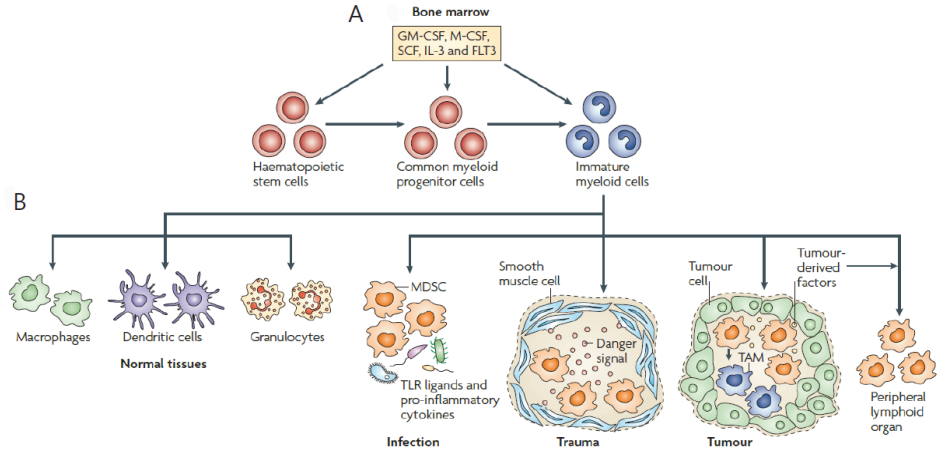

Figure 6. MDSC origin and accumulation: (A) myeloid cells from the bone marrow, including immature cells, are mediated by granulocyte/macrophage colony-stimulating factor (GM-CSF), macrophage CSF (M-CSF), stem-cell factor (SCF), interleukin-3 (IL-3) and FMS-related tyrosine kinase 3 (FLT3). (B) Acute and chronic infections, trauma, sepsis, and tumors promote the accumulation of immature cells, including MDSC (Gabrilovich & Nagaraj, 2009).

1.7.2 Monocytes in ILDs

Monocytes are mononuclear leukocytes derived from the common myeloid progenitor niche. In the human and mouse blood, monocytes represent 10% of total cells, and 5% of total leukocytes (Das et al., 2015). Human monocytes are classified in three different subsets, according to CD14 and CD16 expression: classical, intermediate, and non-classical. Classical monocytes are defined as $CD14^{+++}CD16^{+}$, intermediate monocytes as $CD14^{+}CD16^{+}$ and non-classical monocytes $CD14^{+}CD16^{++}$ (Ziegler-Heitbrock, 2007). Classical monocytes account for approximately 85% of total monocytes. Intermediate and non-classical monocytes represent 5 and 10% of total monocytes, respectively (Passlick, Flieger, & Ziegler-Heitbrock, 1989). Mouse monocytes are classified in classical and non-classical, according to Ly6C expression. In mouse, classical monocytes are classified as $Ly6C^{high}$ and non-classical monocytes $Ly6C^{low}$ (Auffray et al., 2007). Moreover, in human and mouse classical monocytes are defined as $CCR2^{hi}CX3CR1^{low}$ cells and non-classical monocytes as $CCR2^{low}CX3CR1^{hi}$ cells (Shi & Pamer, 2011) (Auffray et al., 2007) (Ginhoux & Jung, 2014) (figure 7).

The role of classical monocytes in humans and mice has been broadly explored whereas non-classical monocytes phenotype, function and recruitment are still unclear (Jung, 2018). As an illustration, cell tracing studies in mice showed that monocytes in injured tissues present a classical $CCR2^{+}$ phenotype. In the tissue, classical $CCR2^{+}$ monocytes contribute to inflammation and angiogenesis (Florez-Sampedro et al., 2018). Furthermore, CCR2 is an important chemokine necessary for monocytes to exit the bone marrow as well supply peripheral monocyte pools (Patel et al., 2017) (Ginhoux & Jung, 2014) (Jung, 2018) (figure 7). The fates of classical monocytes after recruitment from the bone marrow are: 1) to migrate from blood to tissue or 2) remain in the blood and differentiate into intermediate monocytes and later non-classical monocytes (Patel et al., 2017).

The role of non-classical monocytes in mice has been described as resident and patrolling cell because they regulate and remain in the vascular system (Geissmann, Jung, & Littman, 2003). However, there is no substantial evidence that the same

phenotype and function occur in humans (Narasimhan, Marcovecchio, Hamers, & Hedrick, 2019). Non-classical monocytes in humans and mice are characterized by high expression of CX3CR1. The unique ligand of CX3CR1 is fractalkine (CX3CL1) which is known for regulating monocytes survival (D'Haese, Demir, Friess, & Ceyhan, 2010; Landsman et al., 2009). For example, in liver fibrosis mouse model non-classical CX3CR1^{+} monocytes might supply tissue macrophage pools, and regulate immune responses to injury and infection via M2 differentiation, contributing to regression of fibrosis (Ishida, Gao, & Murphy, 2008) (Brempelis & Crispe, 2016). In kidney fibrosis non-classical monocytes CX3CR1^{+} cells induce generation of reactive oxygen species (ROS), and production of fibrotic mediators, as TGF-β and collagen-I, perpetuating fibrosis (Hochheiser et al., 2013) (Shimizu et al., 2011). In airway inflammation, CX3CR1 axis has been described to increase immune cells influx (Mionnet et al., 2010). Overall, the role of CX3CR1-fractalkine axis is shaped by every specific tissue and environment.

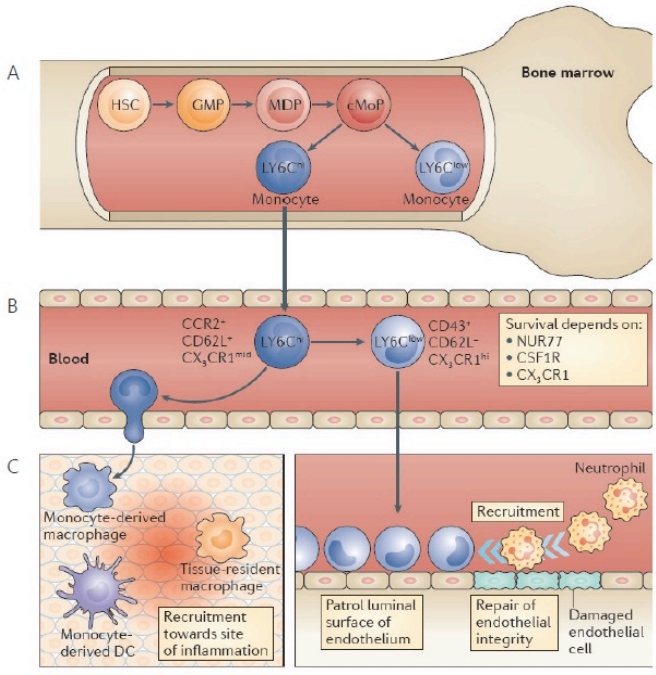

Figure 7. The phenotype of mouse monocyte: (A) monocytes are originated in the bone marrow from the hematopoietic stem cells (HSC) mediated macrophage and

dendritic cell (DC) precursor (MDP) and common monocyte progenitor (cMoP). (B) Circulatory classical (Ly6C^{hi}) and non-classical (Ly6C^{low}) show different phenotype and function. (C) Classical monocytes are rapidly recruited to sites of inflammation where non-classical monocytes patrol the luminal surface of endothelial cells. The precise role of non-classical monocytes under pathological conditions is still unclear. CSF1R (colony-stimulating factor 1 receptor), GMP (granulocyte–macrophage progenitor) (Ginhoux & Jung, 2014) last update (Jung, 2018).

Non-classical monocytes adhesion and migration are mediated by fractalkine-CX3CR1 binding (Jung, 2018). Recently, it has been shown that increased levels of fractalkine in the lung of scleroderma and patients were associated with ILD progression (Hoffmann-Vold et al., 2018). Additionally, non-classical monocytes participate in RA initiation and progression (Misharin et al., 2014) and showed increased migration from peripheral blood to synovial inflamed tissue (Kawanaka et al., 2002). More recently, single cells RNA-sequencing identified in lung fibrosis mouse model a transitional population of monocyte-derived CX3CR1^{+} cells that were localized in the fibrotic niche and contributed to fibroblast accumulation (Aran et al., 2019). However, the mechanisms involved in non-classical monocyte phenotype and recruitment by CX3CR1-fractalkine axis in ILD has not yet been explored.

2. Objectives

Immune system dysregulation has gained important attention in ILD field. Due to deep investigation in characterizing the innate immune cells and their contribution to pulmonary fibrosis pathophysiology we have opened an interesting topic not yet explored: the phenotype of MDSC and monocytes subsets in ILD. This thesis aims to characterize the myeloid immune cells abundance, recruitment mechanisms and their function in ILD patients.

To study the comprehensive immunophenotype of MDSC in IPF patients, here was aimed: 1) to quantify circulating MDSC in the peripheral blood and lungs tissue-resident; 2) to investigate MDSC as potential biomarker; and 3) to assess the function of MDSC in the immune network.

To study the comprehensive immunophenotype and cell recruitment mechanism of monocytes subsets in ILDs, here was aimed: 1) to quantify monocytes subsets: classical, intermediate and non-classical in the peripheral blood and lung tissue; 2) to explore the functional markers expressed by monocytes subsets; 3) to depict the role of monocytes recruitment from the peripheral blood to fibrosis site.

3. Material and Methods

3.1 Subjects

The study was performed in accordance with protocols approved by the Ludwig-Maximilians Universität München ethics review board (numbers 180-14 and 454-12). All subjects provided written informed consent for the research study and molecular testing.

Hundred-seventy subjects were included in the MDSC study. Of those, 69 subjects were diagnosed with IPF, 56 with non-IPF ILD (NSIP n=27, HP n= 17, CTD-ILD n=23), 23 with chronic obstructive pulmonary disease (COPD), and 22 were controls.

To explore monocytes immunophenotype in ILD, 105 subjects were recruited. Of those, 36 were diagnosed with NSIP, 28 with HP, 19 with CTD-ILD, and 22 were controls.

The diagnoses of ILD were performed by multidisciplinary consensus, based on the current ATS/ERS criteria (Travis et al., 2013). Control subjects did not have any signs of active infection, inflammation, and/or respiratory symptoms.

3.2 Immune cells isolation and immunophenotyping by Flow Cytometry

Fresh venous blood was collected in EDTA-coated vacutainer tubes (Sarstedt, Nümbrecht, Germany), peripheral blood mononuclear cells (PBMCs) were isolated by collection of buffy coats prepared by density gradient sedimentation (Lymphoprep™ STEMCELL Technologies, Köln, Germany). Approximately, 18ml of blood was diluted in 10ml of phosphate buffer saline (PBS). Next, 12ml of Lymphoprep ™ was slowly added to the diluted blood and centrifuged at 450x g, room temperature, minimum acceleration, no break, for 20 minutes. Thereafter, PBMCs fraction was collected.

For MDSC, 100μL of whole blood was stained with a cocktail of antibodies containing anti-human: Lineage (CD56, CD20, CD19 and CD16), HLA-DR, CD33, CD11b, CD14 and CD66b (Biolegend, San Diego, CA, USA) for 20 minutes at 4°C in the dark. For MDSC characterization, blood cells (lymphocytes, monocytes and granulocytes) were gated in Lineage$^-$ HLA-DR$^-$ CD33$^+$ CD11b$^+$. M-MDSC were defined as Lineage$^-$ HLA-DR$^-$ CD33$^+$ CD11b$^+$ CD14$^+$ and G-MDSC as Lineage$^-$ HLA-DR$^-$ CD33$^+$ CD11b$^+$ CD66b$^+$. PBMCs were stained with CD3, CD4, CD8, CCR7, CD25 (Biolegend, San Diego, CA, USA), and FoxP3 (Becton Dickinson Bioscience, Heidelberg, Germany). In PBMCs, lymphocytes were distinguished as T cells (CD3$^+$), T helper (Th) cells (CD3$^+$CD4$^+$): Th effector (CCR7$^-$) and Th non-effector (CCR7$^+$); T cytotoxic (CD3$^+$CD8$^+$): T cytotoxic effector (CCR7$^-$) and T cytotoxic non-effector (CCR7$^+$). Abnormal T cells were classified as: CD3$^+$CD4$^+$CD8$^+$, suggestive Tregs CD4$^+$CD25$^+$ and Tregs as CD4$^+$CD25$^+$FoxP3$^+$ (table 1).

	Antigen	Fluorophore	Clone	Manufacturer	Isotype
MDSC	CD33	BV421	WM53	Biolegend	Mouse IgG1
	CD56	FITC	HDC56	Biolegend	Mouse IgG1
	CD20	FITC	2H7	Biolegend	Mouse IgG2b
	CD19	FITC	HIB19	Biolegend	Mouse IgG1
	CD16	FITC	3G8	Biolegend	Mouse IgG1
	CD66b	PE	G10F5	Biolegend	Mouse IgM
	CD11b	PerCPCy5.5	ICRF44	Biolegend	Mouse IgG1
	HLA-DR	PECy7	L243	Biolegend	Mouse IgG2a
	CD14	APCCy7	HCD14	Biolegend	Mouse IgG1
Lymphocytes	CD25	BV421	2A3	Biolegend	Mouse IgG1
	CD19	FITC	HIB19	BD Bioscience	Mouse IgG1
	CCR7	PE	150503	Biolegend	Mouse IgG2a
	CD3	AF700	HIT3a	R&D	Mouse IgG2a
	CD8a	PECy7	HIT8a	Biolegend	Mouse IgG1
	CD27	APC	M-T271	Biolegend	Mouse IgG1
	CD4	BV510	RPA-T4	Biolegend	Mouse IgG1
	FoxP3	AF488	259D/C7	Biolegend	Mouse IgG1

Table 1. List of antibodies used for MDSC and lymphocytes analysis by flow cytometry: anti-human antibodies antigen, fluorophore, clone, manufacturer, and isotype.

For monocytes subsets detection, PBMCs were stained with monocyte antibody mix containing anti-human: HLA-DR, CD14, CD16, CX3CR1, CCR2 (Biolegend, San Diego, CA, USA), and CD163 (Becton Dickinson Bioscience, Heidelberg, Germany) (table 2). Monocytes were gated in HLA-DR^{+} cells, followed by classification of classical monocytes (CD14^{+++}CD16^{+}), intermediate monocytes (CD14^{+}CD16^{+}), or non-classical monocytes (CD14^{+}CD16^{++}). Data are presented as % of total monocytes. Canonical markers CCR2, CX3CR1, and CD163 were analyzed in each subset of monocyte and data presented as mean fluorescence intensity (MFI) of total monocytes.

Moreover, monocytes were detected in the whole lung cell suspension. For that, human explanted lungs or biopsies pieces of 1-2 mm^2 were minced and incubated with 0.2% type II collagenase in DMEM medium containing 10% fetal bovine serum (FBS) for 2 hours on a roller at 37°C. Afterwards, lung pieces were meshed using a 400-500 μm filter followed by a 100 μm filter. Cells were centrifuged 450g, 5 minutes at room temperature. Then, pellet was resuspended and cell number was detected by trypan blue staining and Neubauer chamber. Lung myeloid cells were isolated using the CD45 MicroBeads (Miltenyi Biotec; Bergisch Gladbach, Germany). CD45^{+} cells were stained with a mix of antibodies containing anti-human CD15, HLA-DR, CD14, CD16, MERKT, CD206 (table 2).

	Antigen	Fluorophore	Clone	Manufacturer	Isotype
Monocytes	HLA-DR	PE-Cy7	L243	Biolegend	Mouse IgG2a
	CD14	APC-Cy7	HCD14	Biolegend	Mouse IgG1
	CD16	PerCP/ Cy5.5	3G8	Biolegend	Mouse IgG1
	CD192 (CCR2)	BV421	K036C2	Biolegend	Mouse IgG2a
	CX3CR1	FITC	2A9-1	Biolegend	Rat IgG2b
	CD163	PE	GHI/61	BD Biosciences	Mouse IgG1
	CD15	APC	HI98	Biolegend	Mouse IgM
	MERTK	BV421	590H11G1E3	Biolegend	Mouse IgG1
	CD206	PE/Cy7	15-2	Biolegend	Mouse IgG1

Table 2. List of antibodies used for monocytes analysis by flow cytometry: anti-human antibodies antigen, fluorophore, clone, manufacturer, and isotype.

Flow cytometry data acquisition was performed in a BD LSRII flow cytometer (Becton Dickinson, Heidelberg, Germany). For cell sorting, BD FACS ARIA II (Becton Dickinson, Heidelberg, Germany) was used. Data were analyzed using the FlowJo software (TreeStart Inc, Ashland, OR, USA). For setting up the gates, negative thresholds and isotype-labeled controls were used.

3.3 Cell morphology characterization by cytospin

Sorted M-MDSC and G-MDSC were used to perform cytospins. Approximately 1-3 x 10^4 M-MDSC or G-MDSC were centrifuged at 250x g, at room temperature for 5 minutes on cytospin microscope slides. Following the centrifugation, cytospin slides were stained with May-Grünwald-Giemsa dye used to determine the morphology of M-MDSC and G-MDSC. Moreover, cytospin slides were also performed for immunofluorescence staining. For that, slides of M-MDSC and G-MDSC were

stained with anti-human CD33 (catalog number HPA035832) and ITGAM (CD11b) (catalog number AMAb90911) (Atlas Antibodies-Sigma-Aldrich, St Louis, MO, USA). Antibodies were diluted in PBS + 5% BSA + 0.2% Tween, using the concentration of 1:50, 1:250 and 1:2500, respectively. Next, 1:250 dilution of each secondary antibody Alexa Fluor 568 goat anti-rabbit, and Alexa Fluor 488 goat anti-mouse, respectively, was applied and incubated at room temperature (1 hour) in the darkness. Afterwards, slides were counterstained with DAPI (Sigma-Aldrich, St Louis, MO, USA) (1:2500) (1 minute) and cytospin slides were mounted with fluorescent mounting medium (Dako; Hamburg, Germany). Microscopy was performed using Axiovert II (Carl Zeiss AG; Oberkochen, Germany) and images were processed using ZEN 2010 software (Carl Zeiss AG).

3.4 Lymphocytes suppression assay by co-culture of autologous MDSC and PBMC

MDSC and PBMCs were isolated from the same subject for future co-culture. Approximately $5x10^6$ PBMCs were stained with CFSE solution. Fresh CFSE solution was prepared using 5.625ml of PBS and 1μl of CFSE (CellTrace™, ThermoFisher Scientific, Eugene, OR, USA). PBMCs pellet was resuspended in 1ml of sterile PBS and 1ml of CFSE solution. Afterwards, stained-PBMCs were seeded alone or in co-culture with autologous MDSC in a ratio of 1:4, respectively (3-5 wells, 96 wells plate). In both conditions, lymphocyte proliferation was stimulated adding Recombinant Human 100 U/mL IL-2 (BD Pharmingen, San Diego, CA, USA), and 1 μg/mL OKT3 (CD3) (Biolegend, San Diego, CA, USA). Cells were kept in the incubator (37°C in humidified conditions containing 5% CO_2) for four days. Thereafter, to characterize lymphocytes immunophenotype by flow cytometry, the cells were harvested and stained with anti-human: CD4 and CD8 (Biolegend, San Diego, CA, USA). CSFE fluorescence intensity of $CD4^+$ and $CD8^+$ cells was analyzed with flow cytometry (Alexa Fluor 488). The % of CFSE (indicative of cell proliferation) was analyzed between PBMC cultured alone or with MDSC. Data was analyzed with

FlowJo software (TreeStart Inc, Ashland, OR, USA). This protocol has been adapted from previous publications (Rieber et al., 2013) (Kostlin et al., 2014).

3.5 IPF predictor genes expressed in PBMC by qRT-PCR

Frozen PBMCs of IPF patients with high number of MDSC and controls were used for analysis of CD28, ICOS, ITK, and LCK (Table 3). First, RNA was extracted using RNeasy Mini Plus Kit (Quiagen, Venlo, Holland). Approximately 3-5x10^6 PBMCs were homogenized and lysed with 350μl of lysis buffer (Qiagen buffer RLT Plus) and transferred to the gDNA eliminator column placed in a 2ml collection tube followed by centrifugation (8000x g, room temperature, 30 seconds). Then, the flow-through solution was mixed with 350μl of 70% ethanol and transferred to RNeasy spin column placed in a 2ml collection tube followed by centrifugation (8000x g, room temperature, 15 seconds). The flow-through was discarded. Then, 700μl of buffer RW1 was added into the same column followed by centrifugation (8000x g, room temperature, 15 seconds). The flow-through was discarded. Then, 500μl of buffer RPE was added into the same column followed by centrifugation (8000x g, room temperature, 15 seconds). The flow-through was discarded. The previous step was repeated with 2 minutes of centrifugation. Then, the column was placed in a new collection tube and 30μl of RNase-free water was added into the column followed by centrifugation (8000x g, room temperature, one minute). The flow-through was collected for measuring mRNA concentration, using a NanoDropTM 1000 spectrophotometer (NanoDrop Tech. Inc; Wilmington, DE, USA) at 260 nm.

After obtaining mRNA, RNA denaturation and reverse transcription was performed. For denaturation, mRNA was exposed to a temperature of 70°C for 10 minutes (lid at 75°C) (Eppendorf Mastercycler® pro, Germany). Thereafter, reverse transcription was performed using MuLV reverse transcriptase (Applied Biosystems, Carlsbad, CA, USA) and random hexamer primers (Applied Biosystems) and exposed to 20°C for 10 minutes, 43°C for 75 minutes, 99°C for 5 minutes finishing with long exposure to 4°C. The obtained cDNA was used for performing qRT-PCR.

For qRT-PCR a 96-well format for LightCycler® 480 DNA SYBR Green I Master (Roche; Penzberg, Germany) was used. For housekeeping gene and standardization of gene expression, we used GAPDH (Table 3).

Gene	FW	REV
GAPDH	TGA CCT CAA CTA CAT GGT TTA CAT G	TTG ATT TTG GAG GGA TCT CG
CD28	TCC CCT ATT TCC CGG ACC TTC TAA	AAG CTA TAG CAA GCC AGG ACT CCA
ICOS	TGT TGC CAG CTG AAG TTC TGG T	GGT CGT GCA CAC TGG ATG AAT ACT
ITK	CAG CCT GGC ATA CTT TGA AGA TCG	GGC ATG GGA TGC TGA TGT CAC TTT
LCK	GAC AGC GCC AGA AGC CAT TAA CTA	TGG GTG ACA ATT TCC GTC AGC A

Table 3. List of genes used for IPF prediction by qRT-PCR: forward (FW) sequence and reverse (REV) sequence of GAPDH, CD28, ICOS, ITK, and LCK.

3.6 MDSC and monocytes in the lungs by immunofluorescence

Lung tissue sections from control (tissue tumor-free areas) and ILD subjects were used to localize and quantify myeloid cells: MDSC and monocytes subsets in the lung.

Immunofluorescence staining was performed in lung tissue embedded in paraffin. For that, slides were deparaffinized by incubating overnight at 60°C, following by rehydration where slides were twice immersed in xylol (5 minutes, each), transferred to 100% ethanol (2 minutes, each), once in 90% ethanol (1 minute), 80% ethanol (1 minute), 70% ethanol (1 minute), and finally flushed with distillated water (30 seconds) to wash away the ethanol. Next, for antigen retrieval step slides were emerged in citrate buffer solution (pH 6.0) and placed into a Decloaking Chamber which was heated up at 125°C (30 seconds), 90°C (10 seconds), afterwards the slides slowly cooled down to room temperature. Then, slides were washed three times in Tris buffer, and blocked in 5% BSA – Tris buffer solution (1 hour) to prevent non-specific binding. Slides were placed in a wet chamber, primary antibodies were

added and slides were incubated at 4°C, overnight. The slides were rinsed three times with Tris buffer, and 1:250 dilution of each secondary antibody was applied and incubated at room temperature (1 hour) in the darkness. Slides were counterstained with DAPI (Sigma-Aldrich; St Louis, MO, USA) (1:2500) (1 minute). Once again, the slides were rinsed three times with Tris buffer, and covered with Fluorescence Mounting Medium (Dako, Hamburg, Germany).

For MDSC detection in the lung, we used explanted lungs from controls lung section (n=3) and pulmonary fibrosis lung sections (n=3; IPF n=2, HP n=1) and previously recruited to measure the circulating MDSC. The slides were stained with anti-human CD33 (catalog number HPA035832) (1:50) and ITGAM (CD11b) (catalog number AMAb90911) (1:250) (Atlas Antibodies-Sigma-Aldrich, St Louis, MO, USA). Also, CD33 and α-SMA (catalog number A5228, Sigma-Aldrich, ST Louis, MO, USA) (1:1000) and CD11b and collagen type I (1:200) (600-401-103-0.1, Rockland, Oxfordshire, UK). Afterwards, 1:250 dilution of each secondary antibody was applied: Alexa Fluor 568 goat anti-rabbit, and Alexa Fluor 488 goat anti-mouse, respectively for CD33 and CD11b; Alexa Fluor 568 goat anti-rabbit, and Alexa Fluor 488 goat anti-mouse, respectively for CD33 and α-SMA; Alexa Fluor 568 goat anti-mouse, and Alexa Fluor 488 goat anti-rabbit, respectively for CD11b and collagen I.

For monocyte subset detection in the lung, we used explanted lungs from four tumor-free areas (controls) and six ILD patients (NSIP n=2, HP n=4). The slides were tripled-stained with anti-human von Willebrand Factor (ab11713), CD14 (ab181470) (Abcam, Cambridge, UK), CD14 (BAF383, R&D Systems, Abingdon, UK), CD16 (ab109223, Abcam, Cambridge, UK), Fc gamma RIII/CD16 (NBP-42228, Novus Biologicals, Littleton, Colorado, USA) (CX3CR1 (ab8021, Abcam, Cambridge, UK), CD163 (NBP2-36494, Novus Biologicals, Littleton, Colorado, USA), CD68 (M0814, DAKO, Glostrup, DK), CX3CL1 (ab89229, Abcam, Cambridge, UK), acetylated tubulin (ab125356, Abcam, Cambridge, UK), collagen type I (600-401-103-0.1, Rockland, Oxfordshire, UK), and AXL (AF154SP, R&D Systems, Abingdon, UK). Primary antibodies were diluted using the antibody diluent (Zytomed Systems, Berlin, Germany), vWF (1:100), CD14 (1:100), and CD16 (1:200), CX3CR1 (1:500), and

CD163 (1:200), CD68 (1:50), CX3CL1 (1:100), acetylated tubulin (1:200), collagen type I (1:200), and AXL (1:200).

Microscopy was performed using Axiovert II (Carl Zeiss AG; Oberkochen, Germany) and images were processed using ZEN 2010 software (Carl Zeiss AG). For quantification of monocytes, the number of as $CD14^+$, and $CD14^+CD16^+$ cells (CD14 red fluorophore, and CD16 green fluorophore) in the tissue was normalized as % of total cells (DAPI positive). Five pictures per slide were taken and double positive cells localized in the parenchyma and outside the vessel, stained for vWF (far red fluorophore), were quantified.

3.7 Monocyte's protein quantification by ELISA

CC Chemokine Ligand 2 (CCL2) (catalog number DCP00) and fractalkine (CX3CL1) (catalog number DCX310) were used to quantify monocytes' chemokines levels in plasma and tissue homogenate by enzyme-linked immunosorbent assay (ELISA) (Quantikine Kit R&D Systems, Abingdon, UK). First, for lung homogenate, human lung tissue was pulverized in liquid nitrogen and homogenized in one volume of lysis buffer (1M Tris HCl pF 7.5, 5M NaCl, 100% NP-40, 10% Sodium-deoxycholat, 0.1% SDS). Samples were subsequently centrifuged at 10,000g for 15 minutes at 4°C, and the supernatant was collected to measure protein levels by BCA Protein Assay Kit (Pierce, ThermoFisher, Rockford, IL, USA). Protein aliquots prepared with 100μg of lung were used to measure levels of CCL2, and 200μg were used to measure levels of fractalkine. For plasma, we used 1:1 (in Calibrator Diluent RD6Q) and neat samples for quantification of CCL2 and fractalkine, respectively.

For CCL2, first 50μl of assay diluent RD1-83 diluent was added in each well. Then, 200μl of prepared sample and standards (included in the kit) was added per well and incubated at room temperature for 2 hours. Samples were aspirated and wells were washed with Wash Buffer (the wash step was repeated 4 times). Next, 200µL of human-CCL2 conjugate was added to each well and incubated at room temperature for 1 hour. Human-CCL2 conjugate was aspirated from each well which was washed with Wash Buffer (the washing step was repeated 4 times). Afterwards, 200µL of

Substrate Solution was added to each well and incubated at room temperature for 30 minutes. Finally, 50μL of Stop Solution was added in each well and the optical density was determined using a microplate reader set to 450nm, and wavelength correction of 540nm (Sunrise microplate reader, TECAN, Männedorf, Switzerland). CCL2 data was calculated by a generation of a four parameter logistic (4-PL) curve-fit (GraphPad Prism, version 7.0, GraphPad Software, San Diego, CA, USA). All experiments were performed in technical duplicates.

For fractalkine, first 100μl of RD1-88 assay diluent and 100μl of samples and standards (included in the kit) were added per well and incubated at 4°C for 3 hours. Then, samples were aspirated and wells were washed with Wash Buffer (the wash step was repeated 4 times). Next, 200μl of cold human-fractalkine conjugate was added in each well and incubated at 4°C for 1 hour. Afterwards, human-fractalkine conjugate was aspirated from each well following by washing with Wash Buffer (the wash step was repeated 4 times). 200µL of Substrate Solution to each well and incubated at room temperature for 30 minutes. Lastly, 50μL of Stop Solution was added in each well and the optical density was determined using a microplate reader set to 450nm, and wavelength correction of 540nm (Sunrise microplate reader, TECAN, Männedorf, Switzerland). Fractalkine data was calculated by a generation of a log/log curve-fit (GraphPad Prism, version 7.0, GraphPad Software, San Diego, CA, USA). All experiments were performed in technical duplicates.

3.8 Monocyte subsets function by endothelial cell adhesion assay

Immortalized murine endothelial cells (SVEC) were used to analyze monocyte adhesion. SVEC were cultivated and activated with TNF-α (10ng/mL) for 4 hours, at 37°C in humidified conditions containing 5% CO_2. Monocytes were isolated from PBMC using the Pan Monocyte Isolation Kit followed by CD16 MicroBeads (Miltenyi Biotec; Bergisch Gladbach, Germany), resulting in a separation of $CD14^+$ and $CD16^+$ monocytes. We performed a competitive assay where $CD16^+$ monocytes ILD patient were labeled with green cell dye (LeukoTracker™, Cell Biolabs, INC.; San Diego, CA, USA), and $CD16^+$ monocytes from control were labeled with red cell dye (Red Cell

Tracker™ Red CMTPX dye, Life Technologies; Carlsbad, CA, USA). CD16+ labeled monocytes were resuspended in two different conditions: 1) chemokine free (PBS 2% FBS) and 3) fractalkine (PBS 2% FBS + 200ng/ml fractalkine) (Peprotech; Rocky Hill, NJ, USA) (figure 7). Subsequently, activated endothelial cells were co-cultured with freshly labeled CD16+ monocytes from control sample and CD16+ monocytes from ILD sample (1:1) for 15 minutes at 37°C in humidified conditions containing 5% CO_2. Non-adherent cells were washed away, and adherent cells were fixed with 4% paraformaldehyde (PFA) for 15 minutes at room temperature. Adherent monocytes were imaged using a confocal microscope (LSM710, Carl Zeiss, 10x), and images were acquired by 6x6 tile scan, covering the whole surface area of each well. Adherent CD16+ monocytes were quantified using Imaris' statistical analysis tool Software (Bitplane; version 8.1.2, Concord, MA, USA), where the total number of spot objects, representing the total number of cells were determined. This protocol has been adapted from previous publication (Gamrekelashvili et al., 2016). Data was normalized according to control (chemokine free), and adherent cells were defined by adhesion index (AI), as previously reported (Lo Buono et al., 2011).

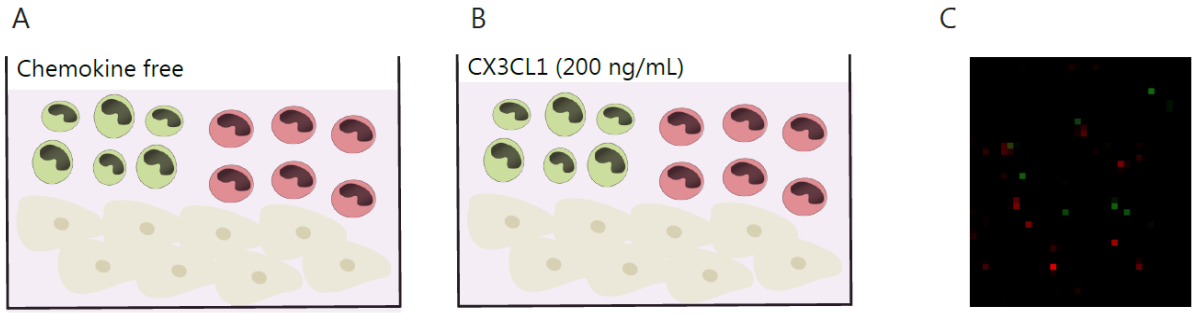

Figure 7. Monocytes adhesion assay: (A) CD16+ monocytes co-cultured with endothelial cells for 15 minutes. (B) CD16+ monocytes co-cultured with endothelial cells and fractalkine (CX3CL1) for 15 minutes. Non-adherent cells were washed away and adherent cells were fixed with 4% PFA. (C) CD16+ monocytes control were quantified using confocal microscopy (LSM710; Carl Zeiss).

3.9 Monocyte subsets function by chemotaxis migration assay

Isolated monocytes seeded into a transwell (Corning® HTS Transwell® 96 wells permeable 5µM pore; Sigma-Aldrich; Kennebunk, ME, USA). To verify whether the migration of monocyte subsets responded to different stimuli, we had three different conditions in the lower chamber: chemokine free (RPMI 1640 + 0.5% BSA), fractalkine (RPMI 1640 + 0.5% BSA + 200ng/ml fractalkine) and fractalkine with antibody blocking fractalkine (RPMI 1640 + 0.5% BSA + 200ng/m fractalkine + 200ng/m mAb-fractalkine) (figure 8). Monocytes were incubated at 37°C in humidified conditions containing 5% CO_2 for 3 hours. Thereafter, migratory cells were harvested and stained with an antibody mix containing anti-human HLA-DR, CD14, and CD16 followed by flow cytometry. Data acquisition was performed in a BD LSRII flow cytometer (Becton Dickinson, Heidelberg, Germany). Migratory monocytes data were analyzed using the FlowJo software (TreeStart Inc, Ashland, OR, USA). Negative thresholds for gating were set according to isotype-labeled controls. Data were normalized using control wells (chemokine free) as an indicator of conversion efficiency, migration index (MI) according to previous publications (Lo Buono et al., 2011).

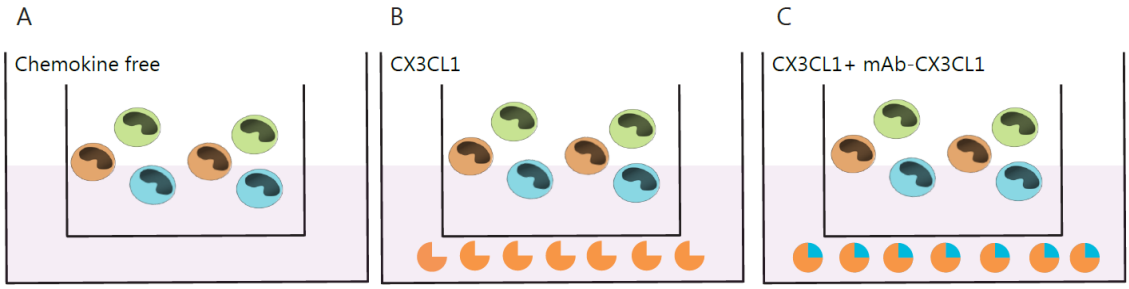

Figure 8. Monocytes migration assay: (A) Monocyte were isolated and added into a transwell (5μM pore membrane). (B) In the bottom of the transwell was added fractalkine (CX3CL1). (C) In the bottom of the transwell was added fractalkine (CX3CL1) together with monoclonal antibody blocking fractalkine (CX3CL1).

3.10 Statistical analysis

Three and more group comparisons were analyzed using the one-way analysis of variance, with non-parametric Kruskal-Wallis test, followed by Dunn's multiple comparison test. For, two group comparisons were analyzed non-parametric or paired Student *t*-test or Mann-Whitney test. Associations between variables were established using linear regression and Pearson correlation. Statistical analyses and significance was defined as *p* less than 0.05.

For MDSC, results are presented as scatter dot plots with mean ± SD. Data was analyzed using GraphPad Prism (version 5.0, GraphPad Software; San Diego, CA, USA). For monocytes, results are presented as box and whiskers vertical graphs with mean ± standard deviation. Data was analyzed using GraphPad Prism (version 7.0, GraphPad Software; San Diego, CA, US

4. Results

4.1 MDSC

The MDSC work presented in this thesis has been published in the ERJ, 2016 (PMID: 27587556); Fernandez I.E, **Greiffo F.R,** et al. (Fernandez et al., 2016) (Appendix).

4.1.1 Patients demographics

The cohort of the subjects in the immunophenotyping characterization of MDSC included patients diagnosed with IPF, non-IPF ILD (NSIP, HP and CTD-ILD), and COPD. Subjects without diagnose of chronic diseases and inflammation were included as controls (Table 3).

Characteristics	Control	IPF	Non-IPF ILD	COPD
	22	69	56	23
Age (years)	55.32±7.27	59.78±11.33**	61.44±8.33*	65.61±11.09
Gender				
Female	11 (50%)	55 (79.7%)	30 (53.5%)	11 (47.8%)
Male	11 (50%)	14 (20.3%)	26 (46.5%)	12 (52.1%)
ILD type				
NSIP	-	-	27 (48.2%)	-
HP	-	-	17 (30.3%)	-
CTD-ILD	-	-	12 (21.4%)	-
Smoking status	-	2.8% (1/ 36)	7.1% (2/ 28)	26.3% (5/ 19)
Current	5 (22.7%)	5 (7.2%)	0	1 (4.3%)
Former	6 (27.2%)	40 (57.9%)	26 (46.4%)	22 (95.6%)
Nonsmoker	11 (50%)	24 (34.7%)	30 (53.6%)	0
DLCO (%predicted)	-	33.8±16.7	32.5±16.3	25.3±18.7
VCmax (%predicted)	-	61.6±17.8	61.3±19.2	61.1±26.6††

Table 3. Subjects demographics: data are presented as % and number of affected patients. Idiopathic pulmonary fibrosis (IPF); Non-specific interstitial pneumonia (NSIP); Hypersensitivity pneumonitis (HP); Connective-tissue diseases (CTD); Chronic obstructive pulmonary disease (COPD). Lung function data are presented as Mean±SD, diffusing capacity of the lung for carbon monoxide (DLCO); maximum vital capacity (Vcmax). * represents $p<0.05$ when compared with control ** represents $p<0.01$ when compared with control.

4.1.2 MDSC immunophenotyping in the peripheral blood

Peripheral blood MDSC were characterized by Lineage$^-$ HLA-DR$^-$ CD33$^+$ CD11b$^+$. M-MDSC were defined as Lineage$^-$ HLA-DR$^-$ CD33$^+$ CD11b$^+$ CD14$^+$ and G-MDSC as Linage$^-$ HLA-DR$^-$ CD33$^+$ CD11b$^+$ CD66b$^+$. Isotype control was used as a threshold of positive-negative populations (figure 9A). To confirm the morphology of M-MDSC and G-MDSC, cells were sorted for staining. Cytospin immunofluorescence stainings of CD33 and CD11b confirmed the nuclei morphology of monocytic and granulocytic MDSC, respectively (figure 9B and 9C).

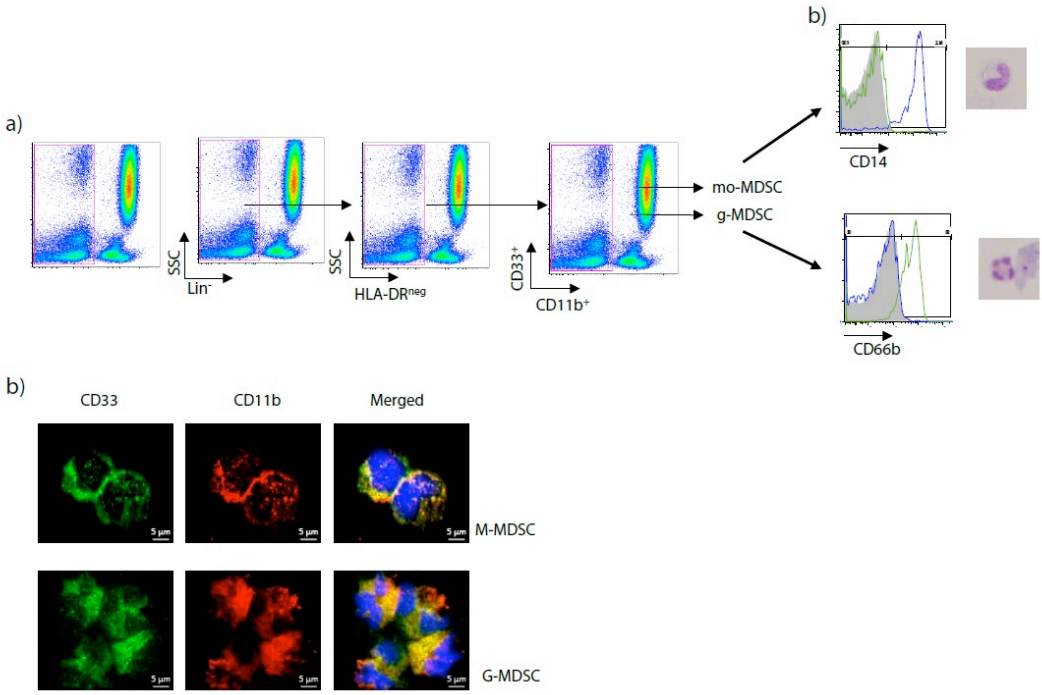

Figure 9. Characterization of human MDSC in the peripheral blood: (A) Flow cytometry analysis is represented by dot-plot graphs of peripheral blood after red blood cells lysis. (B) M-MDSC are represented in the histogram plots in green and G-MDSC in blue. Isotype is represented in gray. Cytospin staining show monocytic and granulocytic nuclei morphology of M-MDSC and G-MSDC. (C) CD33 (green) CD11b (red) DAPI (blue) immunofluorescence of sorted M-MDSC and G-MDSC. Scale bar is 5μm.

4.1.3 MDSC is increased in the peripheral blood of IPF and non-IPF patients

MDSC abundance showed significantly increased in IPF (30.99±15.61%, p=0.0075) and non-IPF ILD patients (31.63±15.61%, p<0.05), when compared with controls (18.96±8.17%). MDSC abundance in COPD did not significantly change when compared with control (25.63±13.94%, p=NS) (figure 10A).

Next, we quantified the predominant MDSC phenotype in IPF. M-MDSC were significantly increased and G-MDSC were significantly decreased in IPF when compared with control (figure 10B-C).

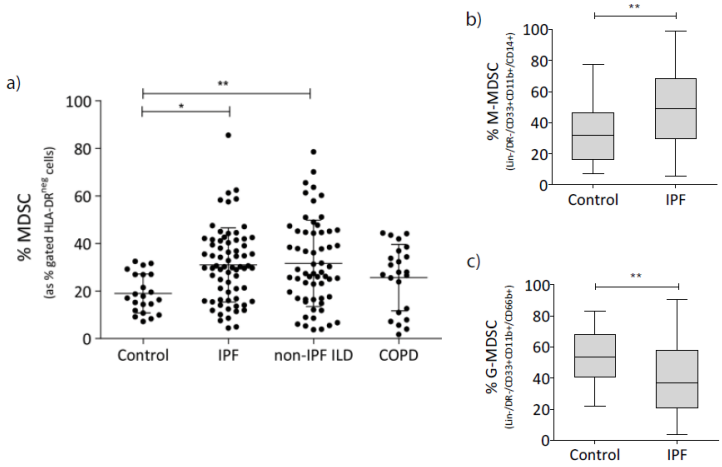

Figure 10. MDSC is increased in the whole blood of ILD: (A) Scatter dot plots show the % of MDSC (gated in HLA-DR negative cells). Control n=22, IPF n=69, non-IPF

ILD n=56, COPD n= 23. (B) % of M-MDSC (gated in CD33+ CD11b+ cells). Control n=22, IPF n=69. (C) % of G-MDSC (gated in CD33+ CD11b+ cells). Control n=22, IPF n=69. Statistical analysis was performed using one-way analysis of variance (ANOVA) followed by non-parametric Kruskal-Wallis test and Dunnnett's multiple comparison test. For two groups, non-parametric two-tailed Mann-Whitney *U* test. * represents p<0.05 and **p<0.01 when compared with control.

4.1.4 MDSC abundance correlates with pulmonary function test in IPF

To explore whether the abundance of MDSC had clinical relevance, we correlated the number of MDSC with pulmonary function test (i.e. VCmax). We found that when abundance of MDSC was higher the lung function was worse. Abundance of MDSC and VCmax significantly correlated in all patients (IPF, non-IPF ILD and COPD) pooled together (*p*= 0.0027, r= -0.24) (figure 11A) and IPF alone (*p* <0.0001, r=-0.48) (figure 11B). However, number of MDSC and VCmax did not show significant correlation in non-IPF ILD (*p*= 0.5, r= -0.07) (figure 11 C) and COPD (*p*= 0.5, r= -0.14) (figure 11D).

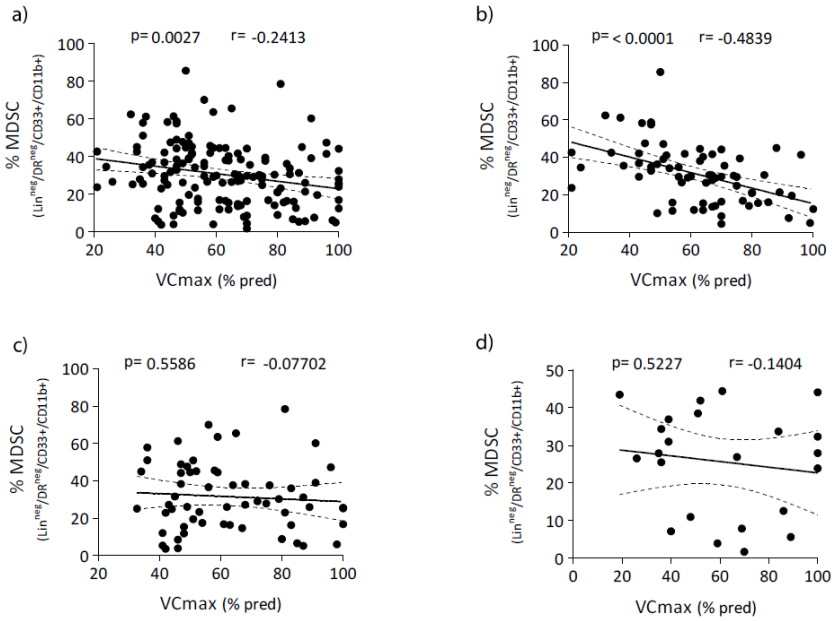

Figure 11. Increased number of MDSC correlates with VCmax decline in IPF: (A) MDSC number negatively correlated with VCmax (% predited) in all diseases (IPF,

non-IPF ILD and COPD). (B) MDSC and VCmax correlation in IPF. (C) MDSC and VCmax correlation in non-IPF ILD. (D) MDSC and VCmax correlation in COPD. Correlation and statistical analysis were determined by Pearson correlation and Student's t distribution.

Moreover, follow-up patients allowed us to study MDSC and VCmax correlation over time. For that, we calculated delta (Δ) MDSC and Δ VCmax and then substrate the difference of values between visits (V) (Δ=V2-V1). Longitudinal analysis showed that MDSC number was reflected on the lung function in IPF only (p=0.0389, r=-0.5773) (figure 12a). When we pooled together all the other diseases we did not observe a correlation MDSC-VCmax (figure 12b).

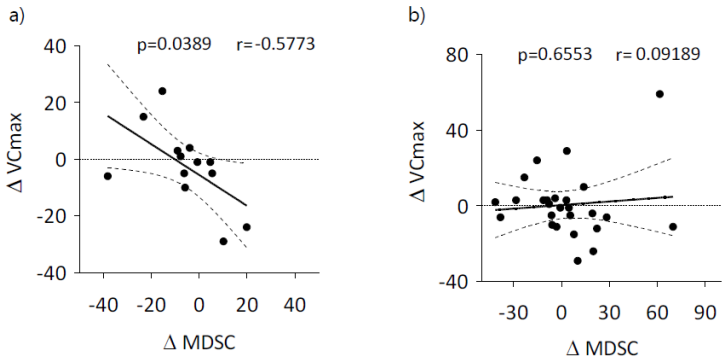

Figure 12. Longitudinal analysis show that the increased number of MDSC correlates with VCmax decline in IPF disease course: (A) ΔMDSC and ΔVCmax correlation in IPF (n=14). (B) ΔMDSC and ΔVCmax correlation in all diseases (IPF n=14, non-IPF ILD 11, COPD n=2). Correlation and statistical analysis were determined by Pearson correlation and Student's t distribution.

4.1.5 MDSC suppress lymphocytes proliferation

To investigate the suppressive function of MDSC in lymphocytes, we performed a co-culture system with autologous MDSC and lymphocytes. $CD4^+$ and $CD8^+$ cells when cultured together with MDSC decreased their proliferation capacity of 70.61±18.73%

and 83.69±7.68%, respectively. The suppressive effect of MDSC was observed in all patients together (IPF and non-IPF), as well as in IPF alone (figure 13).

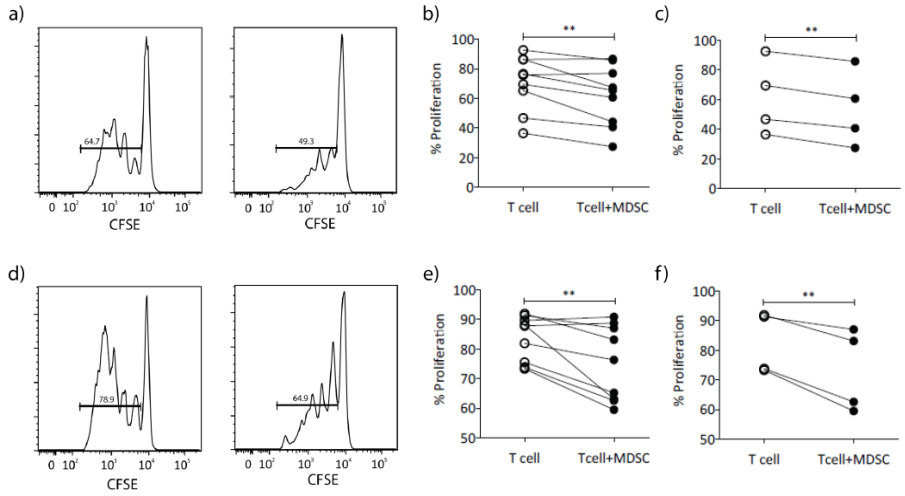

Figure 13. MDSC suppress the proliferation of lymphocytes: (A) Histogram shows CFSE incorporation in PBMC. Each peak represents one proliferation cell-cycle of $CD4^+$ cells for all patients (IPF n=4 and non-IPF ILD n=5) and only IPF, respectively. (B) Quantification $CD4^+$ cells proliferation of all patients. (C) Quantification $CD4^+$ cells proliferation of IPF patients. (D) Proliferation analysis of $CD8^+$ cells in all patients and only in IPF, respectively. (E) Quantification $CD8^+$ cells proliferation of all patients. (F) Quantification $CD8^+$ cells proliferation of IPF patients. Statistical analysis was performed using paired t-test. * represents $p<0.05$ and ** $p<0.01$

4.1.6 IPF patients with high number of MDSC show immunosuppressive phenotype

To determine the immunosuppressive interaction between MDSC and lymphocytes, we profiled the lymphocytes in all patients used in the characterized MDSC abundance. Lymphocytes gating strategy is represented below (figure 14). T helper cells and T cytotoxic cells (effector and non-effector) did not show any significant change when compared with control (figure 15). We found a significant decrease of $CD3^+$ $CD4^+$ $CD8^+$ (so-called abnormal T cells) in non-IPF ILD when compared with control (1.36±1.3% vs 3.14±2.8%, p= 0.0079) (figure 15G). Moreover, $CD4^+$ $CD25^+$

cells (suggestive of Treg cells) were increased in IPF and non-IPF ILD when compared with control (52.96±21% *p*= 0.0002, 55.78±19.8% *p*= 0.0002, 32.8±17.7%, respectively) (figure 16A). So we went deeper into the analysis of Treg cells and found that $CD4^+$ $CD25^+$ $FoxP3^+$ cells significantly correlated with MDSC (p= 0.0484, r=0.3326) (figure 16B). Moreover, patients with MDSC number higher than 40% presented increased mRNA levels of co-stimulatory T cell signals represented by CD28, ICOS, ITK and LCK gene expression (figure 16C).

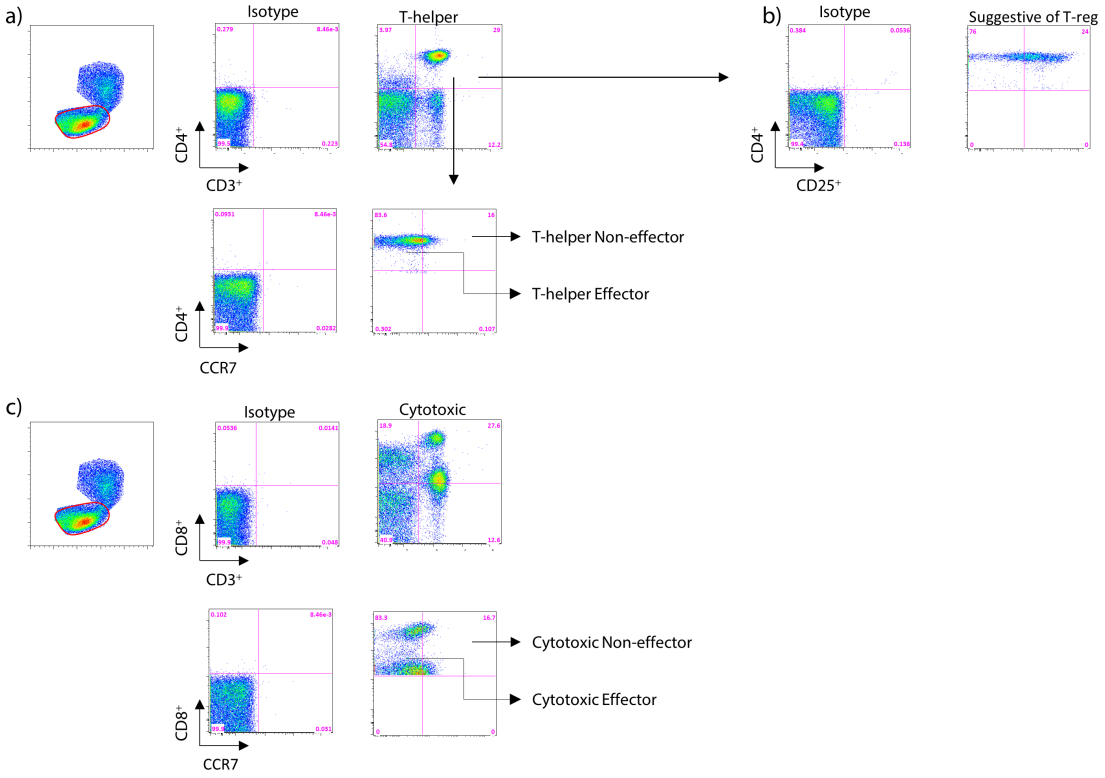

Figure 14. Lymphocytes immunophetyping by flow cytometry: (A) PBMC were stained with lymphocytes mix and depicted according to the surface markers. Flow cytometry dot-plot shows lymphocytes gated for T helper, T helper effector and T helper non-effector cells. (B) Suggestive Treg cells ($CD3^+$ $CD4^+$ $CD25^+$). (C) T cytotoxic, T cytotoxic effector and non-effector cells. In all analysis isotype was used to differentiate negative/positive cells.

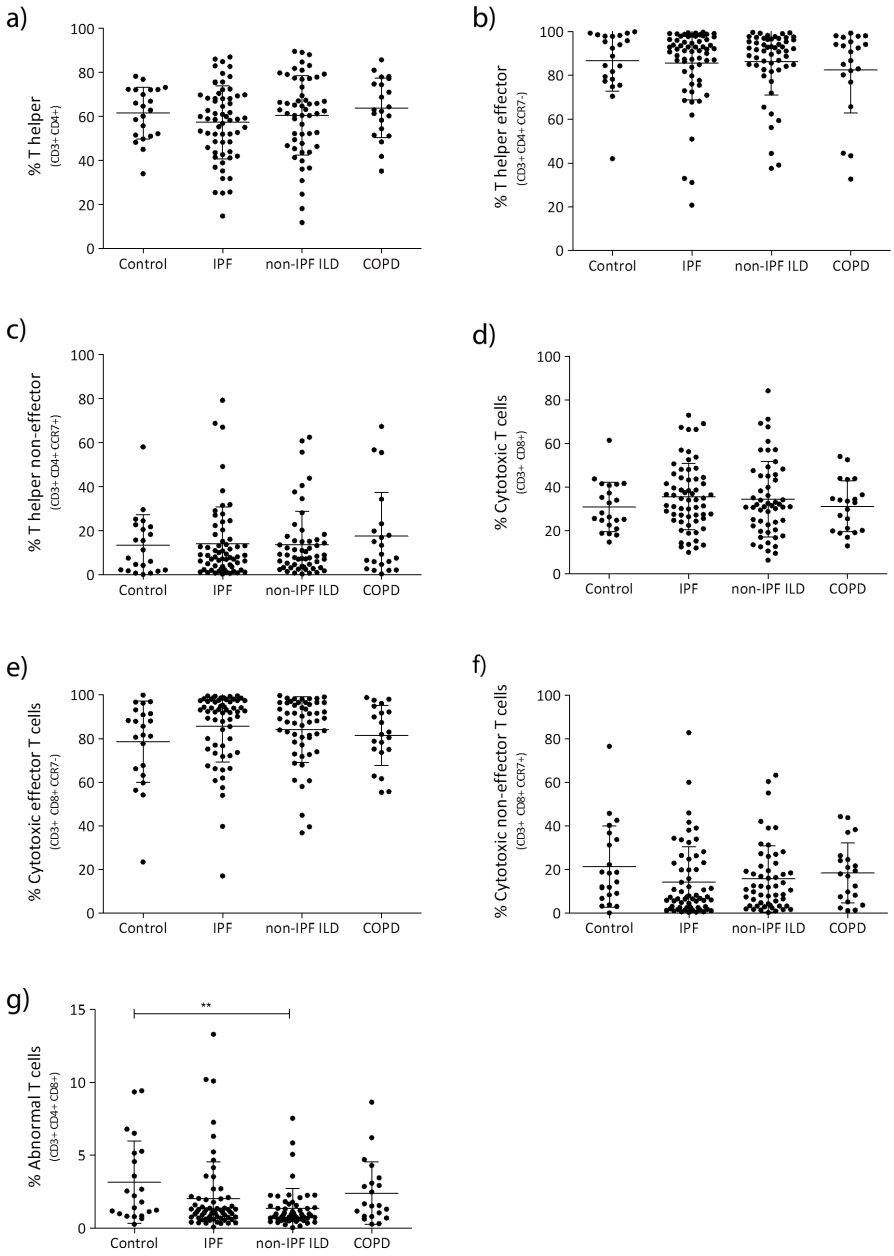

Figure 15. Quantification of lymphocytes immunophetyping: (A) Scatter dot-plot shows the % of T helper cells gated in lymphocytes. (B) T helper effector cells ($CD3^+$ $CD4^+$ $CCR7^-$). (C) T helper non-effector cells ($CD3^+$ $CD4^+CCR7^+$). (D) Cytotoxic T cells ($CD3^+$ $CD8^+$). (E) Cytotoxic effector T cells ($CD3^+$ $CD8^+$ $CCR7^-$). (F) Cytotoxic non-effector T cells ($CD3^+$ $CD8^+$ $CCR7^+$). (G) Abnormal T cells ($CD3^+$ $CD4^+$ $CD8^+$). Control n=22, IPF n=69, non-IPF ILD n=56, COPD n= 23. Statistical analyses were performed by ANOVA one-followed by non-parametric Kruskal-Wallis test and Dunnnett's multiple comparison test. **$p<0.01$ when compared with control.

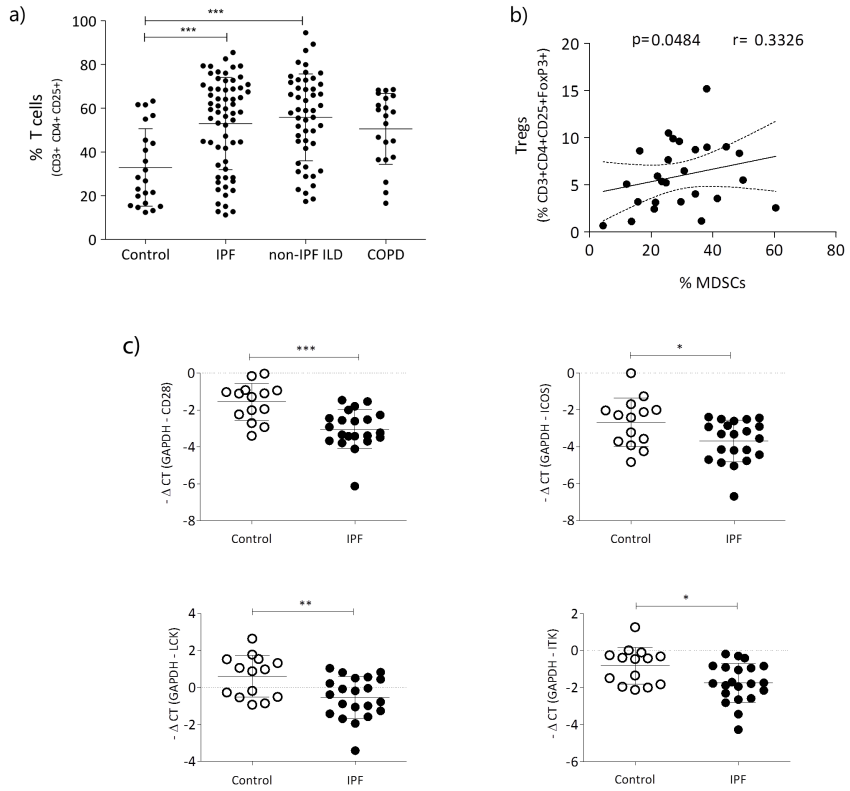

Figure 16. Immune-signatures are dysregulated in IPF patients with high number of MDSC: (A) Scatter dot-plot shows the % of T cells in Control n=22, IPF n=69, non-IPF ILD n=56, COPD n= 23. Statistical analyses were performed by ANOVA one-followed by non-parametric Kruskal-Wallis test and Dunnnett's multiple comparison test. (B) MDSC-Treg cells correlation in IPF. Correlation and statistical analysis were determined by Pearson correlation and Student's t distribution. (C) qPCR quantification of CD28, ICOS, LCK and ITK. Control n=14, IPF n=21. Statistical analysis was performed using paired t-test. * represents $p<0.05$, ** $p<0.01$ and *** $p<0.001$ when compared with control.

4.1.7 MDSC phenotype is neighboring fibrotic regions in IPF lung

To investigate whether MDSC were localized in IPF lung tissue, we used explanted lungs to perform sequential immunofluorescence staining. We found that $CD33^+$ $CD11b^+$ cells, suggestive of MDSC, were present in the fibrotic lungs. Moreover, lung

MDSC were present in the parenchyma around fibrotic areas positive for α-SMA and collagen I (figure 17).

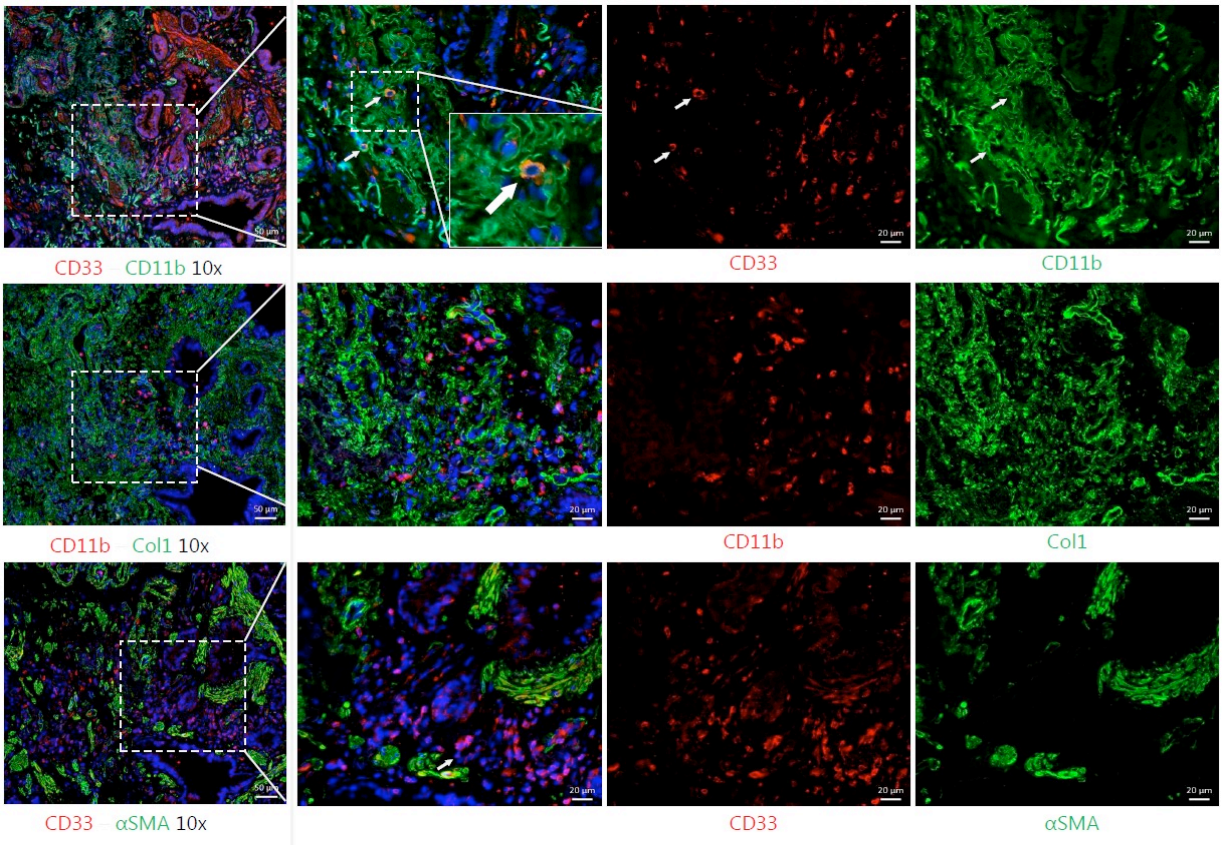

Figure 17. Lung-MDSC cells are present in the fibrotic areas in IPF: (A) Immunofluorescence staining of fibrotic lungs (IPF n=2, HP n=1) shows CD33 (red) and CD11b (green) DAPI (blue). Double positive cells are indicated with squares and arrows. (B) CD11b (red) collagen I (green). White squares are the areas in a higher magnification (C) CD33 (red) α-SMA (green). Scale bar= 50μm and 20μm.

4.2 Monocytes

The monocytes work presented in this thesis has been submitted for future publication as **Greiffo F.R,** et al.

4.2.1 Patients demographics

The cohort of the subjects in the immunophenotyping characterization of monocytes subsets includes patients diagnosed with NSIP, HP and CTD-ILD. Subjects without diagnose of chronic diseases and inflammation were included as controls (Table 4).

Characteristics	Control	NSIP	HP	CTD-ILD
	22	36	28	19
Age (years)	55.32±7.27	59.78±11.33	61.44±8.33*	65.61±11.09**
Gender				
Female	9 (40.9%)	15 (41.6%)	11 (39.3%)	18 (94.7%)
Male	13 (59.1%)	16 (58.4%)	17 (60.7%)	1 (5.3%)
Smoking Status				
Current	-	1 (2.8%)	-	-
Former	7 (31.8%)	17 (47.2%)	9 (32.2%)	10 (52.6%)
Never	15 (68.2%)	18 (50%)	19 (67.8%)	9(47.4%)
Biopsy	-	63.8% (23/ 13)	32.2% (9/ 19)	5.3% (1/ 18)
Lung comorbidities	-	2.8% (1/ 36)	7.1% (2/ 28)	26.3% (5/ 19)
PAH		-	2	5
CPFE		1	-	-
Treatment	-	83.4% (30/ 6)	89.3% (25/ 3)	68.4% (13/ 6)
Immunosuppressor		3	-	2
Glucocorticoid		12	16	3
Immunosuppressor + glucocorticoid		15	9	8
DLCO (%predicted)	-	34.26±14.22	30.17±17.26	51.06±26.8†
FVC (%predicted)	-	56.91±18.17	55.56±19.52	72.06±18.09††

Table 4. Subjects demographics: data are presented as % and number of affected patients (yes/no). Non-specific interstitial pneumonia (NSIP); hypersensitivity pneumonitis (HP); connective-tissue diseases (CTD); pulmonary artery hypertension (PAH), PAH was determined by echocardiography detecting an increase in mean pulmonary artery pressure >25 mmHg; combined pulmonary fibrosis and emphysema (CPFE). Immunosuppressor therapy includes azathioprine, methotrexate, mycophenolic acid, and rituximab. Lung function data are presented as Mean±SD, diffusing capacity of the lung for carbon monoxide (DLCO); forced volume capacity of the lung (FVC). * represents $p<0.05$ when compared with control ** represents $p<0.01$ when compared with control † represents $p<0.05$ when compared with NSIP and HP and †† represents $p<0.01$ when compared with NSIP and HP.

4.2.2 Circulating non-classical monocytes are decreased in ILD

Monocytes were measured and quantified in PBMCs isolated from fresh peripheral blood (Figure 18A). Classical monocytes, defined as HLA-DR^{+}CD14^{+++}CD16^{-}, were significantly increased in NSIP and HP subjects compared with controls (89.5±6.8% *vs* 85.78±4.59%, p<0.05 and 90.91±4.89% *vs* 85.78±4.59%, p<0.01 respectively) (Figure 18B). Intermediate monocytes (HLA-DR^{+}CD14^{+}CD16^{+}) abundance did not show differences in NSIP, HP and CTD-ILD subjects when compared with control (Figure 18C). Non-classical monocytes, defined as HLA-DR^{+}CD14^{+}CD16^{++}, were significantly decreased in NSIP, HP, and CTD-ILD subjects compared with controls (6.55±5.21% *vs* 10.34±3.41%, p<0.01, 5.71±4.41% *vs* 10.34±3.41%, p<0.001 and 6.62±4.42% *vs* 10.34±3.41%, p<0.05, respectively) (Figure 18D).

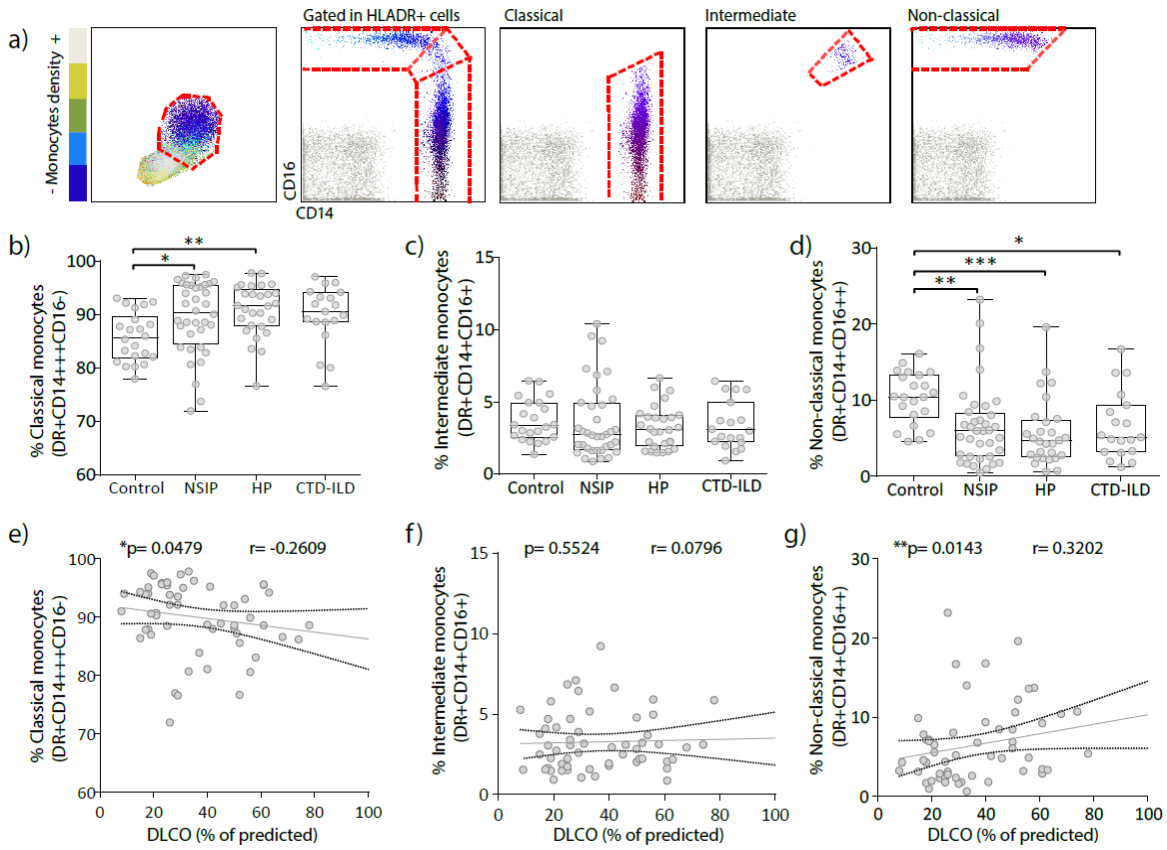

Figure 18. Circulating monocytes show decreased composition of non-classical monocytes and correlate with DLCO in ILD: (A) PBMC were stained with mAbs, and

each monocyte subset was previously defined by HLA-DR^{+} cells and gated according to CD14 and CD16 expression, CD14^{+++}CD16^{-} as classical monocytes, CD14^{+}CD16^{+} as intermediate monocytes, and CD14^{+}CD16^{++} as non-classical monocytes. Isotype was used as a negative control and is represented by gray dots. (B) Flow cytometry analysis shows from total monocytes the percentage of classical monocytes. (C) Intermediate monocytes. (D) Non-classical monocytes. Control (n=22), NSIP (n=36), HP (n= 28), CTD-ILD (n=19). Statistical analysis was performed using one-way analysis of variance with non-parametric Kruskal-Wallis test, followed by Dunn's multiple comparison test. * represents $p<0.05$, and ** represents $p<0.01$, compared with control. (E) Percentage of classical monocytes correlated with DLCO (% predicted) in ILD (n=58). (F) percentage of intermediate monocytes correlated with DLCO (% predicted). (G) Percentage of non-classical monocytes correlated with DLCO (% predicted). For statistical analysis, p values were calculated by Student's t distribution and Pearson correlation. * represents $p<0.05$ and ** $p<0.01$.

Further, we correlated the percentages of circulating monocytes with the forced vital capacity (FVC) and diffusing lung capacity for carbon monoxide (DLCO). The abundance of classical, intermediate, and non-classical monocytes was not significantly correlated with the FVC (% of predicted) (Figure 19D-F). However, classical monocytes and non-classical monocytes abundances were significantly correlated with the DLCO (% of predicted) ($r=-0.2609$, $p<0.05$, and $r=0.3202$, $p=0.01$, respectively) (Figure 19A-B).

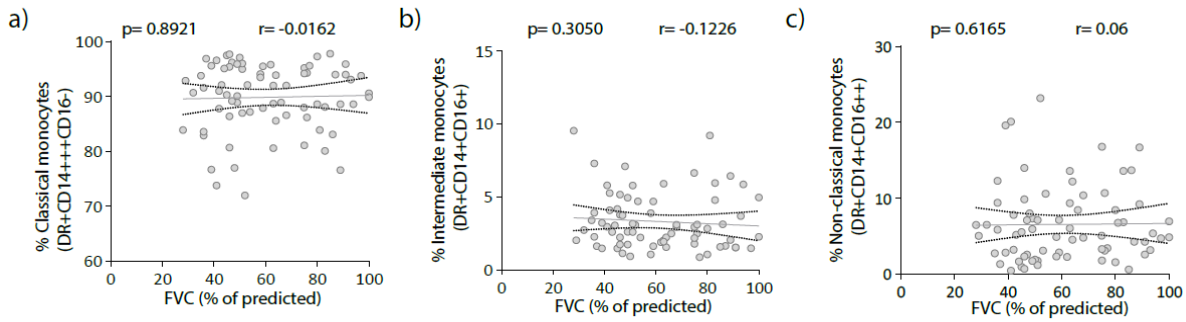

Figure 19. Circulating non-classical monocytes do not correlate with FVC: (A) Percentage of classical monocytes correlated with FVC (% predicted) in ILD (n=66). (B) Percentage of intermediate monocytes correlated with FVC (% predicted). (C) Percentage of classical monocytes correlated with FVC (% predicted). For statistical analysis, p values were calculated by Student's t distribution and Pearson correlation.

Next, NSIP, HP and CTD-ILD subjects were grouped as ILD and divided according to treatment: 1) Naïve/untreated, 2) Immunosuppressor (Imm), 3) Glucocorticoid (GC) and 4) Immunosuppressor with glucocorticoid (Imm+GC) (Table 4). Classical monocytes were significantly increased in patients treated with GC and Imm+GC ILD compared with control (93.02±4.35% *vs* 85.78±4.59%, p<0.01, and 90.3±4.67% *vs* 85.78±4.59% p<0.05, respectively), as well in GC-treated patients when compared with treatment-naive (93.02±4.35% *vs* 87.56±6.4%) (Figure 20A). Intermediate monocytes did not show difference in naïve and treated ILD subjects when compared with control (Figure 20B). Non-classical monocytes were significantly decreased in GC, and Imm+GC treated patients when compared with control (3.6±2.86% *vs* 10.34±3.41%, and 5.64±3.38% *vs* 10.34±3.41%, p<0.001, respectively) (Figure 20C), as well in GC-treated patients when compared with treatment-naïve (3.6±2.86%, *vs* 8.81±4.94%, respectively, p<0.01) (Figure 20C).

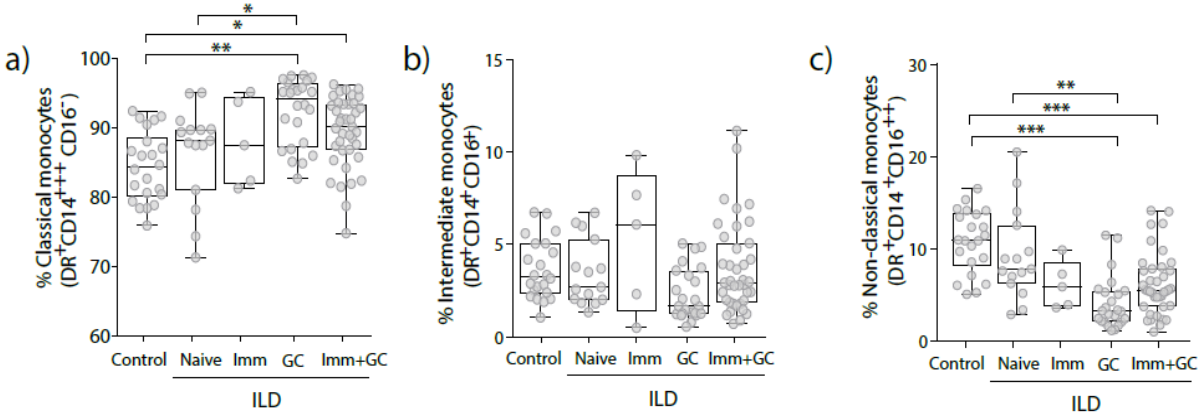

Figure 20. Circulating monocytes composition in ILD is associated with treatment: PBMCs were stained with mAbs, and each monocyte subset was previously defined by HLA-DR+ cells and gated according to CD14 and CD16 expression,

$CD14^{+++}CD16^{-}$ as classical monocytes, $CD14^{+}CD16^{+}$ as intermediate monocytes, and $CD14^{+}CD16^{++}$ as non-classical monocytes. Flow cytometry analysis show from total monocytes the percentage of (A) classical monocytes; (B) intermediate monocytes; (C) non-classical monocytes. Control (n=22), ILD naïve (n=15), ILD immunosuppressor (Imm) (n=5), ILD glucocorticoid (GC) (n=31), ILD immunosuppressor with glucocorticoid (Imm+GC) (n=32). Statistical analysis was performed using one-way analysis of variance with non-parametric Kruskal-Wallis test, followed by Dunn's multiple comparison test. * represents $p<0.05$, ** represents $p<0.01$ and *** represents $p<0.001$, compared with control or ILD naïve.

4.2.3 Canonical kinetic and scavenger receptors expression is altered in non-classical monocytes in ILD

To fully characterize the immunophenotype of the monocyte populations in ILD, we explored the chemokine-receptor expression profile, which distinguishes different monocyte subsets (CCR2 in classical monocytes, CX3CR1 in non-classical monocytes, and CD163 scavenger receptor in myeloid lineages) (Figure 21A). We observed that CCR2 mean fluorescence intensity (MFI) in classical monocytes was significantly decreased in ILD subjects when compared with controls (35296±13922 *vs* 45104±10034, $p<0.001$) (Figures 21B). CX3CR1 was decreased in ILD subjects in classical and non-classical monocytes when compared with control (3571±1774 *vs* 4783±1732, $p<0.01$ and 8724±3183 *vs* 10785±2394, $p<0.01$, respectively) (Figures 21C and 3F). In contrast, the scavenger receptor CD163 expression was increased in non-classical monocytes in ILD subjects compared with control (612.2±588.4 *vs* 323.5±64.5, $p<0.05$) (Figures 21D and 21G).

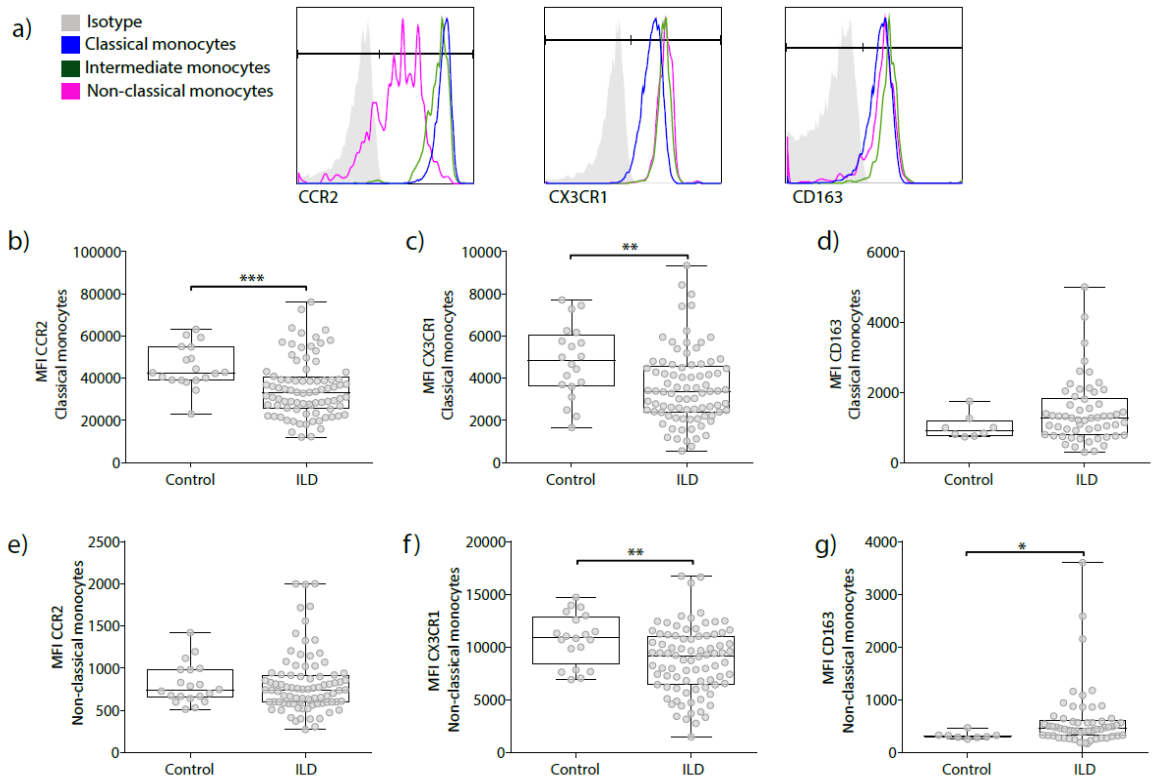

Figure 21. Non-classical monocytes show decreased CX3CR1 and increased CD163 expression in ILD. Box and whiskers with dot plot diagrams of flow cytometry analysis show the (A) mean fluorescence intensity (MFI) of CCR2, CX3CR1 and CD163. (B) $CCR2^{+}$ classical monocytes; (C) $CX3CR1^{+}$ classical monocytes; (D) $CD163^{+}$ classical monocytes; (E) $CCR2^{+}$ non-classical monocytes; (F) $CX3CR1^{+}$ non-classical monocytes; (G) $CD163^{+}$ non-classical monocytes. For A,B, E, F: control (n=20), ILD (n=83). For D and G control (n= 8), ILD (n= 57). Statistical analysis was performed using non-parametric two-tailed Mann-Whitney t test. ** represents $p<0.01$ and * represents $p<0.05$ compared with control.

4.2.4 Fractalkine (CX3CL1) drives non-classical monocyte migration and accumulation in the lung parenchyma of ILD patients

In order to understand the mechanisms involved in the kinetic changes of non-classical monocytes in ILD, we quantified levels of CCL2 and fractalkine (CX3CL1) in plasma and lung homogenates of control and ILD lung tissue. We found increased CCL2 levels in ILD plasma when compared with controls (301.4±212.5 pg/mL *vs*

128.7±88.21 pg/mL, p<0.001) (Figure 22A). Moreover, CCL2 levels in the lung tissue homogenate of ILD and controls did not show a significant difference (Figure 22A). In ILD, CCL2 levels were significantly increased in plasma when compared to lung tissue (301.4±212.5 pg/mL *vs* 185.8±134.3 pg/mL, p<0.05) (Figure 22A). Further, plasma and tissue concentrations of fractalkine (CX3CL1) in ILD patients were significantly increased when compared with controls (0.8166±0.4632 ng/mL *vs* 0.5163±0.2377 ng/mL, p<0.01, and 2.049±0.7354 ng/mL *vs* 1.062±0.4795 ng/mL, p<0.001, respectively) (Figure 22B). Controls and ILD subjects showed higher levels of CX3CL1 in the lung tissue than in the plasma (1.062±0.4795 ng/mL *vs* 0.5163±0.2377 ng/mL, p<0.01, and 2.049±0.7354 ng/mL *vs* 0.8166±0.4632 ng/mL, p<0.001) (Figure 22B).

Next, to understand the chemoattractant potential of fractalkine (CX3CL1), and receptor responsiveness, we performed functional assays in the presence and absence of the ligand. In co-culture with endothelial cells, CX3CL1 did not show influence on non-classical monocyte adhesion (figure 22C). In contrast non-classical monocyte migration was significantly increased in the presence of fractalkine (CX3CL1) in ILD subjects (1.38±0.57 fold change *vs* 1±0, p<0.01) (figure 22D). Moreover, monoclonal fractalkine (CX3CL1) antibody decreased non-classical monocytes migration when compared with CX3CL1-induced migration and control conditions in ILD subjects (0.80±0.85 fold change *vs* 1.38±0.57 fold change and 0.80±0.85 fold change *vs* 1±0, respectively, p<0.05) (Figure 22D).

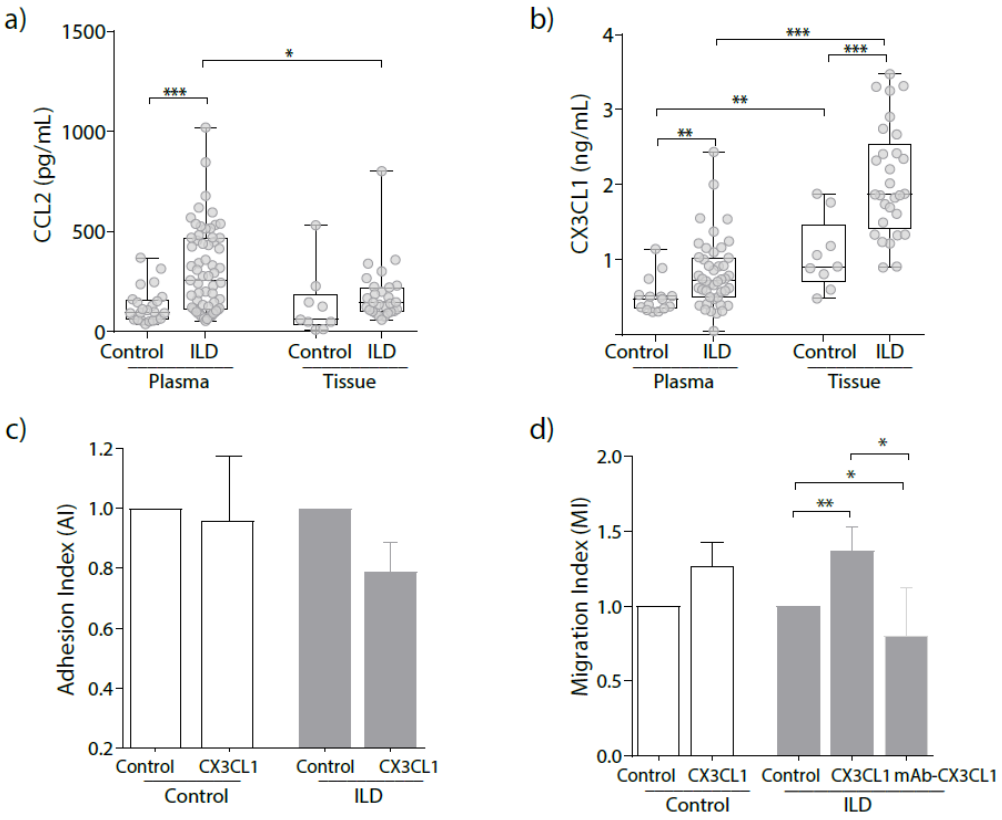

Figure 22. Fractalkine is increased in the lung and drives the migration of pro-fibrotic non-classical monocytes in ILD: Enzyme-linked immune assay (ELISA) for CCL2 and fractalkine were performed in lung tissue homogenate. (A) CCL2 (pg/mL) in plasma (control n=23, and ILD n=63), and lung tissue (control n=9, and ILD n=28); (B) CX3CL1 (ng/mL) in plasma (control n=15, and ILD n=44), and lung tissue (control n=9, and ILD n=29). (C) *In vitro* adhesion assay of $CD16^{+}$ monocytes on the activated endothelial cells (TNF-α, 4 hours), control wells were used as an indicator of conversion efficiency. Control (n=5) ILD (n=5). (D) *In vitro* migration assay of non-classical monocytes, control wells were used as an indicator of conversion efficiency. Control (n=13), ILD (n=14). For functional assays, 3-5 experimental replicates were use in each experiment. Statistical analysis was performed using non-parametric two-tailed Mann-Whitney t test. * represents $p<0.05$ compared with control ** represents $p<0.01$ compared with control *** represents $p<0.001$ compared with control.

Finally, to investigate the accumulation of monocytes in the tissue, we performed immunofluorescence staining of lung tissue sections from control and ILD subjects. ILD sections showed double positive CD14 and CD16 cells, exclusive monocyte markers, outside the vessels (Figure 23A). Quantification of $CD14^{+}CD16^{+}$ myeloid cells localized in the lung parenchyma of explanted ILD subjects was significantly increased when compared to controls (0.6744±0.2224% *vs* 0.3803±0.1001%, $p<0.05$) (Figure 23A). Moreover, immunofluorescence staining showed $CD14^{+}CD16^{+}$ cells expressing $CX3CR1^{+}$ and $CD163^{+}$ markers in ILD tissue (Figure 23B-C). Next, we observed $CX3CR1^{+}CD163^{+}$ abundantly in ILD lung tissue (Figure 23D).Lastly, $CX3CR1^{+}$ cells were also positive for CD68 in ILD (figure 23E).

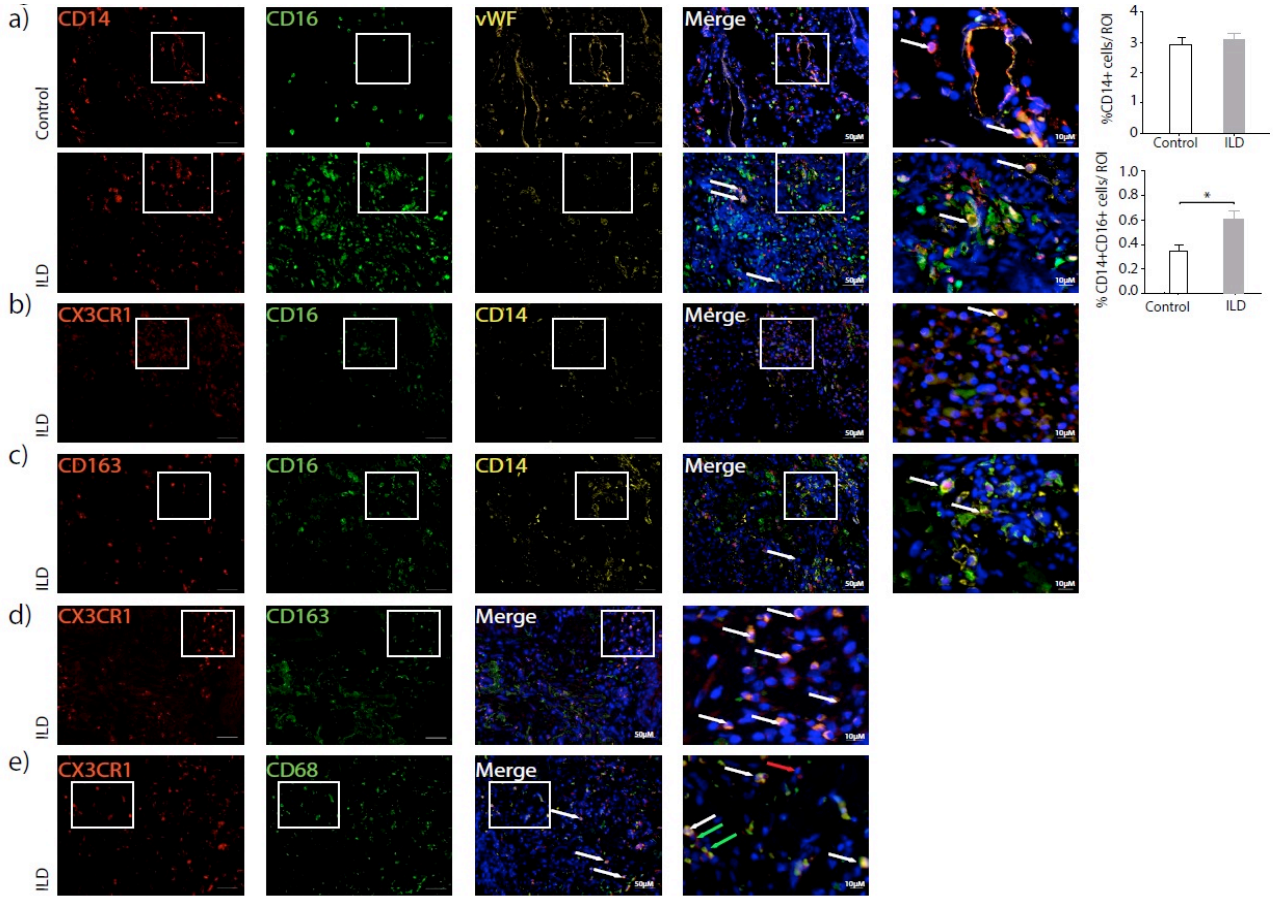

Figure 23. Non-classical monocytes are increased in the lung parenchyma in ILD: (A) Immunofluorescence triple staining was performed using explanted lungs from control, and ILD. Explanted lungs were stained for CD14 (red), CD16 (green), and Von Willebrand factor (vWF) (yellow). Double positive cells are indicated with squares and arrows; Graphs bars show the quantification of $CD14^{+}$ and $CD14^{+}CD16^{+}$

myeloid cells in the lung parenchyma of control and ILD as % of total cells. Control (n= 3), ILD (n=6). (B) CD14 (yellow), CD16 (green), CX3CR1 (red). Triple positive cell is indicated with squares and arrows. (C) CD14 (yellow), CD16 (green), CD163 (red). Triple positive cells are indicated with squares and arrows. (D) CX3CR1 (red), and CD163 (green). (E) CX3CR1 (red), and CD68 (green); CX3CR1 positive cells are indicated with red arrows and CD68 with green arrows. Double positive cells are indicated with squares and arrows. Cell nuclei are stained by DAPI (blue). All the pictures were taken using magnification of 20x (scale bar= 50μm), white squares represent higher magnification (scale bar= 10μm). Control (n=3), ILD (n=3). Statistical analysis was performed using non- parametric two-tailed Mann-Whitney t test. * represents $p<0.05$ compared with control.

4.2.5 Fractalkine (CX3CL1) is expressed by the lung epithelium and lung non-classical monocytes express phagocytic phenotype in ILD

In order to know the lung cell type which is contributing to increased fractalkine (CX3CL1) in ILD, we performed immunofluorescence staining that showed CX3CL1 expression on acetylated tubulin positive cells and on bronchial epithelial regions (Figure 24A). To explore phenotypic and functional features of NCM, we looked myeloid mature markers, as CD206, and for receptors involved in the apoptotic cell clearance and phagocytosis, such as AXL and MERKT. In ILD, immunofluorescence analysis revealed the expression of AXL in $CD14^{+}CD16^{+}$ cells (Figure 24B), and flow cytometry analysis demonstrated that $CD14^{+}CD16^{++}$ myeloid cells express higher levels of MERKT, and mannose receptor (CD206) than $CD14^{+}$ cells (Figure 24C).

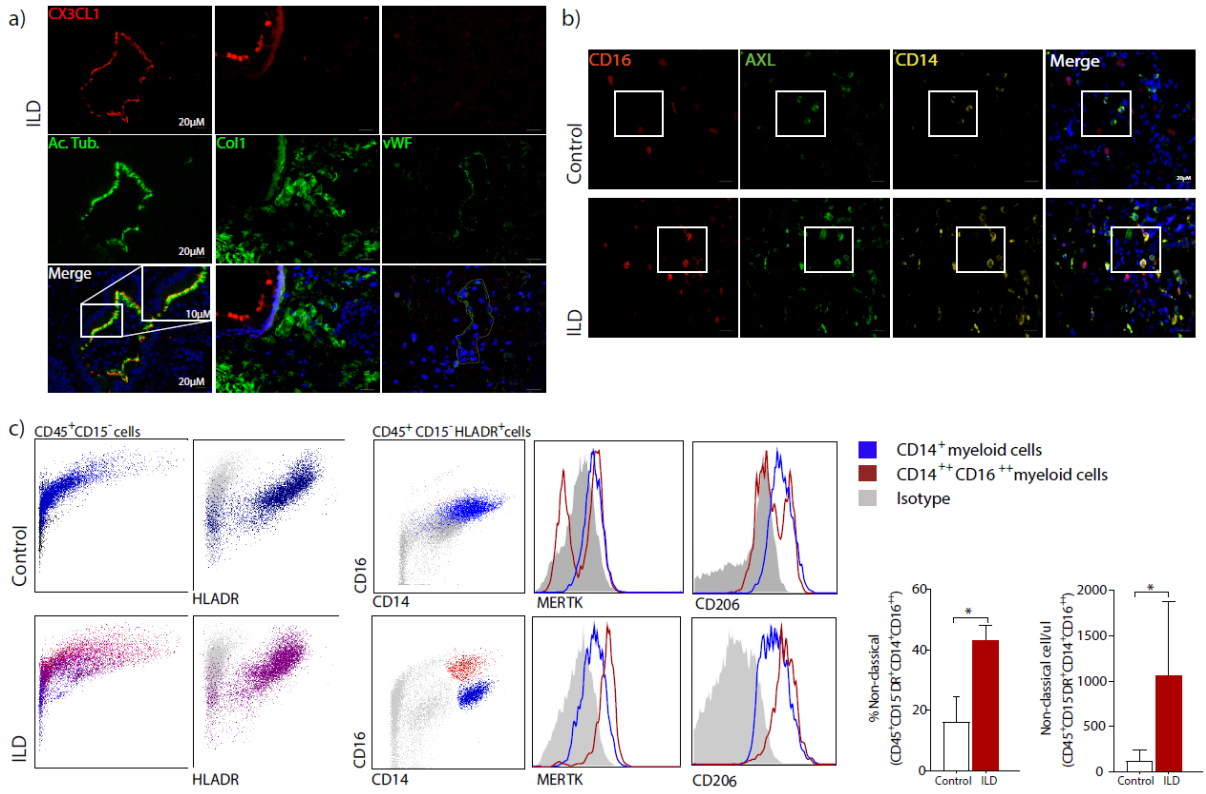

Figure 24. Fractalkine is iexpressed on lung epithelium and non-classical monocytes expressed phagocytic phenotype in ILD lungs: (A) Immunofluorescence staining was performed using explanted lungs and stained for CX3CL1 (red) and acetylated tubulin, or collagen type I, or Von Willebrand factor (green). (B) Triple immunofluorescence staining for CD14 (yellow), CD16 (red), and AXL (green). Pictures were taken using magnification of 40x (scale bar= 20μm), white squares represent higher magnification (scale bar= 10μm). Cell nuclei are stained by DAPI (blue). Control (n=3), non-IPF ILD (n=3). (C) Flow cytometry analysis and quantification (percentage and absolute numbers) of $CD45^+$ lung cells suspension. Monocytes were gated in $CD15^-$ $HLADR^+$ cells. Control (n=4), ILD (n=8).

5. Discussion

This thesis focuses on the functional characterization of circulatory MDSC and monocytes trafficking to the lung in ILD. In IPF, the number of MDSC is increased in the peripheral blood. The higher the number of MDSC, the more limited the lung function of the patient is. In ILD, pro-fibrotic non-classical monocytes (NCM) are decreased in the peripheral blood and increased into the fibrotic lungs. NCM-derived cells in the ILD lungs co-stained with CX3CR1, M2-like and phagocytic markers.

Myeloid cells contribution to lung remodeling, as well as repair and regeneration in ILD has gained important attention in the last years. Recently, a mouse study using GFP-membrane localized myeloid lineage as fibroblast-like cells in the skin wound which suggests a mesenchymal phenotype of myeloid progenitor (Sinha et al., 2018). In cell culture system, increased number of myeloid cells showed to contribute to organoid formation and suggested to revert lung injury in lung regeneration in a mouse model (Lechner et al., 2017). Here, MDSC and monocytes, both derived from myeloid progenitor cell niche, were quantified by flow cytometry. In MDSC quantification, cell abundance correlated with disease severity and suggested to be a potential biomarker for IPF (Fernandez et al., 2016). Classical monocytes were found to be increase in the peripheral blood of ILD patients while non-classical monocytes were decreased. Our studies show that myeloid cells abundance is an important predictor of disease status and predictor of tissue injury. Cell abundance is an important and the first one result to be questionable in cell recruitment the site of injury (Yona et al., 2013). Importantly, the results here presented showed imbalance between compartments and recruitment of cells in response to the injury. Recently, scRNA-seq identified in lung fibrosis mouse model a transitional population of monocyte-derived CX3CR1^{+} cells that were localized in the fibrotic niche and contributed to fibroblast accumulation (Aran et al., 2019). Further, the abundance of MDSC, a cell type which is recruited in case of injury, are also related to the recruitment of tumor-associated macrophages (Ugel, De Sanctis, Mandruzzato, & Bronte, 2015).

Lately, it has been assumed that the crosstalk between mesenchymal and myeloid cells is an important regulator of tissue injury (Reyfman et al., 2018), as well repair (Lechner et al., 2017). Indeed, the activation and proliferation of stromal cells showed to be correlated with immunosuppressive factor, alteration on the cell surface and production of growth factors (Nowarski, Jackson, & Flavell, 2017). Here, MDSC and monocytes showed to contribute to ILD and increase lung injury mechanisms. Importantly, MDSC and monocytes were phenotypically described and classified according to cell surface expression characterizing cell subsets. The characterization of cell subsets is important to functional assessment (Yoon et al., 2014). This is illustrated with the results from Jason Rock's laboratory, as well as the results presented here. In these, 1) tissue regeneration driven by CCR2+ myeloid cells (Lechner et al., 2017) and 2) our data which tissue injury is suggested to be driven by an imbalance in the CX3CR1- fractalkine axis increased the infiltration of pro-fibrotic non-classical monocytes. Therefore, we emphasize that the phenotype analysis of immune-stromal interaction cells is crucial. Next, for a better and clearer discussion, the following text is divided in MDSC and monocytes sub-sections.

5.1 MDSC

The MDSC discussion presented in this thesis has been partly published by Fernandez I.E, **Greiffo F.R**, et al. PMID: 27587556, ERJ, 2016 (Appendix 1). Here, we showed the accumulation of MDSC in the peripheral blood and lung tissue in non-IPF ILD patients. Moreover, the higher number of MDSC worse the lung function showed to be in cross-sectional as well longitudinal analysis. Next, increased circulatory $CD4^+CD25^+$ T regulatory cells were detected in IPF. Additionally, MDSC and Tregs ($CD4^+CD25^+$ $FoxP3^+$) showed a positive correlation. Further, IPF patients with high number of MDSC showed decreased RNA levels of CD28, ICOS, ITK, and LCK in PBMC. Finally, culturing autologous MDSC and lymphocytes revealed the functional assessment of MDSC decreasing $CD4^+$ and $CD8^+$ cells proliferation. Taking together, we showed a new immunosuppressive role in the circulating blood which reflects disease status in IPF.

5.1.1 Immunosuppressive phenotype and function of MDSC

It is known that the innate and adaptive immune cells can enhance the secretion of pro-fibrotic factors contributing to fibrogenesis (Wynn, 2011). Immunosuppressive therapy in IPF (e.g. prednisone and azathioprine) has been not recommended due to its harmful effects. Furthermore, immunosuppressive therapy showed to increase mortality in IPF patients (Raghu, Anstrom, King, Lasky, & Martinez, 2012). Our data shows that there is a MDSC-immunosuppressive network in the peripheral blood and in the lungs of IPF patients. Therefore, in our opinion the immunosuppressive therapies used to treat IPF patients in the past will perpetuate the limited immune defense and so the lung injury.

Furthermore, T cells dysregulation play an important role in IPF (Lo Re, Lison, & Huaux, 2013). Importantly, lymphoid tissue formation has been reported to be involved in fibrotic niches of IPF lungs increasing the migration of activated T and B cells (Marchal-Somme et al., 2006). Moreover, circulating $CD25^{+}$ $FoxP3^{+}$, suggestive of T reg, and $CD4^{+}$ cells express CD28, a marker which related to worse prognosis in IPF (Gilani et al., 2010). Also, IPF patients showed to have low abundance of Treg cells in the BAL (Kotsianidis et al., 2009). In our data we identified decrease $CD4^{+}CD25^{+}FoxP3^{+}$ cells in IPF which correlated with the abundance of MDSC. . In summary, the less MDSC number, less T reg cells were circulating in the peripheral blood of IPF patients. Additionally, autologous cell culture of MDSC and lymphocytes showed that the proliferation of CD4 and CD8 positive lymphocytes was decreased. Here, our data confirmed the immunosuppression role driven by lymphocytes in IPF. Strikingly, we reported for the first time that MDSC play a role in the immunosuppression response in IPF blood and tissue.

5.1.2 MDSC biomarker

In cancer, measurement of MDSC has been considered a biomarker clinical outcome. Moreover, MDSC measurement can help to identify mechanisms involved

in disease progression, therapy response and survival in cancer (Walter et al., 2012) (Wang et al., 2014). Also, MDSC abundance has been shown to correlate with cancer stage (Vasquez-Dunddel et al., 2013). In past years, IPF has been compared with cancer diseases. It seems that IPF and cancer share many of pathogenic pathways, such as Tregs, PDGF, TGF-ß, and now MDSC. Therefore, we think that MDSC are a potential biomarker for IPD which reflects disease status, data presented here. In our opinion, MDSC quantification and mechanisms can reflect disease prognosis. For the future, MDSC quantification should be done in different cohorts. Finally, longitudinal studies will clarify MDSC applicability in medical treatment and survival.

5.1.3 MDSC in the lung tissue

MDSC in the lung tissue have been described in non-small cell lung cancer. Within the lung, high abundance of MDSC interplays with tumor development and disease development (Srivastava et al., 2008) (Feng et al., 2012) (Zhang et al., 2009). Moreover, in other lung diseases (i.e. cystic fibrosis, tuberculosis, pulmonary hypertension and COPD) MDSC number is increased and showed to be associated with pathophysiology (Rieber et al., 2013) (du Plessis et al., 2013) (Yeager et al., 2012). In COPD, recent work demonstrated an effector T-cell dysfunction composed by T regs, MDSC and PD-1 exhausted effector T cells (Kalathil et al., 2014). In our data, the number of MDSC in COPD patients did not show a significant increase. In fact, our COPD cohort was younger than Kalathil et al.'s cohort. Also, Kalathil et al.'s cohort presented worse lung function data than our cohort. In this line, Verschoor et al. showed that MDSC abundance is affected by age (Verschoor et al., 2013). We are aware of the differences between our IPF and control cohorts. The control group has an average of 55.4 years old which is younger than the IPF group with an average of 68.2 years old. In our opinion, the difference of 12.8 years (IPF and controls) is much less than Verschoor et al.'s study which the health young adults presented an average of 32 years old (20 years younger than the average age of controls used here).

Next, the abundance of MDSC inversely correlated with pulmonary function test, VCmax. IPF patients showed a better correlation of MDSC and VCmax than non-IPF and COPD patients. This could be due to differences in pathophysiology. As referenced in the introduction, IPF has the worse prognosis and faster progression than other ILD, as well applicable to COPD. Moreover, we showed $CD33^{+}CD11b^{+}$ cells neighboring fibrotic areas in the lung tissue. This data suggests a migratory capacity of MDSC to the site of injury, as well supports the negative correlation between circulating MDSC and worse VCmax. Recently, we measured MDSC by flow cytometry in the lung cell suspensions of ILD and control lungs (figure 25). Strikingly, our new data fully supports MDSC phenotype analysis and quantification in lung tissue.

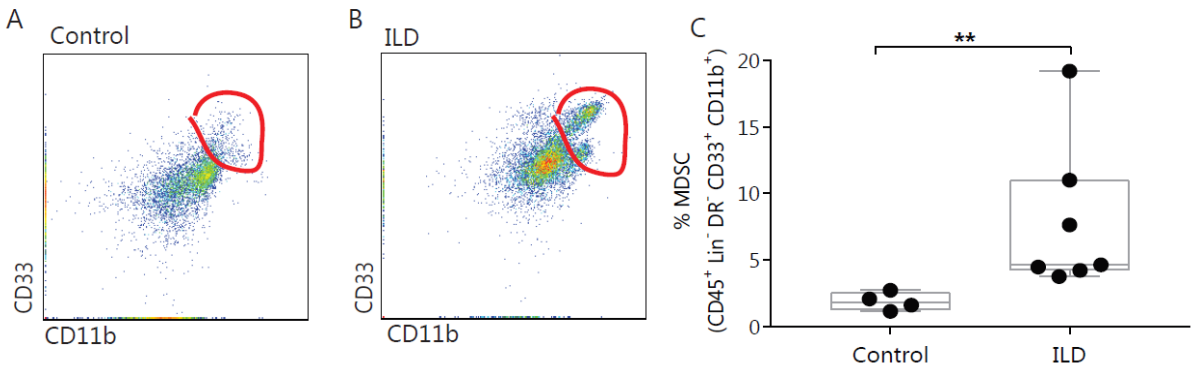

Figure 25. MDSC characterization and quantification by flow cytometry in control and ILD lungs: (A) FACS plot of lung cell suspension in control. Beads isolated CD45+ cells stained and gated in Linage negative (Lin^{-}): CD56, CD20, CD19, CD16, CD3; HLA-DR negative, CD33 and CD11b double positive. (B) ILD (HP) lung cells. (C) Quantification of MDSC in control (n=4) and ILD (IPF n= 3, NSIP n=2, HP n=3). Statistical analysis was performed using non-parametric two-tailed Mann-Whitney t test. ** represents $p<0.01$ compared with control (unpublished data).

5.1.4 MDSC profiling

Cell profiling is value tool to investigate fibrosis. For instance, transcriptome data in the blood of IPF versus control identified 1428 genes expressed in mild IPF and 2790 genes expressed in severe IPF (Yang et al., 2012). Moreover, four genes expressed in PBMCs have been described as important IPF outcome predictor. CD28, ICOS, ITK, and LCK are IPF predictors. Interestedly, the downregulation of these four genes showed to be a better outcome than only clinical data (Herazo-Maya et al., 2013). Here, we showed that IPF patients with high number of circulating MDSC presented downregulation of decreased RNA levels of CD28, ICOS, ITK, and LCK in PBMCs. Therefore, our data supports the downregulation of these genes in IPF versus control, as well the role of MDSC as an important player in IPF.

Moreover, the characterization and interplay of MDSC and other immune cells is crucial for therapeutic target. MDSC is known to suppress the function of immune cells inducting pro-fibrotic factors (i.e. Tregs, TGF-ß) (Marvel & Gabrilovich, 2015). Further, it has been described that MDSC can differentiate into other cell types, such as tumor-associated macrophages and dendritic cells, at the site of injury (cancer) (Corzo et al., 2010; Franklin et al., 2014) (Zhong et al., 2014). Both, macrophages and dendritic cells can be derived from monocytes. Also, our data show monocytic MDSC is more predominant than granulocytic MDSC in IPF. Therefore, we sought to characterize the differences between circulatory MDSC and monocytes. Autologous MDSC and monocytes from IPF patients (n=10) were sorted out by flow cytometry and magnetic beads, respectively. Label-free quantitative mass spectrometry revealed 7000 proteins in total. Comparing the MDSC and monocytes sets of proteins, 502 proteins were enriched in MDSC and 1224 in monocyte. Cell-cell communication showed a combination of 200 ligands and 153 receptors between MDSC and monocytes. Autocrine signaling edges: 1) monocyte to monocyte showed a combination 339 proteins; and 2) MDSC to MDSC showed a combination 290 proteins. Monocyte to MDSC showed a combination 311 proteins and MDSC to monocytes, 316 proteins (figure 26).

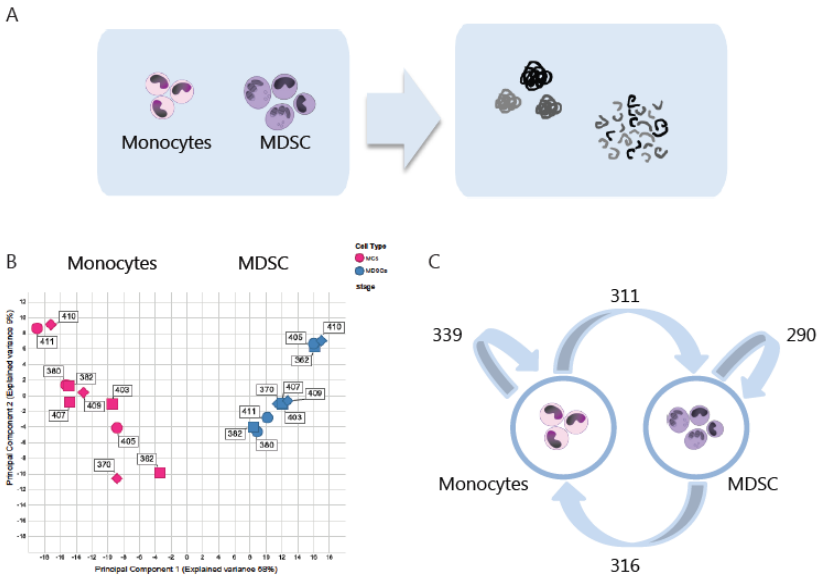

Figure 26. MDSC and monocytes proteomics data. (A) Autologous monocytes and MDSC protein isolation. (B) Vulcan plot analysis of exclusive proteins expressed by monocytes or MDSC. (C) Autocrine and paracrine signals in monocytes and MDSC. Principal component analysis (PCA) was done by Prof. Alistair Forrest and his group (Harry Perkins Institute of Medical Research, Murdoch, Australia) (unpublished data).

5.2 Monocytes

The monocytes discussion presented here is part of the publication "CX3CR1-fractalkine axis drives kinetic changes of monocytes in fibrotic interstitial lung diseases" for future publication. We used a multi-compartment (blood and lung) approach to show that CX3CR1-fractalkine axis plays functional implications on pro-fibrotic non-classical monocytes (NCM) recruitment in ILD (Figure 27). In ILD, peripheral blood NCM were decreased and positively correlated with worse DLCO which resembled a severe disease phenotype. Mechanistic studies indicated that monocytes-derived cells in the lung tissue were recruited from the circulation to the lungs through CX3CR1-fractalkine interaction. Our findings suggest decreased abundance of NCM CX3CR1^{+} in the peripheral blood due to a fractalkine imbalance between lung and blood compartments mediating the increased CD14^{+}CD16^{++} myeloid cells population expressing CX3CR1 and M2-like markers in ILD lungs.

These analyses support a new perspective of myeloid cells phenotype and recruitment in ILD.

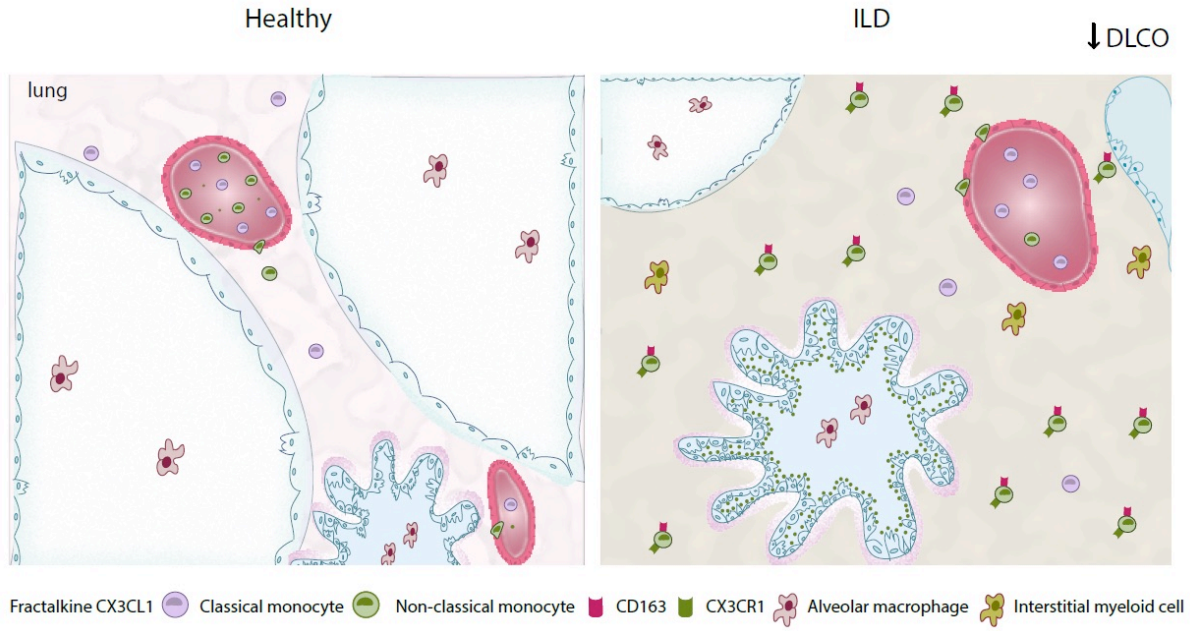

Figure 27. CX3CR1-fractalkine axis enhances pro-fibrotic non-classical monocyte migration into ILD lungs: **r**epresentative scheme shows an overview of monocyte subsets role and function in healthy (left) and ILD (right) lungs. Non-classical monocytes are decreased in the blood of ILD patients. Diffusing lung capacity of carbon monoxide (DLCO) is decreased in ILD. Fractalkine (CX3CL1) levels are higher in the lungs than in the blood of ILD patients, and expressed by epithelial cells. Non-classical monocyte migration is increased in the presence of fractalkine in ILD. Non-classical monocytes-derived cells express CX3CR1, CD163, CD206, AXL and MERKT in ILD lungs.

5.2.1 Monocytes subsets and abundance in the peripheral blood

Monocyte subset frequencies are well defined in human as approximately 85% classical (CM), 5% intermediate (IM) and 10% non-classical (NCM). However, under pathological conditions the frequencies of monocyte subsets vary and respond differently as a consequence of the stimuli (Boyette et al., 2017). Frequencies of circulating classical and non-classical monocytes have been reported to increase in cases of high inflammation, such as severe infection, rheumatoid arthritis,

atherosclerosis, Crohn's disease, and hematological malignancy (Soehnlein et al., 2008; J. Yang, Zhang, Yu, Yang, & Wang, 2014; Ziegler-Heitbrock, 2015). High inflammatory diseases switch the percentage of monocytes due increases in TNF-α, rheumatoid factors, IL-6, IL-1ß, and granulocytes (Soehnlein et al., 2008; J. Yang et al., 2014). Our results show that CM were significantly increased whereas NCM were significantly decreased, in the peripheral blood in ILD when compared with control. When we correlated these results with DLCO, we observed that higher number of CM, as well as, lower numbers of NCM significantly correlated with worse DLCO. Recently, a longitudinal study reported increased abundance of monocytes in the peripheral blood of early stage-ILD patients significantly associated with lung abnormalities and lower FVC (Podolanczuk et.al, 2018). However, FVC did not show a significant correlation with monocytes subsets, PFT (DLCO and FVC) indicated that our cohort included patients with severe lung function parameters suggestive of late inflammation phase and extensive fibrotic status of ILD. This might explain the differences on our data and inflammatory diseases that showed increased frequencies of circulating CM and NCM (Ziegler-Heitbrock, 2015) (J. Yang et al., 2014).

In the past, non-classical monocytes in mice were shown to be associated with the initial inflammatory response by releasing tumor necrosis factor alpha (TNF-α) developing inflammatory arthritis (Misharin et al., 2014). We think that these results might be due to a vascular injury, which is known to happen in pulmonary fibrosis, and a possible NCM infiltration into the lung injury. On the other hand, we think that the correlation between NCM and DLCO parameters suggests being a result of NCM accumulation on the pulmonary vessels decreasing the DLCO.

Another important point to discuss is the effect of glucocorticoid treatment on monocytes subsets. Our cohort included treated ILD and a few number of naive patients (untreated). Thus, to address to point in depth, we performed experiments in which we isolated monocytes from controls and treated them with different doses of methylprednisolone, as previously reported (Frankenberger, Haussinger, & Ziegler-Heitbrock, 2005). Then, we found that CM and NCM treated with methylprednisolone for 24 hours did not show changes in cell number. However, we found increased

number of intermediate monocytes (IM) treated with 10^{-9} M of methylprednisolone (figure 28). Not long ago, it has been described that the abundance of intermediate monocytes is associated to systemic glucocorticoid treatment in uveitis patients (Liu et al., 2015). Here, we did not find increased numbers of circulating IM in ILD. Taking together, our results show that steroid therapy does not affect mature circulating monocytes populations in ILD. However, in our case, it might influence monocyte activation and migration, as previously showed in healthy volunteers (Ehrchen et al., 2007). Moreover, in the study of Varga et al. dexamethasone treatment in cultured monocytes decreased the expression CX3CR1 and CD163 (Varga et al., 2008). We think that these findings support our data which show decreased CX3CR1 expression in NCM in treated ILD patients. On contrary, we show increased CD163 expression in NCM. In our opinion, the fact that only NCM showed increased expression of CD163 in treated ILD patients is suggestive of potential pro-fibrotic and M2 like macrophage phenotype.

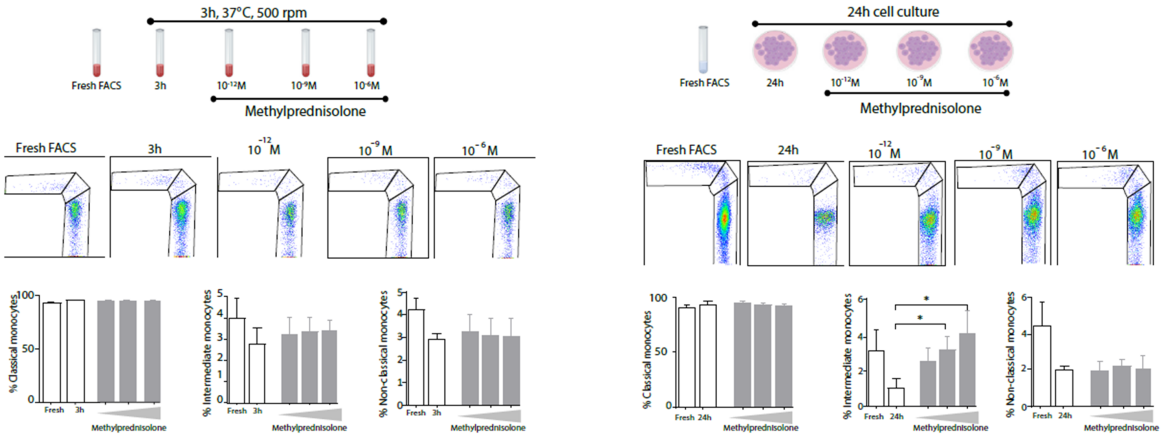

Figure 28. Glucocorticoid effect on monocytes (whole blood and isolated monocytes): different concentrations of methylprednisolone were added or not in cell culture medium of freshly isolated monocytes. Flow cytometry was performed to quantify percentages of classical, intermediate and non-classical monocytes. For methylprednisolone experiments (n=3). Statistical analysis was performed using non-parametric two-tailed Mann-Whitney t test. * represents $p<0.05$ compared with

control ** represents p<0.01 compared with control *** represents p<0.001 compared with 24h without methylprednisolone.

5.2.2 Non-classical monocytes infiltration into fibrotic lungs

Next, we sought to determine if circulating NCM are decreased in the peripheral blood of ILD due to an active adhesion to the endothelium or migration to the injured organ contributing to pulmonary fibrosis. In this line, CCR2 and CX3CR1 are known to be chemokine receptors which are important in monocyte phenotyping, as well in subset function (Ziegler-Heitbrock, 2007). In our data, we observed that ILD patients with a low frequency of non-classical monocytes also showed decreased expression of chemokine receptors in the peripheral blood. Here, global MFI levels of CCR2 were decreased in classical monocytes and CX3CR1 were decreased in CM and NCM. Importantly, when chemokine receptors are engaged in chemotaxis, they can be transiently removed from the cell surface by ligand-receptor internalization or clathrin-mediated endocytosis (Springer, 1994). Thus, we think that an active receptor-ligand interaction might explain the decrease of CCR2, and CX3CR1 in non-IPF ILD patients.

We know that chemokine receptors are highly responsive to their ligands (Landsman et al., 2009; Osafo-Addo & Herzog, 2017). For instance, CCR2 responds to multiple ligands, including CCL2 (Nomiyama, Osada, & Yoshie, 2013). On contrary, CX3CR1 responds exclusively to its ligand fractalkine (CX3CL1) (Nomiyama et al., 2013). The major role of the CX3CR1-fractalkine axis is to mediate chemotaxis, adhesion, and transmigration of leukocytes (Ge et al., 2016). In our data, we observed increased CCL2 and fractalkine levels in the plasma in ILD versus control. However, in the lungs, only fractalkine was increased in ILD versus control. When we analyzed the differences of CCL2 and fractalkine levels between compartments, lung and plasma: 1) CCL2 plasma levels were higher than in the lungs in ILD patients; 2) fractalkine levels in the lung were higher than in the plasma in ILD patients. In our opinion, this might suggest active monocyte recruitment from the bone marrow by CCL2 and supporting our data by the increase in classical monocytes in the circulation and

could explain the decreased levels of CCR2 by receptor internalization, as previously described (Cardona et al., 2008). Also, our data show an imbalance of fractalkine levels between the blood and lung compartments, which we think might be related to an increased infiltration of $CD14^{+}CD16^{+}$ myeloid cells into fibrotic lungs. Following-up in the function of fractalkine, we performed migration and adhesion assays in the presence of CX3CL1. First, NCM adhesion capacity in the presence of CX3CL1 did not show changes. However, we observed that in ILD patients only, CX3CL1 increased NCM migration.

CX3CR1-fractalkine axis is a key-mediator of monocyte adhesion and migration (Lee, Lee, Song, Lee, & Chang, 2018). In fibrosis, for instance in the skin, CX3CR1 axis regulated tissue fibrosis by TGF-β and CTGF production and enhancing collagen deposition (Arai et al., 2013). In our data, we showed that the source of fractalkine in pulmonary fibrosis is the bronchium epithelium. Certainly, the crosstalk between myeloid and epithelial cells is an important regulator of lung-immunity, whereas monocytes and M2-like macrophages modulate ATII survival and proliferation (Lechner et al., 2017). In this line, we also detected an increased expression of the CD163 scavenger receptor exclusively in NCM in ILD. CD163 is a scavenger receptor, and marker of macrophage alternative activation (Pilling, Fan, Huang, Kaul, & Gomer, 2009). CD163 is a marker related to cell debris and apoptotic body removal. Furthermore, CD163 showed to be highly expressed in cultured fibrocytes (Canton, Neculai, & Grinstein, 2013), $CD14^{+}$ circulating cells in scleroderma-ILD patients, and in the tissue of several types of ILD (S. K. Mathai et al., 2010; Prasse et al., 2006). Also, the scavenger receptor CD163 expression is considered an innate immune sensor due to the TNF-α production under infection (Fabriek et al., 2009). Therefore, the higher expression of CD163 in our cohort together with $CX3CR1^{+}CD68^{+}$ myeloid cells in the lung parenchyma of ILD patients, might suggest a M2-like macrophage signature of NCM. In summary, these results highlight an important link between $CD16^{+}$ monocytes, CX3CR1, CD163 expression, and monocyte-derived macrophages in the lung tissue. Additionally, macrophages expressing CX3CR1 may support a potential role of NCM progenitor cells of macrophages in the lung.

5.2.3 Non-classical monocytes phenotype in the fibrotic lungs

In fact, depicting myeloid cell function for therapeutic or regenerative medicine applications requires a comprehensive understanding of what drives the localization and fate of these cells (Misharin et al., 2017). In this line, genetic linage tracing experiments show that increases in alveolar macrophages during fibrosis is attributable to recruited monocytes-derived cells, carrying a fibrotic transcriptome profile (Misharin et al., 2017). A recent study using CX3CR1 knockout mice showed decrease mRNA and protein levels of TGF-ß in mouse model of pulmonary fibrosis on days 3, 7 and 14 (Ishida et al., 2017). More recently, scRNA-seq data showed that fibrotic lung-macrophages expressing CX3CR1 are localized on fibroblast-site increasing the secretion of PDGF (Aran et al., 2019). Although the approach we used here did not trace circulating NCM CX3CR1^{+} cells, it has been proved by genetic linage tracing experiments that increases in alveolar macrophages during fibrosis, is attributable to recruited monocytes-derived cells carrying a fibrotic transcriptome profile (Misharin et al., 2017).

In our data, we found expression of fractalkine by the bronchium epithelium which we think is a modulator of non-classical monocyte migration in ILD. On these thoughts, we know that loss of epithelial cell integrity as one of the hallmarks in lung fibrosis (Rock et al., 2011). We found that only in ILD, CD14^{+}CD16^{+} cells expressed AXL. Our results are consistent with previous findings which showed rare immune cells localized in the fibrotic lung parenchyma expressing AXL (Espindola et al., 2018). Recently, AXL which is part of the TAM (Gas6/TYRO3, AXL, MERKT) family, has been reported as an important player in epithelial cell injury and an important target to decrease lung fibrosis (Espindola et al., 2018; Fujino, Kubo, & Maciewicz, 2017). We observed CD14^{+}CD16^{++} myeloid cells increased in the ILD lungs. We found that only in ILD, CD14^{+}CD16^{+} cells expressed AXL. Here, we show that NCM in the fibrotic parenchyma of ILD patients in expressed AXL. Therefore, we think that the rare immune cells described by Espindola et al. (Espindola et al., 2018) are NCM which migrate to extravascular compartment though fractalkine which has been

cleavage in response to epithelial cell injury known to happened in pulmonary fibrosis. Linked to CD163 scavenger receptor, AXL and MERTK signaling contributes to the “eat-me signals” which recognizes phagocytosis process by receptor activation (Li, 2012). Furthermore, $CD14^{+}CD16^{++}$ myeloid cells in the ILD lung expressed MERTK and macrophage mannose receptor CD206.

6. Conclusions and future directions

Pulmonary fibrosis is a detrimental and complex disease. Ultimately, disease progression leads to alteration of the lung pathophysiology and death. The treatment is limited, for IPF the prescription of pirfenidone and nintedanib (both anti-fibrotic drugs) will slow-down disease progression. NSIP, HP and CTD-ILD are treated with glucocorticoid which may not be benefic to fibrosis. Therefore, there is an urgent need of a complete understanding and identification of cellular and molecular players in all types of ILD. With that, it would be possible to determine in-depth mechanisms of effective therapies.

In our first study presented here, MDSC has been suggested to be a novel and potential biomarker for IPF. Also, MDSC affected lymphocytes response. Therefore, the control of MDSC abundance and migration to the lungs via exclusive targets expressed by MDSC can reduce immune dysregulation in IPF. Moreover, network analysis of autocrine and paracrine signatures found in MDSC and monocytes lead to targets in which can be applicable in new treatment. Identification of specific proteins expressed by MDSC leads a potential research field.

Second, the monocytes study presented here showed that monocytes phenotypes may help the management of pulmonary fibrosis and provide novel therapeutic strategies to either restore monocyte function or modulate recruitment. In this study we identified a compartmental imbalance of fractalkine levels mediating the migration of NCM-CX3CR1 into human fibrotic lungs. Furthermore, NCM-derived cells expressed M2-like phenotype and phagocytosis markers in the ILD lungs. Therefore, targeting CX3CR1-fractalkine axis may aid the management of end-stage ILD and provide novel therapeutic strategies to either restore monocyte function or modulate recruitment. Interestingly, fractalkine cleavage has been reported to be associated with over-expression of disintegrin and metalloproteinase 10 (ADAM10) (Hundhausen et al., 2003). The fractalkine shedding via ADAM10 is currently under

investigation of our group and collaborators (ERS short term fellowship – October 2018).

7. Appendix

Publications, peer-reviewed and review articles, part of this thesis.

Peer-reviewed article

Peripheral blood myeloid-derived suppressor cells reflect disease status in idiopathic pulmonary fibrosis

Fernandez IE, Greiffo FR, Frankenberger M, Bandres J, Heinzelmann K, Neurohr C, Hatz R, Hartl D, Behr J, Eickelberg O. European Respiratory Journal, 48 (4). doi: 10.1183/13993003.018262015. (2016).

Peripheral blood myeloid-derived suppressor cells reflect disease status in idiopathic pulmonary fibrosis

Isis E. Fernandez[1], Flavia R. Greiffo[1], Marion Frankenberger[1], Julia Bandres[1], Katharina Heinzelmann[1], Claus Neurohr[2,3], Rudolf Hatz[2], Dominik Hartl[4,5], Jürgen Behr[2,3] and Oliver Eickelberg[1]

Affiliations: [1]Comprehensive Pneumology Center, Ludwig-Maximilians-University, University Hospital Grosshadern, and Helmholtz Zentrum München, Member of the German Center for Lung Research, Munich, Germany. [2]Asklepios Fachkliniken München-Gauting, Munich, Germany. [3]Comprehensive Pneumology Center, Medizinische Klinik und Poliklinik V, Klinikum der Ludwig-Maximilians-Universität, Member of the German Center of Lung Research (DZL), Munich, Germany. [4]Children's Hospital of the University of Tübingen, Pediatric Infectiology, Immunology and Cystic Fibrosis, Tübingen, Germany. [5]Roche Pharma Research and Early Development (pRED), Immunology, Inflammation and Infectious Diseases (I3) Discovery and Translational Area, Basel, Switzerland.

Correspondence: Oliver Eickelberg, Comprehensive Pneumology Center, Ludwig-Maximilians-University and Helmholtz Zentrum München, Max-Lebsche-Platz 31, 81377 Munich, Germany.
E-mail: oliver.eickelberg@helmholtz-muenchen.de

ABSTRACT Idiopathic pulmonary fibrosis (IPF) is a fibroproliferative disease with irreversible lung function loss and poor survival. Myeloid-derived suppressor cells (MDSC) are associated with poor prognosis in cancer, facilitating immune evasion. The abundance and function of MDSC in IPF is currently unknown.

Fluorescence-activated cell sorting was performed in 170 patients (IPF: n=69; non-IPF interstitial lung disease (ILD): n=56; chronic obstructive pulmonary disease (COPD): n=23; healthy controls: n=22) to quantify blood MDSC and lymphocyte subtypes. MDSC abundance was correlated with lung function, MDSC localisation was performed by immunofluorescence. Peripheral blood mononuclear cell (PBMC) mRNA levels were analysed by qRT-PCR.

We detected increased MDSC in IPF and non-IPF ILD compared with controls (30.99±15.61% *versus* 18.96±8.17%, $p \leqslant 0.01$). Circulating MDSC inversely correlated with maximum vital capacity ($r = -0.48$, $p \leqslant 0.0001$) in IPF, but not in COPD or non-IPF ILD. MDSC suppressed autologous T-cells. The mRNA levels of co-stimulatory T-cell signals were significantly downregulated in IPF PBMC. Importantly, $CD33^{+}CD11b^{+}$ cells, suggestive of MDSC, were detected in fibrotic niches of IPF lungs.

We identified increased MDSC in IPF and non-IPF ILD, suggesting that elevated MDSC may cause a blunted immune response. MDSC inversely correlate with lung function only in IPF, identifying them as potent biomarkers for disease progression. Controlling expansion and accumulation of MDSC, or blocking their T-cell suppression, represents a promising therapy in IPF.

@ERSpublications
Circulating myeloid-derived suppressor cells are increased in IPF and inversely correlate with lung function http://ow.ly/6rDm301BpvC

This article has supplementary material available from erj.ersjournals.com

Received: Nov 04 2015 | Accepted after revision: June 15 2016 | First published online: Sept 01 2016

Support statement: This work was supported by the Helmholtz Association and the German Center for Lung Research. Funding information for this article has been deposited with the Open Funder Registry.

Conflict of interest: Disclosures can be found alongside this article at erj.ersjournals.com

Introduction

Idiopathic pulmonary fibrosis (IPF) is a chronic and lethal fibroproliferative disease of the lung, with unknown aetiology. IPF is characterised by an irreversible loss of lung function with a median survival, or time to lung transplantation, of 2–3 years after diagnosis. The natural history of IPF is highly variable and unpredictable between patients [1]. In the past years, many advances have been accomplished with respect to better delineating dominant pathomechanisms and improved diagnosis, monitoring or treatment of IPF. These efforts have led to the approval of two new therapeutics, pirfenidone and nintedanib, which slow down lung function decline in IPF [2].

While the exact pathophysiology of IPF remains unknown, several key drivers of disease initiation and progression have been unravelled, including repetitive microinjuries to the bronchial and alveolar epithelium [3], aberrantly activated fibroblast phenotypes, and excessive extracellular matrix (ECM) accumulation [4]. While nonspecific immunosuppressive therapy remained without benefit in a number of clinical studies, recent findings of gene expression signatures and peripheral blood biomarker profiling have highlighted the possibility of immune system dysfunction in IPF pathogenesis (*e.g.* correlating gene expression levels with B- and T-cell activation [5–8]).

Importantly, innate and adaptive immunity contributes to fibrogenesis in a number of organs [9]. The recent literature has provided increasing evidence for a pro-inflammatory signature in peripheral blood and lung tissue of IPF patients, including aberrantly activated lymphocyte/monocyte populations [10]. In IPF, circulating leukocyte phenotypes, for instance $CD4^+$ T-cells, display reduced levels of CD28, suggesting persistent antigen-driven proliferation and possibly clonal exhaustion [6]. These data are supported by recent transcriptome analysis of peripheral blood mononuclear cells (PBMCs) in which the co-stimulatory T-cell signal (assessed by mRNA levels of CD28, ICOS, LCK and ITK) was downregulated and predicted poorer survival in IPF patients [7]. Semaphorin (Sema) 7a-positive T-regulatory (T-reg) cells are increased in rapidly progressive IPF patients [5], thus supporting the role of dysregulated T-cell responses in IPF.

Myeloid-derived suppressor cells (MDSCs) are a heterogeneous population of immature myeloid cells with potent suppressor capabilities, which are associated with poor prognosis in cancer [11]. MDSCs contribute to tumour-immune cell evasion by suppressing T-cell responses [12]. Currently, MDSCs are not classified by a standard leukocyte lineage marker, since MDSCs are comprised of various immature cells of myeloid origin, including myeloid-progenitor cells, immature monocytes or dendritic cells, or immature granulocytes. Two important subsets of human MDSCs have been reported: monocytic MDSC (mo-MDSC) with a $lineage^{neg}/HLA\text{-}DR^{neg}/CD33^+/CD11b^+/CD14^+$ phenotype, and granulocytic MDSC (g-MDSC) with a $lineage^{neg}/HLA\text{-}DR^{neg}/CD33^+/CD11b^+/CD14^-/CD15^+/CD66b^+$ phenotype [13]. The accumulation of MDSCs is a common finding in malignancies, including lung cancer, but also in many other pathological conditions, such as transplantation [14], infection [15] or autoimmunity [16]. In nonsmall cell lung cancer, patients with higher amounts of peripheral MDSCs had poorer survival or response to chemotherapy [17]. In chronic inflammatory processes of the lung, such as tuberculosis (TB) [18] or *Pseudomonas aeruginosa* infection secondary to cystic fibrosis [19], MDSCs induce T-cell suppression to avoid immune surveillance and undermine host defence. In COPD, a suppressive network comprised by T-reg cells, $PD\text{-}1^+$ T-cells and MDSCs counteract the inflammatory immune reaction and mitigate innate antibacterial and antiviral properties [20].

Importantly, the contribution of MDSCs in fibrotic lung disease, including IPF, has not been elucidated at all to date [21]. Therefore, in this study we performed, for the first time, an in-depth characterisation of MDSCs in the peripheral blood and lung tissue of IPF patients and correlated their levels with parameters of disease severity. Intriguingly, MDSCs inversely correlate with lung function and can be detected in lung tissue of IPF patients, highlighting their potential contribution to IPF pathogenesis.

Materials and methods

For in-depth details on the material and methods, refer to the supplementary material.

Patients and control group

We prospectively included 170 patients in the analysis, divided into 69 IPF, 56 non-IPF ILD (hypersensitivity pneumonitis: n=17, nonspecific interstitial pneumonia: n=27, connective tissue disease-ILD: n=12) and 23 COPD patients, as well as 22 healthy controls. Patients were recruited at the Comprehensive Pneumology Center (Munich, Germany) from June 2014 to July 2015 (table 1). 22 healthy volunteers (table 1) were free from signs of current infection, inflammation or respiratory symptoms at the time of blood sampling. Informed written consent was obtained for all participants, study methods were approved by the local ethical review board. Diagnosis of IPF was performed by multidisciplinary consensus, based on current American Thoracic Society/European Respiratory Society criteria [22].

DOI: 10.1183/13993003.01826-2015

TABLE 1 Patient demographics and clinical characteristics

Characteristics	Control	IPF	Non-IPF ILD	COPD
Subjects	22	69	56	23
Age years	55.4±6.4	68.2±11.1**	62.5±10.4*	58.3±6.4
Sex				
Male	11 (50%)	55 (79.7%)	30 (53.5%)	11 (47.8%)
Female	11 (50%)	14 (20.2%)	26 (46.4%)	12 (52.1%)
ILD type				
CTD-ILD			12 (21.4%)	
HP			17 (30.3%)	
NSIP			27 (48.2%)	
Smoking status#				
Current	5 (22.7%)	5 (7.2%)	0	1 (4.3%)
Former	6 (27.2%)	40 (57.9%)	26 (46.4%)	22 (95.6%)
Nonsmokers	11 (50%)	24 (34.7%)	30 (53.6%)	0
D_{LCO} % pred		33.8±16.7	32.5±16.3	25.3±18.7
VC_{max} % pred		61.6±17.8	61.3±19.2	61.1±26.6

Data are presented mean±SD, unless otherwise stated. IPF: idiopathic pulmonary fibrosis; ILD: interstitial lung disease; COPD: chronic obstructive pulmonary disease; CTD: connective tissue disease; HP: hypersensitivity pneumonitis; NSIP: nonspecific interstitial pneumonia; D_{LCO}: diffusing capacity of the lung for carbon monoxide; VC_{max}: maximum vital capacity. #: subjects with ⩾5 pack-years of cigarette smoking. *: p<0.05 *versus* healthy controls; **: p<0.01 *versus* healthy controls.

Cell isolation and flow cytometry analysis

For immunophenotyping, fresh venous blood was collected in EDTA-coated vacutainer tubes (Sarstedt, Nümbrecht, Germany). Briefly, whole blood or PBMC buffy coats were used for flow cytometry detection of MDSC and lymphocyte subtypes. MDSC were gated as lineage^{neg}/HLA-DR^{neg}/CD33^{++}/CD11b^{+}/CD14^{+} or lineage^{neg}/HLA-DR^{neg}/CD33^{+}/CD11b^{+}/CD66b^{+}, and data presented as % gated HLA-DR^{neg} cells. %mo-MDSC and %g-MDSC was determined and presented as % gated CD33^{++} CD11b^{+} and CD33^{+} CD11b^{+}, respectively. Lymphocyte subtypes were determined as T-cells (CD3^{+}), T-helper (CD3^{+}CD4^{+}) (effector (CCR7^{-}) and non-effector (CCR7^{+})), T-cytotoxic (CD3^{+}CD8^{+}) (effector (CCR7^{-}) and non-effector (CCR7^{+})), abnormal T-cells (CD3^{+}CD4^{+}CD8^{+}) and T-reg cells (CD4^{+}CD25^{+} and CD4^{+}CD25^{+}FoxP3^{+}), with the antibody list detailed in figure E1 and table E1, as previously reported [23]. For whole blood staining, 100 µL was incubated with an antibody mix for MDSC (table E1) for 20 min at 4°C in the dark. Erythrocytes were lysed with a Coulter Q-Prep working station (Beckman Coulter, Germany), as previously reported [24]. For lymphocyte analysis, PBMCs were prepared from blood samples using density gradient sedimentation (Lymphoprep; STEMCELL Technologies, Cologne, Germany). Trypan blue staining was used for differentiation between viable and nonviable cells, and showed viability of >90% for all cells used in this study. After gradient separation, cells were stained with lymphocyte antibody mix for 20 min at 4°C in the dark. Data acquisition was performed in a BD LSRII flow cytometer or a BD fluorescence-activated cell sorter (FACS) ARIA II (both Becton Dickinson, Heidelberg, Germany) if cells were sorted. Data was analysed with FlowJo software (TreeStart Inc, Ashland, OR, USA). Negative thresholds for gating were set according to isotype-labelled controls.

T-cell suppression assay and MDSC co-culture

The T-cell suppression assay and MDSC co-cultures were performed as previously published [19, 25]. Briefly, PBMCs from IPF patients were isolated, stained with CFSE (CellTrace, C34554; ThermoFisher Scientific, Darmstadt, Germany) and stimulated with recombinant human IL-2 (100 U·mL^{-1}; BD Pharmingen, San Diego, CA, USA) and OKT3 (1 µg·mL^{-1}; Biolegend, San Diego, CA, USA). PBMCs were incubated with stimulation media alone or with isolated autologous MDSC. After 4 days, cells were harvested and stained with anti-CD4-PE or anti-CD8-allophycocyanin (Biolegend). CSFE fluorescence intensity of each cell type was analysed by flow cytometry. The percentage of proliferation was analysed for CD8^{+} and CD4^{+} cells cultured alone or in conjunction with MDSC. Data were analysed with FlowJo software. After 96 h of incubation, cells were harvested and stained with anti-CD4-PE (BD Pharmingen) and anti-CD8-allophycocyanin. CFSE fluorescence intensity was analysed by flow cytometry to determine proliferation of CD4^{+} and CD8^{+} T-cells. After 96 h of incubation, cells were harvested and stained with anti-CD4-PE (BD Pharmingen) and anti-CD8-allophycocyanin. CFSE fluorescence intensity was analysed by flow cytometry to determine proliferation of CD4^{+} and CD8^{+} T-cells.

Statistical analysis

Data are presented as scatter plots with mean±SD. Two group comparisons were made using a non-parametric two-tailed Mann–Whitney U-test, parametric test or paired t-test, when specified. Three or more group comparisons were made using one-way ANOVA, with the non-parametric Kruskal–Wallis test followed by Dunnett's test. Associations between variables were established by linear regression and Pearson correlation. GraphPad Prism (version 5.0; GraphPad Software, San Diego, CA, USA) was used for statistical analyses. Significance was defined as $p<0.05$.

Results

Patient demographics

In total, 170 patients and controls were included in this study (table 1). From those, 69 were diagnosed with IPF, 56 with non-IPF ILD (connective tissue disease-ILD: n=12, hypersensitivity pneumonitis: n=17; nonspecific interstitial pneumonia: n=27) and 23 with COPD, and 22 were healthy controls. Patient demographics are shown in table 1.

MDSC are increased in the peripheral blood of patients with lung fibrosis

Whole blood MDSC (defined as lineage^{neg}/HLA-DR^{neg}/CD33^{+}/CD11b^{+} cells) were measured and quantified in freshly drawn blood in all study subjects. Previous reports in several types of cancer [11] or lung disorders have described human circulating MDSCs as monocytic (CD14^{+}) or granulocytic (CD66b^{+}) [13]. In order to set a threshold for positive–negative discrimination, a fluorescently labelled isotype was used as a control for each subject (figure 1a). To exclude definitive differentiated and mature cell populations, a cocktail with lineage-definitive markers was used and positive cells were excluded (figure 1a). This was followed by exclusion of HLA-DR-positive cells and further gating on CD33 and CD11b positivity. Two distinct populations were observed: a CD33^{++}/CD11b^{+}, characterised by strong CD14 expression and monocytic morphology; and a CD33^{+}/CD11b^{+}, characterised by strong CD66b expression and granulocytic morphology (figure 1). We used FACS-sorted monocytic and granulocytic MDSCs to confirm their morphology using cytospins with Diff-quick staining, as well as co-expression of CD33 and CD11b by immunofluorescence staining (figure 1b).

Next, we quantified the abundance of MDSCs (as % gated of HLA-DR^{neg} cells) in all subjects. We observed that the amount of MDSCs was significantly elevated in the peripheral blood of IPF (30.99±15.61%, $p<0.01$) and non-IPF ILD patients (31.63±15.61%, $p<0.05$) when compared with controls (18.96±8.17%) or COPD (25.63±13.94%, p=NS) (figure 2a). Next, to determine which MDSC phenotype was prevalent in IPF patients, we quantified the proportion of mo-MDSC (as % gated CD33^{++}CD11b^{+} cells) and g-MDSC (as % gated CD33^{+}CD11b^{+} cells). Interestingly, we observed that the proportion of mo-MDSC was significantly increased in IPF compared with controls (figure 2b). Inversely, the proportion of g-MDSC was significantly decreased (figure 2c).

Increased MDSC abundance reflects poor lung function specifically in IPF patients

To elucidate the clinical relevance of increased circulating MDSCs, we analysed whether higher numbers of MDSCs correlated with physiological parameters that determine disease status, such as lung function. We observed that, in a cross-sectional analysis, higher numbers of peripheral blood MDSCs inversely correlated with maximum vital capacity (VC_{max} % predicted) ($p<0.0001$, $r=-0.48$) in IPF. The MDSC-VC_{max} correlation remained significant when all patients were pooled together, albeit with a less stringent correlation coefficient ($p=0.0027$, $r=-0.24$) (figure 3). Correlation analysis was also performed for non-IPF ILD and COPD, but no significant correlation was found for these groups ($p=0.5$, $r=-0.07$ and $p=0.5$, $r=-0.14$, respectively).

Although our study was not designed as a prospective longitudinal study, a number of patient revisits occurred in the study period; thus, we were able to analyse the relationship between the change in MDSC and VC_{max} over time in the same patients. As depicted in figure 4, 27 patients were assessed by follow-up analysis (IPF: n=14, non-IPF ILD: n=11, COPD: n=2). While the initial values are included in all patients' analysis (figure 2), we performed an additional analysis for repeat visits by correlating the delta (Δ) MDSC with ΔVC_{max} % predicted ($\Delta=V2-V1$). By using this calculation, we could uncover whether the number of MDSCs changed with declining lung function over time. When patients were analysed altogether a nonsignificant weak negative correlation was observed ($r=0.09189$) (figure 4a). When we analysed only IPF patients, a strong and significant correlation was observed ($r=-0.5773$, $p=0.0389$) (figure 4b).

MDSC from IPF patients effectively suppress T-cell proliferation

To confirm that peripheral blood MDSCs from IPF patients suppressed T-cell proliferation, we isolated and co-cultured PBMCs with autologous MDSCs, and assessed the suppressive function of MDSC *in vitro*. PBMCs were isolated (non-IPF ILD: n=5, IPF: n=4), stained with CFSE and cultured over a period of

DOI: 10.1183/13993003.01826-2015

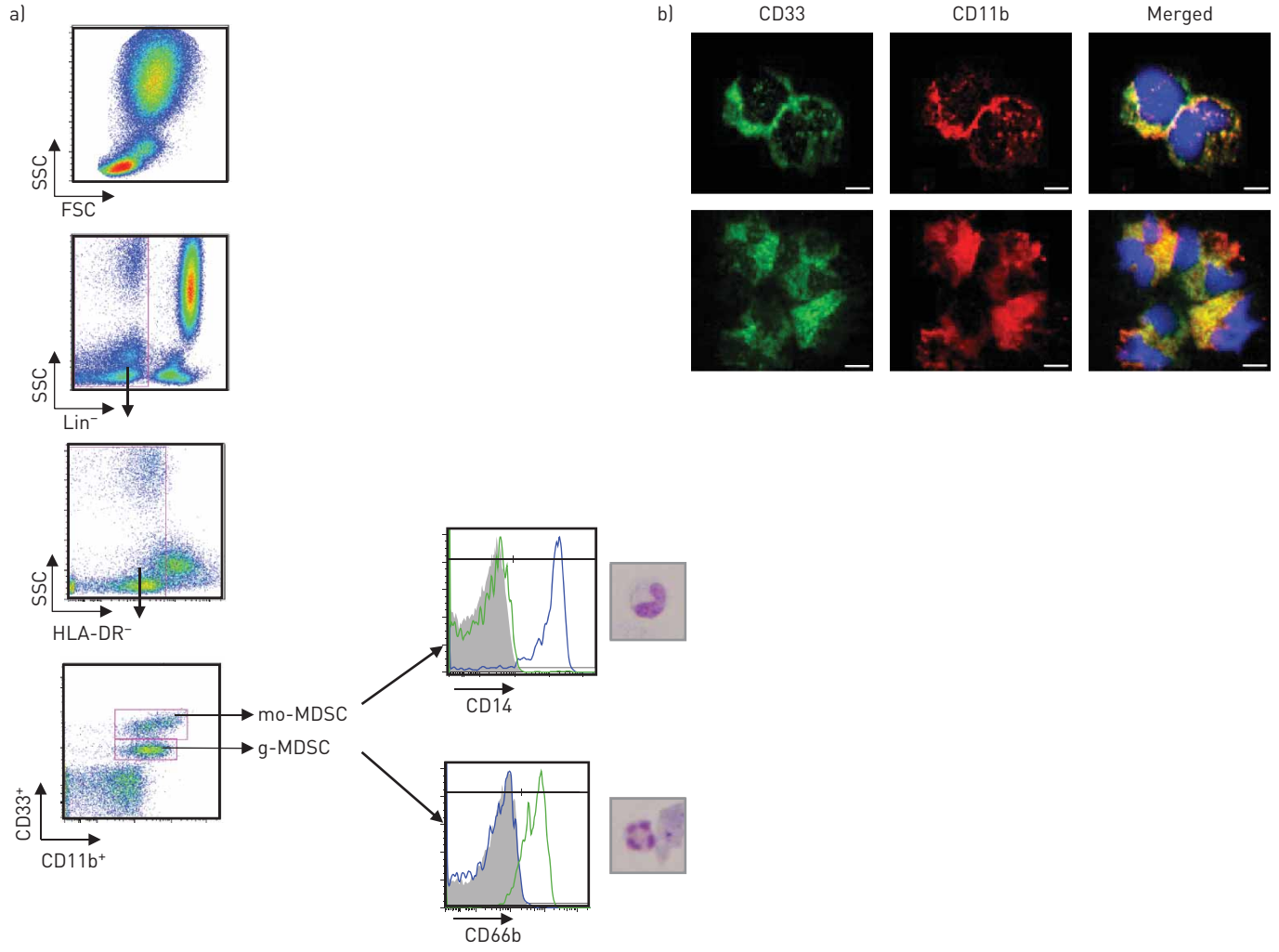

FIGURE 1 Characterisation of human myeloid-derived suppressor cells (MDSC) in whole blood. Representative dot-plots of whole blood flow cytometry analysis after red blood cell lysis. a) Cells were stained with a panel of monoclonal antibody and gated on Lin^{neg}, HLA-DR^{neg}, $CD33^{+}$ $^{+}CD11b^{+}$ and $CD33^{+}CD11b^{+}$, and further characterised as monocytic (mo-MDSC: $CD14^{+}$) or granulocytic (g-MDSC: $CD66b^{+}$), depicted in the histograms as blue and green, respectively. Gates were based on isotype-stained samples, represented as grey in the histograms. Microscopic analysis of Diff-quick stained cytospins of fluorescence-activated cell sorter (FACS)-sorted mo-MDSC and g-MDSC confirmed phenotypic characteristics. b) Immunofluorescence staining of FACS-sorted mo-MDSC (top) and g-MDSC (bottom) are depicted as single channels (CD33 in green; CD11b in red) and merged channels confirmed the co-expression of MDSC markers. Scale bars=5 µm. SSC: side-scattered light; FSC: forward-scattered light; HLA-DR: human leukocyte antigen-DR.

4 days. $CD4^{+}$ and $CD8^{+}$ T-cells showed a baseline proliferation of 70.61±18.73% and 83.69±7.68%, respectively, when cultured alone in stimulation media. When autologous MDSCs were added to these cultures, at a ratio of 1:4 (T cell:MDSC), $CD4^{+}$ and $CD8^{+}$ T-cell proliferation were significantly decreased, confirming MDSC suppressive functions (figure 5a and b).

Patients with IPF exhibit elevated levels of immunosuppressive lymphocytes

Next, we analysed lymphocyte subtypes in all subjects to test the hypothesis that an MDSC-lymphocyte axis might contribute to the immunosuppressive network in IPF. We did not observe significant differences in several T-cell subsets, including T-helper (effector and non-effector) or T-cytotoxic (effector and non-effector) cells (figure E3). However, a significant decrease in abnormal T-cells ($CD3^{+}CD4^{+}CD8^{+}$) was observed in non-IPF ILD (1.36±1.3% *versus* 3.14±2.8%, p=0.0079) when compared with controls (figure E3). When we analysed $CD4^{+}$ $CD25^{+}$ cells, a population that includes T-reg cells, we observed a significant increase in IPF (52.96±21%, p=0.0002) and non-IPF ILD (55.78±19.8%, p=0.0002) when compared with controls (32.8±17.7%) (figure 6a). We performed intracellular FoxP3 staining in lymphocytes of 26 IPF patients to determine T-reg cell abundance and correlated the percentage of T-reg cells with MDSCs. A significant positive correlation between T-reg cells and MDSCs was observed (p=0.0484, r=0.3326) (figure 6b). To substantiate this, we isolated PBMC mRNA of IPF patients with >40% MDSCs and performed

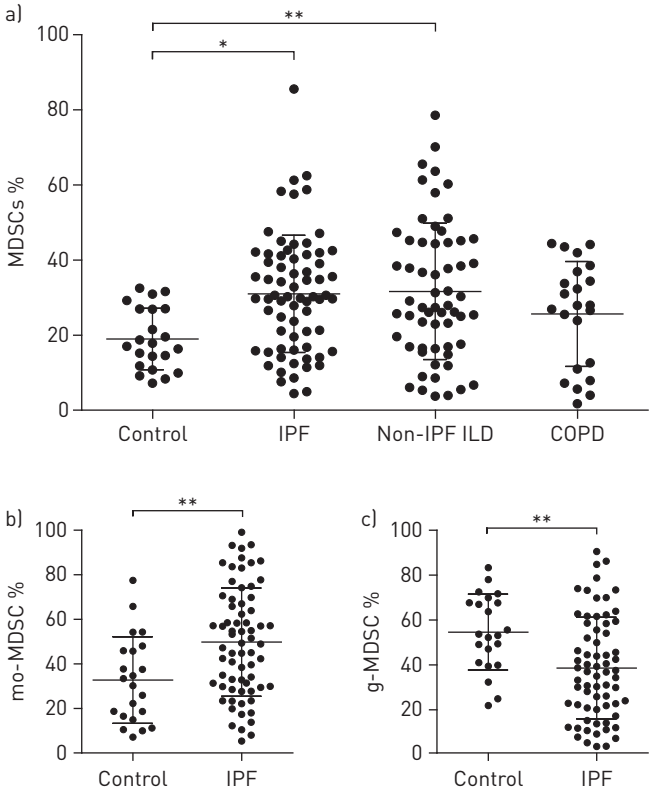

FIGURE 2 Increased abundance of myeloid-derived suppressor cells (MDSC) in lung fibrosis. a) Scatter-plot diagrams from flow cytometry analysis of MDSC counts, as % gated HLA-DR^{neg} cells in 22 healthy controls, 69 idiopathic pulmonary fibrosis (IPF), 56 non-IPF interstitial lung disease (ILD) and 23 chronic obstructive pulmonary disease (COPD) patients. b) Monocytic (mo)-MDSC as % gated CD33^{++}CD11b^{+} and c) granulocytic (g)-MDSC as % gated CD33^{+}CD11b^{+} cells in 22 controls and 69 IPF patients. For statistical analysis, one-way ANOVA with the non-parametric Kruskal–Wallis test, followed by Dunnett's multiple comparison test (a), and non-parametric two-tailed Mann–Whitney U-test (b, c) was used. *: p<0.05 *versus* healthy controls; **: p<0.01 *versus* healthy controls. HLA-DR: human leukocyte antigen-DR.

qPCR analysis for a set of four genes that were recently related to T-cell co-stimulatory signals [7]. Importantly, the mRNA transcripts of CD28, ICOS, ITK and LCK were significantly decreased in IPF patients with high circulating MDSCs when compared with controls (figure 6c).

MDSC are detected in the lungs of IPF patients

To date, tissue-infiltrating MDSCs have been described in several human cancer types, where they have been shown to differentiate, for example, into immunosuppressive tumour-associated macrophages or dendritic cells [26, 27]. To determine whether MDSCs are present in the fibrotic lung, we investigated lung tissue from explants of fibrotic patients (IPF and chronic hypersensitivity pneumonitis) for the presence of CD33^{+}CD11b^{+} positive cells. Sequential immunofluorescence stains from fibrotic lung tissues revealed that CD33^{+}CD11b^{+} double-positive cells, suggestive of MDSC, are present in collagen 1-positive areas and neighbouring α-SMA-positive areas in the fibrotic lung parenchyma outside vessels (figure 7).

Discussion

Our study demonstrates, for the first time, an increased abundance of circulating and tissue-infiltrating MDSCs in patients with IPF and non-IPF ILD. Specifically in IPF, MDSC abundance in the peripheral blood inversely correlates with lung function. We further detected a suppressive function in IPF MDSCs, along with an increase in circulating CD4^{+}CD25^{+} activated T-cells, a correlation between MDSCs and FoxP3-positive T-reg cells, and a decrease in the transcript levels of CD28, ICOS, ITK and LCK in PBMCs. In our opinion, these are remarkable observations due to the following reasons. First, these data strongly support a role for an immunosuppressive environment in the peripheral blood and lungs of IPF patients. Secondly, the tight correlation of increased MDSCs with decreased lung function suggest that MDSCs, at least in part, contribute to disease progression in IPF, which is further substantiated by longitudinal assessments of ΔMDSCs and ΔVC_{max} % pred over time in selected patients. Thirdly, MDSC

DOI: 10.1183/13993003.01826-2015

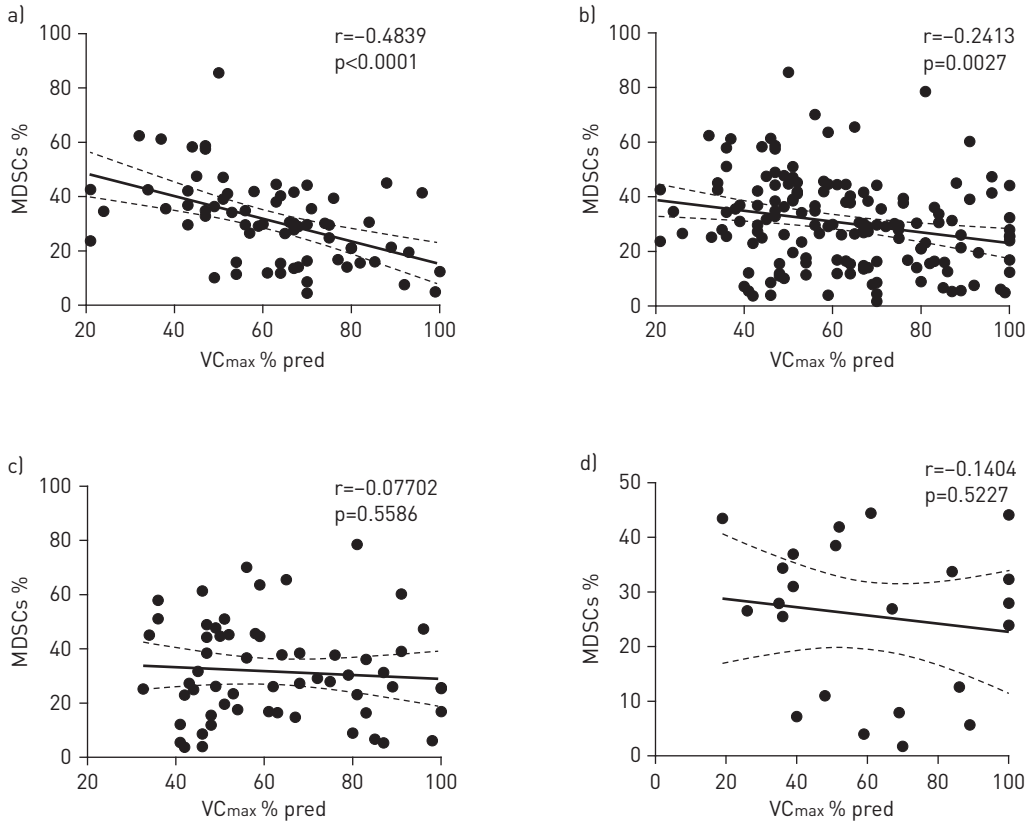

FIGURE 3 Myeloid-derived suppressor cells (MDSC) abundance inversely correlates with maximum vital capacity (VC_{max}) % predicted in idiopathic pulmonary fibrosis (IPF). The percentage of gated MDSC (as % gated HLA-DR^{neg} cells) was inversely correlated with VC_{max}, as % predicted values in a) IPF, b) all subjects, c) non-IPF interstitial lung disease and d) chronic obstructive pulmonary disease. p-values were determined by t-distribution for Pearson correlation.

abundance and/or function are currently manipulated in cancer trials. Targeting MDSC abundance and/or function may, therefore, represent an exciting novel treatment approach in IPF. Altogether, these data reveal that MDSCs are part of an immune-deregulated environment and reflect disease status in IPF.

In recent years, it has become apparent that immune dysregulation is a key contributor to fibrogenesis in a number of organs. The innate and adaptive immune system can enhance the secretion of pro-fibrotic

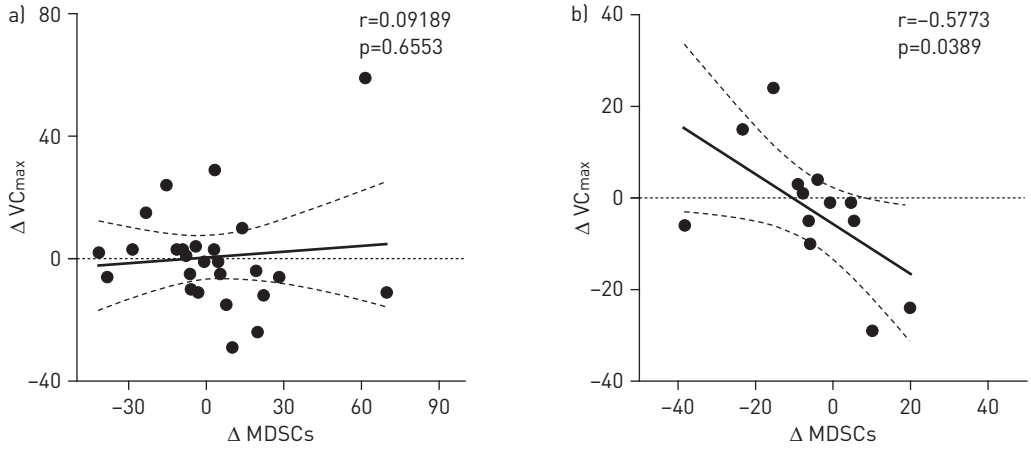

FIGURE 4 Follow-up analysis reveals correlation of myeloid-derived suppressor cells (MDSC) abundance with the disease course of idiopathic pulmonary fibrosis (IPF). Δ % gated MDSC and maximum vital capacity (VC_{max}) % predicted was calculated for patients with consecutive visits for a) all diagnosis (n=27) and b) IPF only (n=14). The ΔVC_{max} and ΔMDSC, calculated from visit 1 to 2, were correlated. p-values were determined by t-distribution for Pearson correlation.

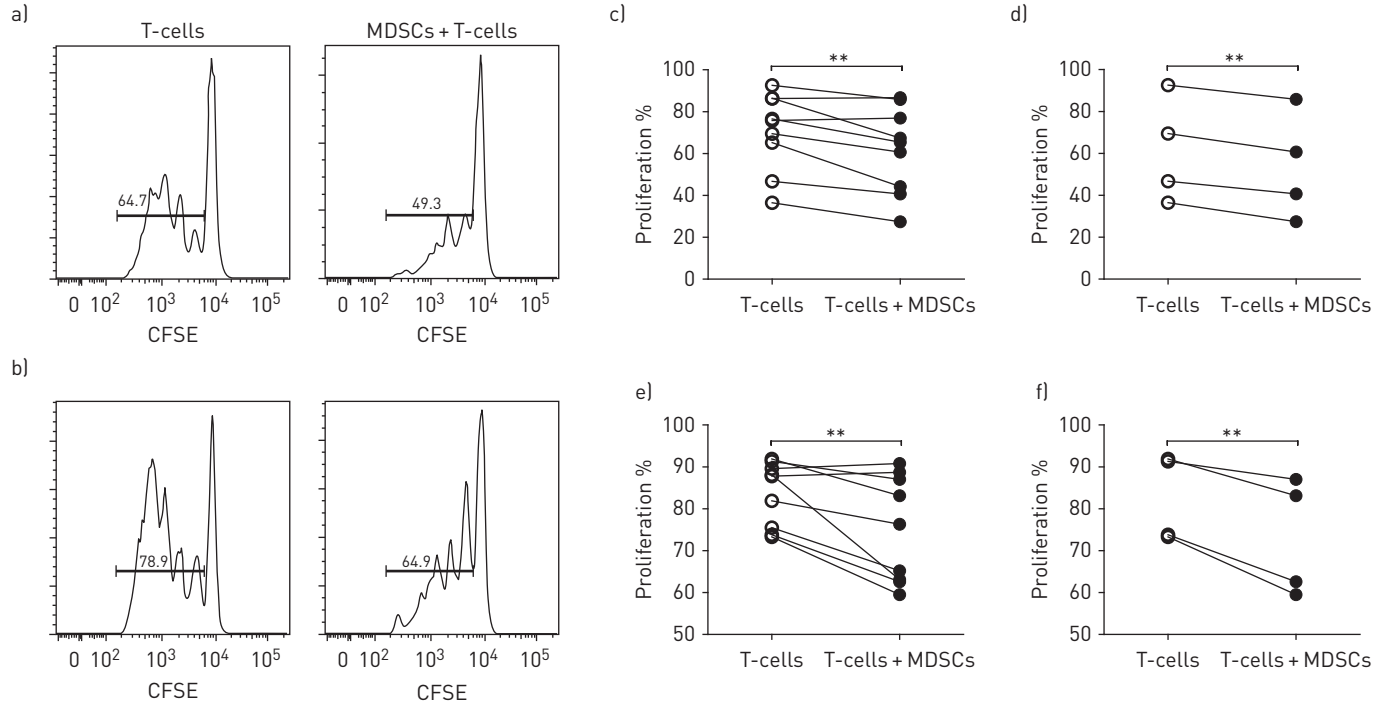

FIGURE 5 Myeloid-derived suppressor cells (MDSC) suppress autologous T-cell proliferation in idiopathic pulmonary fibrosis. Representative histogram of a) $CD4^+$ and b) $CD8^+$ T-cell proliferation, assessed by carboxyfluorescein succinimidyl ester (CFSE) incorporation and measured by flow cytometry, with medium only (left-hand panels) and co-cultured with autologous MDSC (right-hand panels). Quantification of % proliferation of c, d) $CD4^+$ and e, f) $CD8^+$ T-cells alone or in co-culture with autologous MDSC for all patients (n=9) (c, e) or idiopathic pulmonary fibrosis only (n=4) (d, f). For statistical analysis paired t-tests were used. **: p<0.01.

factors that direct the healing/scarring response towards a fibrotic outcome [9]. Historically, harmful effects of global immunosuppressive therapy in IPF (*e.g.* by using prednisone and/or azathioprine) outweighed this possibility, as a randomised controlled trial reported an increased mortality in IPF patients subjected to anti-inflammatory therapy [28]. Herein, we provide compelling evidence for the observation that IPF patients exhibit an immunosuppressive network in the peripheral blood and lungs, driven by MDSCs. Taking this into account, traditional immunosuppressive therapies would, instead, perpetuate the already dysregulated immune environment and be deleterious for disease.

A growing body of literature supports a role for T-cells in IPF pathogenesis [29]. Marchal-Sommé *et al.* [30] reported ectopic formation of secondary lymphoid tissue in fibrotic niches of IPF lungs, supporting enhanced migration and generation of activated T- and B-cell subtypes in IPF. Although several subtypes of activated T-cells have been associated with progression and outcome in IPF, the literature remains controversial to date. Recently, Gilani *et al.* [6] showed that $CD4^+$ T-cells displayed a marked downregulation in the surface expression of CD28 in IPF, which was associated with worse outcome. The $CD4^+CD28^-$ T-cells detected in this study showed a decrease in CD25 and FoxP3 expression. Nonetheless, $CD4^+CD25^+FoxP3^+$ total numbers (non-discriminated by CD28) were not reported in this study. Furthermore, Kotsianidis *et al.* [8] reported that peripheral blood and BAL T-reg cells ($CD4^+CD25^+FoxP3^+$) were decreased in IPF. Importantly, the identification of T-reg subsets in fibrotic conditions of the human lung is more discriminative when $CD4^+/CD25^+/CD27^+$ cells are assessed [31]. Recently, $Sema7a^+/CD4^+/CD25^+/FoxP3^+$ cells were found to be increased in rapidly progressive IPF patients, and adoptive transfer of these cells to transforming growth factor-β overexpressing mice was sufficient to induce fibrosis [5], corroborating the notion that increased T-reg cells induce and/or facilitate fibrogenesis in the lung. In other animal models of fibrosis, depletion of $CD4^+CD25^+FoxP3^+$ cells by administration of a blocking CD25 antibody switched T-helper 2-driven responses towards a T-helper 1 kind and attenuated fibrosis development [32].

Importantly, extensive gene expression profiling in the peripheral blood of IPF patients has recently extended this knowledge. Yang *et al.* [33] first demonstrated that the peripheral blood transcriptome in IPF patients varies from normal individuals by documenting that 1428 and 2790 genes were differentially regulated in mild *versus* severe IPF, respectively, when compared with controls. Extending this observation, Herazo-Maya *et al.* [7] showed that gene expression patterns in PBMCs predict outcome in IPF patients. In that study, decreased expression of CD28, ICOS, LCK and ITK was a stronger outcome predictor than clinical data alone.

DOI: 10.1183/13993003.01826-2015

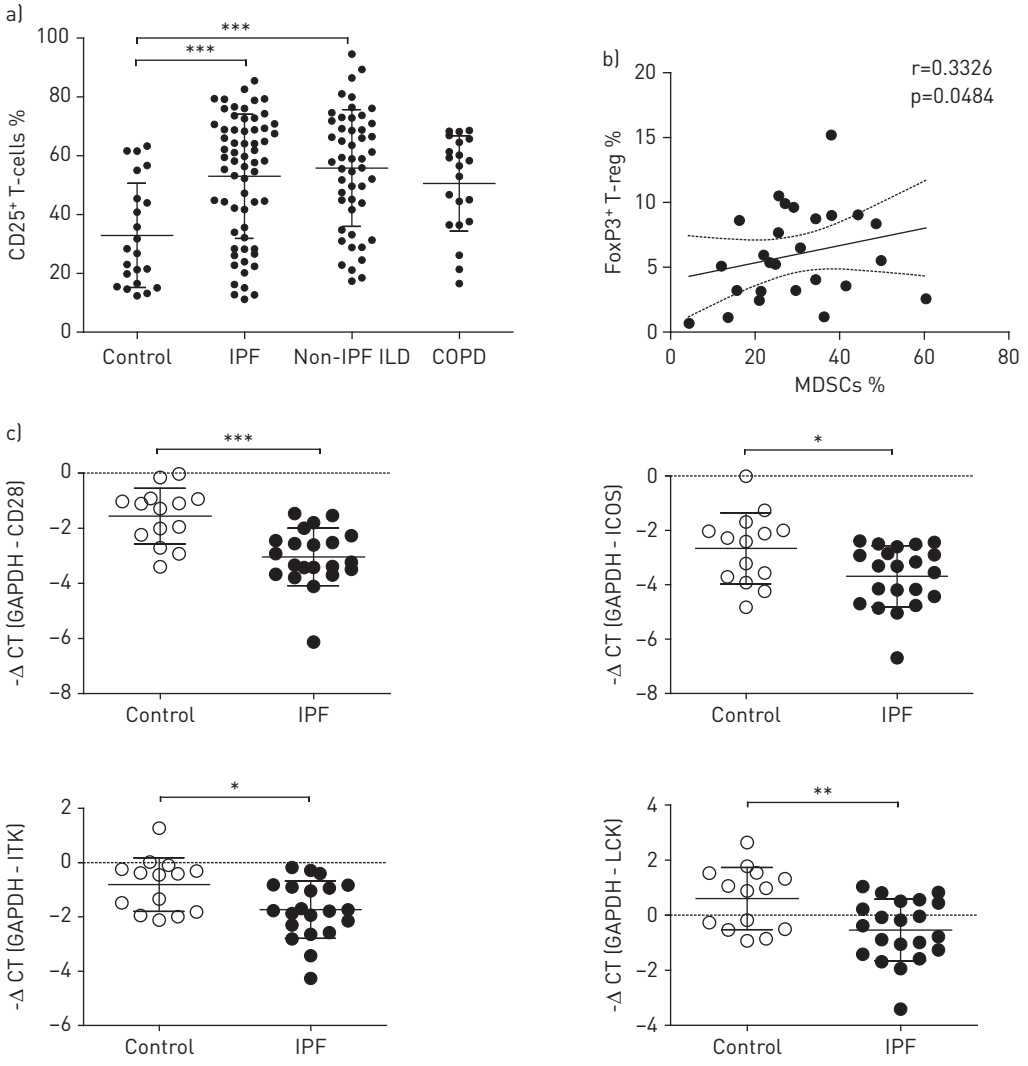

FIGURE 6 $CD25^+$ T-cells, $FoxP3^+$ regulatory T-cells (T-reg) and co-stimulatory T-cell signals are dysregulated in idiopathic pulmonary fibrosis (IPF). a) Scatter-plot diagrams from flow cytometry analysis of $CD25^+$ T-cells (as % gated $CD3^+CD4^+$) in 22 healthy controls, 69 IPF, 56 non-IPF interstitial lung disease (ILD) and 23 chronic obstructive pulmonary disease (COPD) patients. For statistical analysis, one-way ANOVA was used with the non-parametric Kruskal–Wallis test, followed by Dunnett's multiple comparison test. b) Correlation of % $FoxP3^+$ T-reg cells (as % gated $CD4^+CD25^+$) and myeloid-derived suppressor cells (MDSC). p-values were determined by t-distribution for Pearson correlation. c) qPCR analysis of CD28, ICOS, ITK and LCK in peripheral blood mononuclear cell pellets of healthy controls (n=14) and IPF patients (n=21). Non-parametric two-tailed Mann–Whitney U-test was used for statistical analysis. *: $p<0.05$; **: $p<0.01$; ***: $p<0.001$.

Although these data support an important role for immunosuppression in IPF by elucidating the role of T-reg cells, another major innate immunosuppressive cell type, MDSC, has not been investigated at all in lung fibrosis. In the lung, the presence of MDSCs was initially described in advanced nonsmall cell lung cancer [34], where their presence has been widely explored, both clinically [17] and mechanistically [35]. In cystic fibrosis, MDSCs have been associated with *Pseudomonas aeruginosa* infections, demonstrating that this pathogen induced MDSC generation *via* flagellin [19]. In TB, increased MDSC numbers are described to suppress T-cell functions [18]. To this extent, Knaul *et al.* [36] unravelled a complex role of MDSCs in murine TB. MDSCs accumulated in TB lungs, acted as phagocytes and provided a cellular shelter for mycobacteria, which then suppressed T-cell responses and led to increased TB lethality. In pulmonary hypertension, MDSCs are increased and their levels correlated with increased mean pulmonary artery pressure [37]. In COPD, recent work demonstrated an effector T-cell dysfunction composed by T-reg cells, MDSC and PD-1 exhausted effector T-cells [20].

Of note, we did not observe a significant increase in MDSC numbers in COPD patients in our study. This difference could be due to the fact that Kalathil *et al.* [20] investigated an older and more advanced

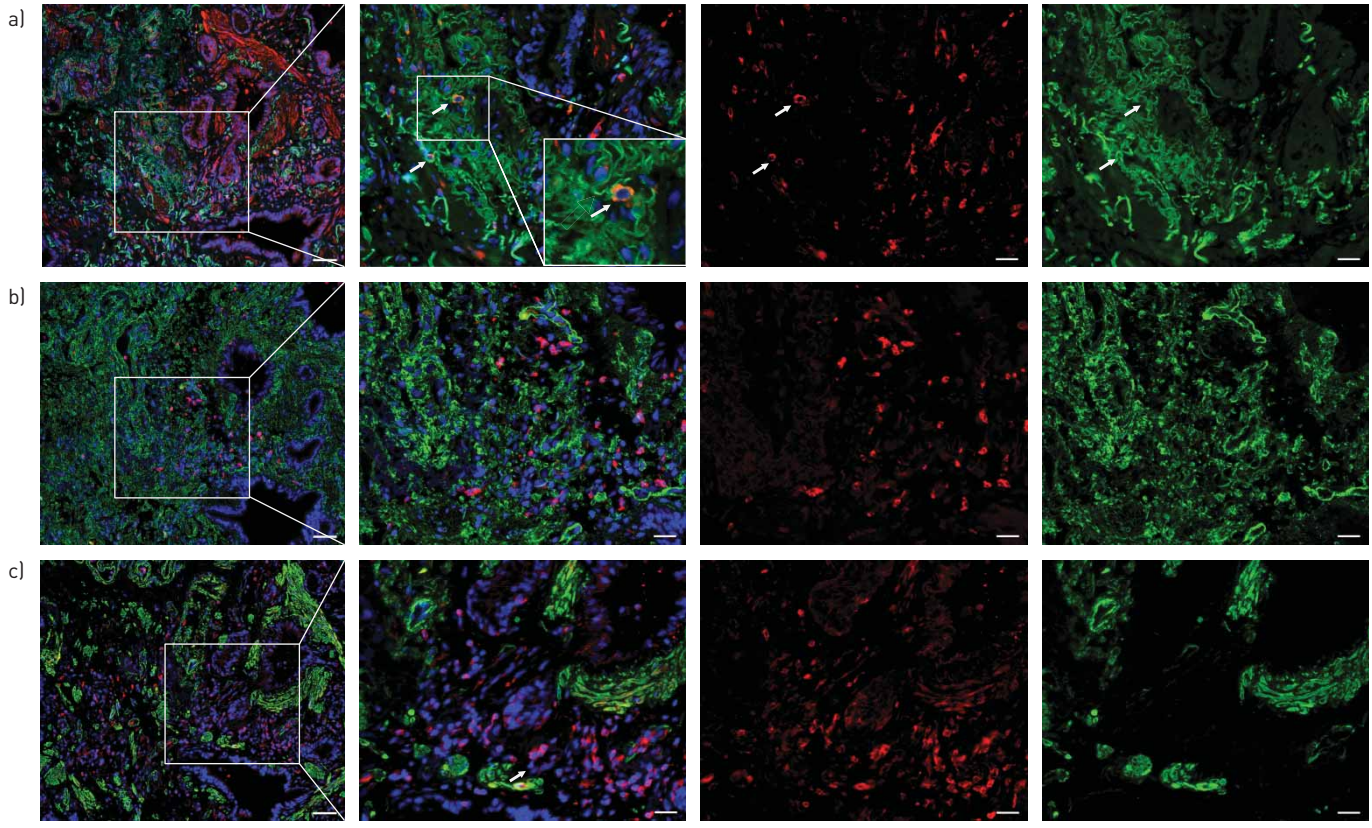

FIGURE 7 $CD33^{+}CD11b^{+}$ cells are present in fibrotic areas of idiopathic pulmonary fibrosis (IPF) lungs. Representative immunofluorescence of sequential cuts from paraffin sections of IPF lungs are shown stained for: a) CD33 (red) and CD11b (green), b) CD11b (red) and collagen 1 (green), and c) CD33 (red) and α-SMA (green). For all, nuclei were counterstained with DAPI (blue). Lower magnifications (left-hand panel) are presented at 10× (scale bar=50 µm). White squares represent higher magnifications (scale bar=20 µm), depicted as merged images and single channel images for the red and green channel. $CD33^{+}CD11b^{+}$ cells are indicated with a white arrow. Sections are representative stains of two IPF patients and one hypersensitivity pneumonitis patient.

COPD population, with worse baseline lung function compared to our cohort. It is also critical to highlight that, due to the diverse strategies to phenotypically define MDSC, it is difficult to compare absolute cell numbers across diseases.

Granulocytic MDSCs are described to be the predominant MDSC subtype in malignancies of several organ systems. Surprisingly, our analysis of MDSC subtypes in IPF revealed that monocytic MDSCs are the predominant subtype in IPF. Peyvandi *et al.* [38] recently demonstrated that modulation of the Fas–FasL pathway did not increase overall MDSC abundance; however, it skewed the MDSC subtype towards a highly suppressive monocytic MDSC subtype. It simultaneously increased the number of tumour-associated macrophages and T-reg cells, and increased tumour growth with decreased survival in a mouse model of lung cancer [38]. We believe that further studies are necessary to clarify the differential contribution of MDSC subtypes to lung fibrosis.

Previous reports have shown that ageing affects MDSC abundance, influencing the progression of age-related pathologies [39]. The age of our IPF population was significantly higher when compared with controls (mean age 68.2 *versus* 55.4 years). However, it is important to note the mean age for the young adult population in the study mentioned above was 32 years, *i.e.* 20 years younger than our control group. Therefore, we consider that the effect of age only for our analysis is minimal.

In repeated visits in our study we demonstrated that increased MDSC numbers over time significantly correlated with the decline in VC_{max}. This was observed in a greater extent in IPF patients than in non-IPF ILD or COPD. We reason for this may be due to the fact that IPF exhibits different disease pathogenesis than non-IPF ILD. Also non-IPF ILD exhibits more variability in its natural history and treatment responsiveness, which may influence data interpretation.

One of the critical roles of MDSCs is their ability to suppress immune cell function, especially by the induction of arginase, COX2, ROS, inducible NOS secretion of transforming growth factor-β and/or

 DOI: 10.1183/13993003.01826-2015

induction of T-reg cells [26], all of which are pro-fibrotic players [40]. At the tumour site, MDSCs can differentiate into tumour-associated macrophages [27, 41] or regulatory dendritic cells [42]. Furthermore, in mouse models of metastatic melanoma and breast cancer, MDSCs were shown to differentiate into fibrocytes, in a KLF4-dependent manner, to support the establishment of lung metastasis [43]. In a murine model of renal fibrosis, fibrocytes generated from a subpopulation MDSC under control of $CD4^+$ cells contributed to renal deposition of collagen type I [44]. A population of circulating MDSC-like fibrocytes was initially reported in metastatic cancer patients by Zhang *et al.* [45], which showed expression of α-SMA, collagen I/V and mediation of angiogenesis. Importantly, circulating fibrocytes numbers are increased in IPF [46] and non-IPF ILD [47], and have been associated with poor prognosis. It is therefore important to define the overlap between FACS-defined MDSC and fibrocytes in future prospective studies.

Ample evidence supports the use of MDSCs as biomarkers for clinical outcomes in cancer patients, specifically when assessing tumour progression and response to therapy [48]. High percentages of circulating MDSCs have been shown to predict resistance to anticancer therapies and shorter survival [49]. Further evidence supporting the promotion of tumour growth, differentiation and metastasis by MDSCs is growing. In diffuse large B-cell lymphoma [50] and melanoma [51], MDSCs are an independent prognostic factor. In head and neck squamous cell carcinoma, MDSC abundance correlated with cancer stage [52]. In gastric [53] and renal carcinoma [54], MDSC inhibited T-cell proliferation and correlated with later stage and shorter overall survival. In breast cancer, MDSCs suppress antitumor immune responses, and correlate with lymph node metastasis [55]. In addition, sufficient evidence from preclinical models and clinical testing of multiple cancers types, such as melanoma [56], breast cancer [57], nonsmall cell lung cancer [58] or metastatic kidney cancer [59], demonstrated that targeting and decreasing MDSC abundance increased the tumour's sensitivity to chemotherapy. Accordingly, novel therapeutic strategies in the above-mentioned diseases aim to eliminate, deactivate or skew MDSC number and/or function [26], and it is probably suitable to explore these interventions in IPF.

IPF has been considered as a cancer-like disorder, due to the activation of common pathogenic pathways and shared mechanisms (*e.g.* expansion of tissue-resident cells, activation of pro-proliferative signalling pathways) that are finally reflected in poor responses to medical treatment and clinical prognosis. Importantly, MDSC abundance in IPF and many cancer types might further support the available data in overlapping mechanism between these two conditions.

In conclusion, our study demonstrates, for the first time, the accumulation of MDSCs in peripheral blood and tissue of IPF patients. MDSCs inversely correlated with lung function, reflecting more advanced disease in IPF patients with high MDSC. These findings might explain dysregulated T-cell responses in IPF. Elevated MDSCs might cause a blunted immune response, which also might be an explanatory link for the increased incidence and burden of lung cancer in IPF. Controlling the expansion and accumulation of MDSCs or blocking their suppressive functions represents promising novel approaches to be used as a therapeutic strategy in IPF patients.

Acknowledgements

We thank Daniela Dietel (Comprehensive Pneumology Center, Ludwig-Maximilians-University, University Hospital Grosshadern, and Helmholtz Zentrum München, Member of the German Center for Lung Research, Munich, Germany) for excellent technical assistance, and the Helmholtz association for supporting this work.

The authors' contributions were as follows. Conception and design: I.E. Fernandez and O. Eickelberg; experimental work, analysis and interpretation: I.E. Fernandez, F.R. Greiffo, M. Frankenberger, J. Bandres, K. Heinzelmann, R. Hatz, C. Neurohr, D. Hartl, J. Behr and O. Eickelberg; drafting the manuscript and intellectual content: I.E. Fernandez and O. Eickelberg.

References

1 King TE Jr, Pardo A, Selman M. Idiopathic pulmonary fibrosis. *Lancet* 2011; 378: 1949–1961.
2 Wuyts WA, Antoniou KM, Borensztajn K, *et al.* Combination therapy: the future of management for idiopathic pulmonary fibrosis? *Lancet Respir Med* 2014; 2: 933–942.
3 Zoz DF, Lawson WE, Blackwell TS. Idiopathic pulmonary fibrosis: a disorder of epithelial cell dysfunction. *Am J Med Sci* 2011; 341: 435–438.
4 Fernandez IE, Eickelberg O. New cellular and molecular mechanisms of lung injury and fibrosis in idiopathic pulmonary fibrosis. *Lancet* 2012; 380: 680–688.
5 Reilkoff RA, Peng H, Murray LA, *et al.* Semaphorin 7a+ regulatory T-cells are associated with progressive idiopathic pulmonary fibrosis and are implicated in transforming growth factor-beta1-induced pulmonary fibrosis. *Am J Respir Crit Care Med* 2013; 187: 180–188.
6 Gilani SR, Vuga LJ, Lindell KO, *et al.* CD28 down-regulation on circulating CD4 T-cells is associated with poor prognoses of patients with idiopathic pulmonary fibrosis. *PloS One* 2010; 5: e8959.
7 Herazo-Maya JD, Noth I, Duncan SR, *et al.* Peripheral blood mononuclear cell gene expression profiles predict poor outcome in idiopathic pulmonary fibrosis. *Sci Transl Med* 2013; 5: 205ra136.
8 Kotsianidis I, Nakou E, Bouchliou I, *et al.* Global impairment of CD4+CD25+FOXP3+ regulatory T-cells in idiopathic pulmonary fibrosis. *Am J Respir Crit Care Med* 2009; 179: 1121–1130.

9 Wynn TA. Integrating mechanisms of pulmonary fibrosis. *J Exp Med* 2011; 208: 1339–1350.
10 Moore BB, Fry C, Zhou Y, *et al.* Inflammatory leukocyte phenotypes correlate with disease progression in idiopathic pulmonary fibrosis. *Front Med* 2014; 1: pii00056.
11 Lindau D, Gielen P, Kroesen M, *et al.* The immunosuppressive tumour network: myeloid-derived suppressor cells, regulatory T-cells and natural killer T-cells. *Immunology* 2013; 138: 105–115.
12 Talmadge JE, Gabrilovich DI. History of myeloid-derived suppressor cells. *Nat Rev Cancer* 2013; 13: 739–752.
13 Damuzzo V, Pinton L, Desantis G, *et al.* Complexity and challenges in defining myeloid-derived suppressor cells. *Cytom Part B Clin Cytom* 2015; 88: 77–91.
14 Lees JR, Azimzadeh AM, Bromberg JS. Myeloid derived suppressor cells in transplantation. *Curr Opin Immunol* 2011; 23: 692–697.
15 Vollbrecht T, Stirner R, Tufman A, *et al.* Chronic progressive HIV-1 infection is associated with elevated levels of myeloid-derived suppressor cells. *AIDS* 2012; 26: F31–F37.
16 Li Y, Tu Z, Qian S, *et al.* Myeloid-derived suppressor cells as a potential therapy for experimental autoimmune myasthenia gravis. *J Immunol* 2014; 193: 2127–2134.
17 Feng PH, Lee KY, Chang YL, *et al.* $CD14^{+}S100A9^{+}$ monocytic myeloid-derived suppressor cells and their clinical relevance in non-small cell lung cancer. *Am J Respir Crit Care Med* 2012; 186: 1025–1036.
18 du Plessis N, Loebenberg L, Kriel M, *et al.* Increased frequency of myeloid-derived suppressor cells during active tuberculosis and after recent *Mycobacterium tuberculosis* infection suppresses T-cell function. *Am J Respir Crit Care Med* 2013; 188: 724–732.
19 Rieber N, Brand A, Hector A, *et al.* Flagellin induces myeloid-derived suppressor cells: implications for *Pseudomonas aeruginosa* infection in cystic fibrosis lung disease. *J Immunol* 2013; 190: 1276–1284.
20 Kalathil SG, Lugade AA, Pradhan V, *et al.* T-regulatory cells and programmed death 1+ T-cells contribute to effector T-cell dysfunction in patients with chronic obstructive pulmonary disease. *Am J Respir Crit Care Med* 2014; 190: 40–50.
21 Kolahian S, Öz HH, Zhou B, *et al.* The emerging role of myeloid-derived suppressor cells in lung diseases. *Eur Respir J* 2016; 47: 967–977.
22 Raghu G, Rochwerg B, Zhang Y, *et al.* An Official ATS/ERS/JRS/ALAT Clinical Practice Guideline: Treatment of Idiopathic Pulmonary Fibrosis. an update of the 2011 Clinical Practice Guideline *Am J Respir Crit Care Med* 2015; 192: e3–e19.
23 Maecker HT, McCoy JP, Nussenblatt R. Standardizing immunophenotyping for the Human Immunology Project. *Nat Rev Immunol* 2012; 12: 191–200.
24 Heimbeck I, Hofer TP, Eder C, *et al.* Standardized single-platform assay for human monocyte subpopulations: lower CD14+CD16++ monocytes in females. *Cytom Part A* 2010; 77: 823–830.
25 Kostlin N, Kugel H, Spring B, *et al.* Granulocytic myeloid derived suppressor cells expand in human pregnancy and modulate T-cell responses. *Eur J Immunol* 2014; 44: 2582–2591.
26 Marvel D, Gabrilovich DI. Myeloid-derived suppressor cells in the tumor microenvironment: expect the unexpected. *J Clin Invest* 2015; 125: 3356–3364.
27 Franklin RA, Liao W, Sarkar A, *et al.* The cellular and molecular origin of tumor-associated macrophages. *Science* 2014; 344: 921–925.
28 Raghu G, Anstrom KJ, King TE Jr, *et al.* Prednisone, azathioprine, and *N*-acetylcysteine for pulmonary fibrosis. *N Engl J Med* 2012; 366: 1968–1977.
29 Lo Re S, Lison D, Huaux F. CD4+ T lymphocytes in lung fibrosis: diverse subsets, diverse functions. *J Leukoc Biol* 2013; 93: 499–510.
30 Marchal-Somme J, Uzunhan Y, Marchand-Adam S, *et al.* Cutting edge: nonproliferating mature immune cells form a novel type of organized lymphoid structure in idiopathic pulmonary fibrosis. *J Immunol* 2006; 176: 5735–5739.
31 Mack DG, Lanham AM, Palmer BE, *et al.* CD27 expression on CD4+ T-cells differentiates effector from regulatory T-cell subsets in the lung. *J Immunol* 2009; 182: 7317–7324.
32 Liu F, Liu J, Weng D, *et al.* CD4+CD25+Foxp3+ regulatory T-cells depletion may attenuate the development of silica-induced lung fibrosis in mice. *PLoS One* 2010; 5: e15404.
33 Yang IV, Luna LG, Cotter J, *et al.* The peripheral blood transcriptome identifies the presence and extent of disease in idiopathic pulmonary fibrosis. *PLoS One* 2012; 7: e37708.
34 Srivastava MK, Bosch JJ, Thompson JA, *et al.* Lung cancer patients' $CD4^{+}$ T-cells are activated *in vitro* by MHC II cell-based vaccines despite the presence of myeloid-derived suppressor cells. *Cancer Immunol Immunother* 2008; 57: 1493–1504.
35 Zhang Y, Liu Q, Zhang M, *et al.* Fas signal promotes lung cancer growth by recruiting myeloid-derived suppressor cells via cancer cell-derived PGE2. *J Immunol* 2009; 182: 3801–3808.
36 Knaul JK, Jorg S, Oberbeck-Mueller D, *et al.* Lung-residing myeloid-derived suppressors display dual functionality in murine pulmonary tuberculosis. *Am J Respir Crit Care Med* 2014; 190: 1053–1066.
37 Yeager ME, Nguyen CM, Belchenko DD, *et al.* Circulating myeloid-derived suppressor cells are increased and activated in pulmonary hypertension. *Chest* 2012; 141: 944–952.
38 Peyvandi S, Buart S, Samah B, *et al.* Fas ligand deficiency impairs tumor immunity by promoting an accumulation of monocytic myeloid-derived suppressor cells. *Cancer Res* 2015; 75: 4292–4301.
39 Verschoor CP, Johnstone J, Millar J, *et al.* Blood $CD33^{+}HLA\text{-}DR^{-}$ myeloid-derived suppressor cells are increased with age and a history of cancer. *J Leukoc Biol* 2013; 93: 633–637.
40 Fernandez IE, Eickelberg O. The impact of TGF-β on lung fibrosis: from targeting to biomarkers. *Proc Am Thorac Soc* 2012; 9: 111–116.
41 Corzo CA, Condamine T, Lu L, *et al.* HIF-1α regulates function and differentiation of myeloid-derived suppressor cells in the tumor microenvironment. *J Exp Med* 2010; 207: 2439–2453.
42 Zhong H, Gutkin DW, Han B, *et al.* Origin and pharmacological modulation of tumor-associated regulatory dendritic cells. *Int J Cancer* 2014; 134: 2633–2645.
43 Shi Y, Ou L, Han S, *et al.* Deficiency of Kruppel-like factor KLF4 in myeloid-derived suppressor cells inhibits tumor pulmonary metastasis in mice accompanied by decreased fibrocytes. *Oncogenesis* 2014; 3: e129.
44 Niedermeier M, Reich B, Rodriguez Gomez M, *et al.* CD4+ T-cells control the differentiation of Gr1+ monocytes into fibrocytes. *Proc Natl Acad Sci USA* 2009; 106: 17892–17897.

 DOI: 10.1183/13993003.01826-2015

45 Zhang H, Maric I, DiPrima MJ, *et al.* Fibrocytes represent a novel MDSC subset circulating in patients with metastatic cancer. *Blood* 2013; 122: 1105–1113.
46 Moeller A, Gilpin SE, Ask K, *et al.* Circulating fibrocytes are an indicator of poor prognosis in idiopathic pulmonary fibrosis. *Am J Respir Crit Care Med* 2009; 179: 588–594.
47 Garcia de Alba C, Buendia-Roldan I, Salgado A, *et al.* Fibrocytes contribute to inflammation and fibrosis in chronic hypersensitivity pneumonitis through paracrine effects. *Am J Respir Crit Care Med* 2015; 191: 427–436.
48 Walter S, Weinschenk T, Stenzl A, *et al.* Multipeptide immune response to cancer vaccine IMA901 after single-dose cyclophosphamide associates with longer patient survival. *Nat Med* 2012; 18: 1254–1261.
49 Wang Z, Zhang Y, Liu Y, *et al.* Association of myeloid-derived suppressor cells and efficacy of cytokine-induced killer cell immunotherapy in metastatic renal cell carcinoma patients. *J Immunother* 2014; 37: 43–50.
50 Tadmor T, Fell R, Polliack A, *et al.* Absolute monocytosis at diagnosis correlates with survival in diffuse large B-cell lymphoma-possible link with monocytic myeloid-derived suppressor cells. *Hematol Oncol* 2013; 31: 65–71.
51 Weide B, Martens A, Zelba H, *et al.* Myeloid-derived suppressor cells predict survival of patients with advanced melanoma: comparison with regulatory T-cells and NY-ESO-1- or melan-A-specific T-cells. *Clin Cancer Res* 2014; 20: 1601–1609.
52 Vasquez-Dunddel D, Pan F, Zeng Q, *et al.* STAT3 regulates arginase-I in myeloid-derived suppressor cells from cancer patients. *J Clin Invest* 2013; 123: 1580–1589.
53 Rodriguez PC, Ernstoff MS, Hernandez C, *et al.* Arginase I-producing myeloid-derived suppressor cells in renal cell carcinoma are a subpopulation of activated granulocytes. *Cancer Res* 2009; 69: 1553–1560.
54 Wang L, Chang EW, Wong SC, *et al.* Increased myeloid-derived suppressor cells in gastric cancer correlate with cancer stage and plasma S100A8/A9 proinflammatory proteins. *J Immunol* 2013; 190: 794–804.
55 Yu J, Du W, Yan F, *et al.* Myeloid-derived suppressor cells suppress antitumor immune responses through IDO expression and correlate with lymph node metastasis in patients with breast cancer. *J Immunol* 2013; 190: 3783–3797.
56 Schilling B, Sucker A, Griewank K, *et al.* Vemurafenib reverses immunosuppression by myeloid derived suppressor cells. *Int J Cancer* 2013; 133: 1653–1663.
57 Verma C, Eremin JM, Robins A, *et al.* Abnormal T-regulatory cells (Tregs: FOXP3+, CTLA-4+), myeloid-derived suppressor cells (MDSCs: monocytic, granulocytic) and polarised T-helper cell profiles (Th1, Th2, Th17) in women with large and locally advanced breast cancers undergoing neoadjuvant chemotherapy (NAC) and surgery: failure of abolition of abnormal treg profile with treatment and correlation of treg levels with pathological response to NAC. *J Transl Med* 2013; 11: 16.
58 Iclozan C, Antonia S, Chiappori A, *et al.* Therapeutic regulation of myeloid-derived suppressor cells and immune response to cancer vaccine in patients with extensive stage small cell lung cancer. *Cancer Immunol Immunother* 2013; 62: 909–918.
59 Mirza N, Fishman M, Fricke I, *et al.* All-trans-retinoic acid improves differentiation of myeloid cells and immune response in cancer patients. *Cancer Res* 2006; 66: 9299–9307.

Review

Systems medicine advances in interstitial lung disease

Greiffo FR, Eickelberg O, and Fernandez IE. European Respiratory Review, 26 (145). doi: 10.1183/16000617.0021-2017. (2017).

Systems medicine advances in interstitial lung disease

Flavia R. Greiffo[1], Oliver Eickelberg[1,2] and Isis E. Fernandez[1]

Affiliations: [1]Comprehensive Pneumology Center, Ludwig-Maximilians-Universität, University Hospital Grosshadern and Helmholtz Zentrum München and Member of the German Center for Lung Research, Munich, Germany. [2]Division of Respiratory Sciences and Critical Care Medicine, Dept of Medicine, University of Colorado, Denver, CO, USA.

Correspondence: Isis E. Fernandez, Comprehensive Pneumology Center, Ludwig-Maximilians-Universität and Helmholtz Zentrum München, Max-Lebsche-Platz 31, 81377 Munich, Germany.
E-mail: isis.fernandez@helmholtz-muenchen.de

@ERSpublications
Systems medicine provides critical advances in understanding and molecular fingerprinting interstitial lung diseases http://ow.ly/phXg30dWVvv

Cite this article as: Greiffo FR, Eickelberg O, Fernandez IE. Systems medicine advances in interstitial lung disease. *Eur Respir Rev* 2017; 26: 170021 [https://doi.org/10.1183/16000617.0021-2017].

ABSTRACT Fibrotic lung diseases involve subject–environment interactions, together with dysregulated homeostatic processes, impaired DNA repair and distorted immune functions. Systems medicine-based approaches are used to analyse diseases in a holistic manner, by integrating systems biology platforms along with clinical parameters, for the purpose of understanding disease origin, progression, exacerbation and remission.

Interstitial lung diseases (ILDs) refer to a heterogeneous group of complex fibrotic diseases. The increase of systems medicine-based approaches in the understanding of ILDs provides exceptional advantages by improving diagnostics, unravelling phenotypical differences, and stratifying patient populations by predictable outcomes and personalised treatments. This review discusses the state-of-the-art contributions of systems medicine-based approaches in ILDs over the past 5 years.

Introduction

Interstitial lung diseases (ILDs) are fibrosing diseases, characterised by a reversible or nonreversible limitation in the gas exchange capacity of the lung, induced by known or unknown causes. This occurs as a secondary effect to the excessive accumulation of cells from distinct sources (*e.g.* mesenchymal, epithelial and inflammatory), wound healing products and extracellular matrix (ECM) in the lung interstitium. ILDs refer to a large group of diseases with a high mortality index, overlapping clinical features, unpredictable clinical progression and no available curative therapies, as is the case for idiopathic pulmonary fibrosis (IPF) [1, 2].

Systems biology is a biology-based interdisciplinary area that studies complex interactions within biological systems, using a holistic approach to biological research. Driven by high-throughput "omic" technologies, it enables multiscale and insightful overviews of cells, organisms and populations. Systems medicine integrates systems biology into modelling of pathological mechanisms, along with clinical parameters. Dynamic analysis between clinical and omics-generated data through bioinformatic and computational tools helps to dissect altered pathways, and to understand disease establishment, progression and remission [3].

Received: March 13 2017 | Accepted after revision: June 15 2017

Support statement: Funding was received from the Helmholtz-Gemeinschaft. Funding information for this article has been deposited with the Crossref Funder Registry.

Conflict of interest: Disclosures can be found alongside this article at err.ersjournals.com

Provenance: Submitted article, peer reviewed.

The application of systems medicine to ILDs seeks to analyse their heterogeneity in a comprehensive manner, with the purpose of identifying biomarkers and genetic factors that improve disease understanding from the physio-pathological and clinical perspectives. While there are many key studies that have increased our knowledge of IPF and other ILDs, this article concisely focuses on omic-related studies, which contributed to the field during the past 5 years. Contributions published prior to this time frame were comprehensively reviewed in 2012 by Herazo-Maya and Kaminski [4].

Systems medicine and ILDs

With scientific advancement and accessibility at reasonable costs, the widespread use of high-throughput omic technologies has increased greatly over the last decade. This phenomenon has had a major impact on our understanding of multiple diseases, where omic-generated data have led to a personalised approach, decreasing mortality and improving survival, *e.g.* in the case of *HER2* (human epidermal growth factor receptor type 2)-positive breast cancer patients or *EGFR* (epidermal growth factor receptor)-mutated patients. Omic-driven personalised medicine has the potential to allow individualised treatment selection, determined by specific characteristics of the patient and disease.

There are overlapping similarities among ILDs subtypes, complicating the precise diagnosis and representing a daily challenge in clinical practice. The available treatment options are limited, increasing the need for molecular fingerprinting of patient populations. Thus, this complex and heterogeneous group of diseases requires the integrated approach of systems medicine to clearly discriminate and better understand them. We consider that advances in multiplex approaches allow us to glimpse critical players in these biological systems (figure 1). However, confirmatory testing of individual interactions is critical to demonstrate the importance at the molecular, cellular and organism level. A combination of holistic and traditional reductionist approaches will thus be needed for further understanding this multifaceted disease process.

Systems medicine in IPF

IPF has the worst prognosis of all ILDs, with a median survival of 3–5 years after diagnosis and no curative treatment available [2, 5]. Distinct clinical phenotypes with different patterns of survival have being described in IPF [5]. Therefore, systems medicine represents a new era for IPF. Interesting biomarkers have been discovered using omic analysis (table 1) and the challenge now is to establish them in routine clinical practice. Currently, only clinical and physiological changes are used to characterise disease progression.

Genomics and transcriptomics

Advances in genomic techniques have allowed high-throughput analysis and discovery of gene deregulation in IPF [6]. In particular, genetic studies have contributed to a better understanding of IPF, *e.g.* the expression of *MUC5B* (mucin 5B) and *TOLLIP* (Toll-interacting protein) [7–9]. Polymorphism in the promoter region of *MUC5B* (rs35705950) is associated with a higher likelihood of IPF development, although patients carrying this allele present a milder disease course and improved survival [7]. *MUC5B* was found expressed in areas of microscopic honeycombing and honeycomb cysts [8]. To date, the precise role of *MUC5B* in the pathophysiology of IPF is unclear.

Furthermore, variants in *TOLLIP* have also been linked to susceptibility and treatment responses in IPF. Single nucleotide polymorphisms within *TOLLIP* (rs5743890/rs3750920) are associated with increased mortality risk (rs5743890) and better response to *N*-acetylcysteine treatment (rs3750920) in IPF patients [9, 10]. Similarly, *DSP* (desmoplakin) variance (rs2076295) is associated with increased risk of IPF. *MUC5B* and *DSP* expression in the lung, especially in the airway epithelium, indicates the contribution of the aberrant epithelium in IPF [11].

Most IPF cases are sporadic. However, genetic variations also include an autosomal dominance pattern of inheritance, leading to familial pulmonary fibrosis. Several studies showed a strong relationship between familial IPF and telomerase mutations and their shortening. Recently, a prospective study performed genetic evaluations of IPF patients and affected relatives, and confirmed a strong relationship between familial IPF and telomerase mutations and shortening [12, 13]. Several studies have reported that familial IPF is associated with variances of the genes *TERT* (telomerase reverse transcriptase), *TERC* (telomerase RNA component), *DKC1* (dyskerin pseudouridine synthase 1), *TINF2* (TERF1 interacting nuclear factor 2), *RTEL1* (regulator of telomere elongation helicase 1) and *PARN* (poly(A)-specific RNase) [12, 13]. Familial IPF also presents mutations within surfactant protein-encoding genes *SFTPA2* (surfactant protein A2) and *SFTPC* (surfactant protein C), and *ABCA3* (ATP-binding cassette subfamily A member 3) [12, 14].

MicroRNAs (miRNAs) are small noncoding RNAs involved in the regulation of gene and protein expression, thus altering cellular phenotypes. IPF patients display downregulation of miRNA levels in

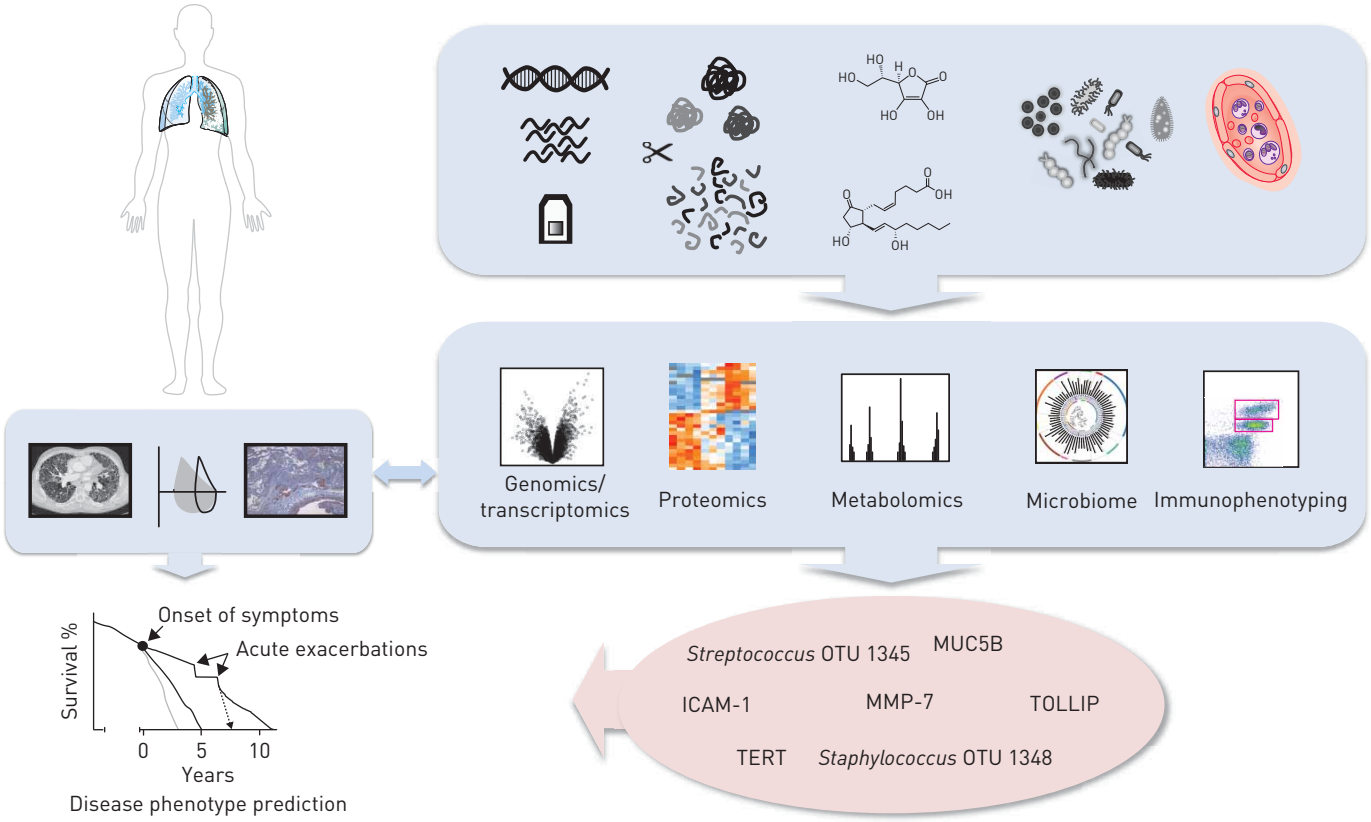

FIGURE 1 Systems medicine-based approaches in interstitial lung diseases seek to analyse biological products (*e.g.* RNA, DNA, proteins, metabolites, microbiome, *etc.*) and, through massive data generation and integration with clinical features, help to identify biomarkers that can predict disease phenotypes. OTU: operational taxonomic unit; MUC5B: mucin 5B; ICAM-1: intracellular adhesion molecule-1; MMP-7: metalloproteinase-7; TOLLIP: Toll-interacting protein; TERT: telomerase reverse transcriptase.

members of the let-7, mir-29 and mir-30 families, and upregulation in members of the mir-155 and mir-21 families, which modulate biological pathways and modify the IPF phenotype [15]. Altered expression of let-7 family members leads to changes in epithelial–mesenchymal transition in lung epithelial cells and inhibition of mir-21 modulates fibrosis [15]. mir-29 is also being explored as a potential target for IPF therapy as it decreases collagen expression in fibrotic lungs [16].

Moreover, IPF shares features with other chronic lung diseases, such as chronic obstructive pulmonary disease (COPD), where the molecular mechanism of lung injury leads to airway fibrosis. Kusko *et al.* [17] revealed a shared mRNA–miRNA transcriptional network between IPF and COPD. Specifically, upregulation of mir-96 in both diseases may control part of the shared disease gene expression network. Kusko *et al.* [17] describe overexpression of mir-96 as a key novel regulator of p53 expression in both epithelial cells and fibroblasts, which modulates the expression of genes related to the "emphysema–IPF" gene network [17]. Currently, miRNA therapy is being explored as a therapeutic option in diverse fibrotic conditions.

Cell-based RNA genomics can also provide an insight into disease features and targetable molecules. In line with the study by Kusko *et al.* [17], single-cell RNA sequencing analysis of IPF and control lungs identified the cross-talk of four distinct lung epithelial cell subtypes (alveolar type 2, goblet, basal and indeterminate) [18]. Xu *et al.* [18] showed that cells isolated from IPF patients express genes associated with activation of canonical transforming growth factor (TGF)-β, HIPPO/YAP, PI3K/AKT, p53 and WNT signalling cascades, which are activated in an integrated network [18]. Myofibroblast differentiation and massive ECM deposition are both ideal targetable phenomena in fibrotic diseases [19]. Parker *et al.* [19] used fibroblasts to explore at the RNA level how proteins present in the ECM of acellular lungs can provoke a feedback loop to normal living cells exposed to an aberrant environment. The results suggest that characterisation of lung proteins, specifically the lung fibrotic ECM, will help to not only determine its composition, but also to define targetable molecules for advanced stages of fibrosis [19].

Advances in genomic technologies show an exciting time ahead, where analysis of the genetic makeup of IPF patients will dictate therapeutic approaches and predict disease outcome. Hence, implementing routine

TABLE 1 Potential interstitial lung disease (ILD) targets identified through systems medicine-based approaches

	Target	Reference(s)
IPF		
Genomics	*MUC5B*	[7, 8]
	TOLLIP	[9]
	let-7, mir-30, mir-155, mir-21	[15]
	mir-29	[15, 16]
Proteomics	CCL24, surfactant protein A2, NF-κB, peroxisome proliferator-activated receptor-γ	[20–22]
	Platelet-derived growth factor receptor-α	[23]
	Ficolin-2, cathepsin-S, legumain, inducible T-cell costimulator, trypsin-3	[25]
Metabolomics	Ornithine	[27]
	Lactate dehydrogenase-5	[28]
	6-Phosphofructo-2-kinase/fructose-2,6-biphosphatase 3	[51]
Microbiome	*Staphylococcus* OTU 1348	[30–32]
	Streptococcus OTU 1345	[30]
Peripheral blood phenotyping	Metalloproteinase-7	[33]
	CD28, inducible T-cell costimulator, lymphocyte-specific protein tyrosine kinase, interleukin-2 inducible T-cell kinase	[34, 35]
	Neoepitopes BGM, C1M, C3M, C5M, C6M, CRPM	[36]
	Plasma B-lymphocyte stimulating factor, B-cells	[37]
	Myeloid-derived suppressor cells	[38]
Familial IPF		
Genomics	*TERT*, *TERC*, *DKC1*, *TINF2*, *RTEL1*, *PARN*	[12, 13]
	SFTPA2, *SFTPC*, *ABCA3*	[12, 14]
Non-IPF ILDs		
Genomics	Telomere length	[43]
	RTEL1	[44]
	DPP9, *DSP*, *FAM13A*, *IVD*, *DISP2*, *OBFC1*, *ATP11A*, *MUC2*	[45]
	ADAMTS4, *ADAMTS9*, *AGER*, *HIF1A*, *SERPINE2*, *SELE*, *RTKN2*, *PI15*	[48]

IPF: idiopathic pulmonary fibrosis; OTU: operational taxonomic unit. See main text for further details of gene symbols.

clinical genotyping and biomarker testing is essential for future patient stratification and personalised treatment.

Proteomics

As a substantial part of systems medicine, proteomics covers information on protein abundance, variation and modification, including their partners and networks, in order to explain cellular processes. Given the impact of aberrant biological processes in IPF, proteomics analysis provides global protein quantification as a critical tool to identify disease-driving molecules and potential targets. The most universal and powerful method for global protein measurement is mass spectrometry, which uses liquid chromatography together with high-resolution tandem mass spectrometry to identify and quantify peptides at a large scale. These techniques, together with bioinformatic tools, contribute to a better understanding of protein biochemistry, nature and interaction.

It is possible that many of the proteins dysregulated in IPF may not cross the lung endothelial barrier or become diluted out by more abundant constituents, thus being undetectable in plasma [20]. Based on this concept, initial studies with proteomics in IPF have been primarily performed in bronchoalveolar lavage fluid (BALF). Osteopontin has been a more strongly validated marker increased in the BALF of IPF patients. Other targets have also been associated with disease, *e.g.* the CC chemokine ligand CCL24, surfactant protein A2, and transcriptional factors NF-κB, peroxisome proliferator-activated receptor-γ and c-Myc [20–22]. Recently, it was reported from proteomics analysis of fibroblast surface fractions that platelet-derived growth factor receptor (PDGFR)-α expression was altered by pro-fibrotic TGF-β in lung

fibroblasts from IPF patients [23]. The authors suggest a potential cross-talk between two critical signalling pathways in fibrosis, *i.e.* TGF-β/PDGFR-α, which affects myofibroblast differentiation in the context of IPF [23], currently insufficiently targeted by approved therapies.

In an iTRAQ (isobaric tag for relative and absolute quantitation)-based proteomics study, Niu *et al.* [24] identified a set of proteins in the serum of IPF patients. The identified targets were related to the protein activation cascade, regulation of response to wounding and extracellular components (see table 1). Unfortunately, no correlation with clinical parameters was performed. Recently, using a 1129-analyte SOMAmer (slow off-rate modified aptamer) array in IPF plasma, a six-analyte index predicted better progression-free survival in IPF. Specifically, high levels of ficolin-2, cathepsin-S, legumain and soluble vascular endothelial growth factor receptor-2, and low levels of inducible T-cell costimulator (ICOS) or trypsin-3 were associated with IPF progression [25]. The use of this index should be further validated in independent cohorts for general applicability.

Metabolomics

Metabolites are the second product of metabolic reactions catalysed by enzymes that naturally occur in the cells, complementing gene and protein expression [26]. Metabolic changes of the lung are involved in IPF pathogenesis, as reported by Kang *et al.* [27]. IPF presented 25 metabolite signatures, which indicated alteration in metabolic pathways of ATP degradation, glycolysis, glutathione biosynthesis and ornithine aminotransferase pathways [27]. Interestingly, ornithine has a negative correlation with forced vital capacity (FVC), suggesting the potential role of ornithine in IPF pathophysiology [27]. Moreover, lactic acid levels and lactate dehydrogenase (LDH)-5 levels were elevated in IPF lungs when compared with controls [28]. Increased levels of LDH-5 activate the TGF-β pathway, inducing myofibroblast differentiation [28].

Microbiome

The human microbiota consists of 10–100 trillion symbiotic microbial cells in a single individual; however, little is known about the contribution of the microbiome to health and disease. Recently, it was reported that IPF patients have higher bacterial load in BALF when compared with controls and the increased bacterial load identifies patients with more rapidly progressive disease [29]. Interestingly, Molyneaux *et al.* [29] found bacterial burden to be independent of *MUC5B* genotype, suggesting a direct connection between host immunity and bacterial load [29]. In addition, it has been described in the COMET cohort that microbial signatures of *Staphylococcus* and *Streptococcus* help predict IPF progression [30]. Disease progression was significantly associated with increased abundance of two specific strains of *Staphylococcus* and *Streptococcus*. The study determined two operational taxonomic units (OTUs) associated with disease progression: *Staphylococcus* OTU 1348 and *Streptococcus* OTU 1345 [30]. This altered microbiome persists over time, which may implicate bacterial communities localised in the lower airways as persistent stimuli for repetitive alveolar injury in IPF [31]. IPF patients from the COMET cohort showed interactions between the host microbiome and progression-free survival [32]. Downregulation of the immune response was associated with changes in the abundance of *Staphylococcus* OTU 1348, which correlated with alterations in circulating leukocyte phenotypes, expression of several Toll-like receptors and fibroblast responsiveness [32].

Peripheral blood phenotyping

In the past, the role of the immune system in IPF has been controversial. However, increasing contributions indicate multiple alterations in the immune compartment of IPF patients, raising interest in the field. The peripheral blood compartment provides an easily accessible liquid biopsy, highly practical to study molecules and cell types as potential biomarkers. IPF patients have an increase in circulating biomarkers, *e.g.* CCL18, metalloproteinase (MMP)-7 and soluble intracellular adhesion molecule-1. To date, MMP-7 is the most validated biomarker to adopt clinically for diagnosis and prognostic evaluation of IPF [33]. Recently, several studies have validated the immunosuppressive environment present in the peripheral blood of IPF patients, showing that the gene expression of CD28, ICOS, lymphocyte-specific protein tyrosine kinase and interleukin-2 inducible T-cell kinase can predict outcome in IPF [34, 35].

In PROFILE, the largest IPF biomarker cohort studied globally, Jenkins *et al.* [36] showed changes in serum concentrations of proteolytically cleaved protein fragments/neopitopes. Levels of fragmented proteins generated by MMP activity and collagen synthesis in the serum of IPF patients were associated with IPF progression, as well as survival rate [36]. Immune cell type dysfunction has also been implicated in IPF. Abnormal B-cells and B-cell stimulator factor are often present in IPF patients, and are highly associated with disease manifestations and patient outcome [37]. Furthermore, myeloid-derived suppressor cells were described as a potent biomarker for IPF, where increased numbers of myeloid-derived suppressor cells measured in the blood of IPF patients correlated with lung function in cross-sectional and longitudinal analysis [38].

Omics in non-IPF ILDs

Non-IPF ILDs are defined by a large group of diseases classified by know causes or associations, *e.g.* idiopathic interstitial pneumonias (IIPs), granulomatous and other forms of ILDs [39]. The majority of non-IPF ILDs are idiopathic nonspecific interstitial pneumonia (NSIP), hypersensitivity pneumonitis, connective tissue disease-associated ILD and sarcoidosis. These diffuse parenchymal lung diseases affect the interstitium of the lung, distort pulmonary architecture and alter the gas exchange ability of the lung. ILDs can have associated causes, or not, but once scarring occurs, it is irreversible. The heterogeneity of non-IPF ILDs is extremely complex, with multiple common features and a high overlap in clinical, radiological and pathological patterns. Therefore, diagnosis requires a multidisciplinary approach and, in some cases, surgical lung biopsy, thus increasing mortality risk [40]. This highlights the need for integrated systems biology platforms to determine the molecular fingerprinting that improves diagnostic accuracy and provides novel targetable molecules.

Kim *et al.* [41] used integrative clustering analysis to integrate multi-omics data and propose an integrative phenotyping framework for identification of disease subtypes. Well-characterised clinical data, mRNA and miRNA profiles were integrated and visualised. Applying this method, clusters of homogeneous disease presentations and intermediate disease characteristics were identified. Validation of this open-access tool with other datasets is needed to support wide clinical usage. The integration of multi-omics data (*e.g.* proteomic, metabolomic, genomic and clinical data) provides a holistic integration of disease-related pathways at multiple levels, giving a futuristic perspective of understanding disease [41]. Using machine learning approaches with high-dimensional transcriptional data, a genomic signature could cluster ILD patients (IIP, NSIP, hypersensitivity pneumonitis and sarcoidosis) with a specificity of 92% (95% CI 81–100%) and a sensitivity of 82% (95% CI 64–95%) for microarray analysis, and a specificity of 95% (95% CI 84–100) and a sensitivity of 59% (95% CI 35–82%) for RNA sequencing. This study continues to support the need for better and less invasive diagnostic methods for ILDs patients [42]. Additionally, telomere length has been shown to be relevant in different ILDs. Telomeres are shorter in ILDs patients when compared with healthy controls, and even shorter in IPF when compared with other IIPs and sarcoidosis [43]. Moreover, a rare loss-of-function variant in *RTEL1* was found in peripheral blood mononuclear cells in one out of 25 families, representing a genetic predisposition for familiar interstitial pneumonia [44]. Fingerlin *et al.* [45] identified 10 risk loci for fibrotic IIP (fIIP), *e.g. DPP9* (dipeptidyl peptidase 9), *DSP*, *FAM13A* (family with sequence similarity 13 member A), *IVD* (isovaleryl-CoA dehydrogenase), *DISP2* (dispatched RND transporter family member 2), *OBFC1* (oligonucleotide/oligosaccharide-binding fold-containing protein 1), *ATP11A* (ATPase phospholipid transporting 11A) and *MUC2* (mucin 2), by genome-wide association studies. Furthermore, by imputing the data of genome-wide genotypes and conducting RNA sequencing studies, they identified new fIIP risk loci in lung tissue. Fibrotic lung tissue showed a deregulation in the human leukocyte antigen region of chromosome 6 (rs7887), involving and reaffirming the role of an immune deregulation in fibrotic ILDs [46].

Using the two-dimensional DIGE (difference in gel electrophoresis) technique and MALDI-TOF-MS (matrix assisted laser desorption ionisation-time of flight mass spectrometry), Korfei *et al.* [47] sought differences between IPF and fibrotic NSIP, reporting that differences in expression of only a few proteins exist between these two entities. Although it is currently a limited and low-sensitivity proteome measuring technique, the authors interestingly reported that intracellular clearance of reactive oxygen species and carbonyl proteins seems to be enhanced in NSIP, due to enhanced expression of antioxidant acting proteins, which may explain the better outcome and survival in patients with NSIP [47].

Assessing the relationship between changes in lung function parameters and gene expression is a helpful method to identify clinically relevant molecules implicated in disease. Steele *et al.* [48] used tissue gene expression profiling of IIPs to analyse differences and similarities among several IIPs, estimating the relationship between gene regulation and disease progression (using percentage predicted values for FVC and diffusing capacity of the lung for carbon monoxide). Some previously reported fibrotic targets were confirmed, *e.g. ADAMTS4* (ADAM metallopeptidase with thrombospondin type 1 motif 4), *ADAMTS9* (ADAM metallopeptidase with thrombospondin type 1 motif 9), *AGER* (advanced glycosylation end-product specific receptor), *HIF1A* (hypoxia inducible factor 1 α subunit), *SERPINE2* (serpin family E member 2) and *SELE* (selectin E), and novel candidates were identified, *e.g. RTKN2* (rhotekin 2) and *PI15* (peptidase inhibitor 15). Gene expression changes in those targets were significantly associated with lung function decline in moderate and severe IIP patients [48].

Conclusions

The pathobiology of pulmonary fibrosis involves adaptive and maladaptive pathways that work on multiple biological levels to disturb organ function. A comprehensive understanding of this complex interaction requires the integration of multiple data types: from DNA sequence variations to transcriptomics to

proteomics and ultimately phenomics, notwithstanding data obtained by classical physiology and pathology across different tissue and cell types. The speed of progress in science and technology applied to medicine in recent years has allowed several endotypes of diseases to be defined: from systems medicine-based approaches, leading to detection of specific targets that subclassify disease, to the possibility of offering personalised treatment, as is the case for EGFR in lung cancer.

Genome editing technologies, such as the CRISPR (clustered regularly interspaced palindromic repeat)-associated protein Cas9 (CRISPR-Cas9) system, provide hope that the discovery of critical gene regulators of disease can be applied to gene correction, such that CRISPR-Cas9-mediated gene correction could theoretically be offered for personalised treatments [49, 50]. Recently, Xie *et al.* [51] showed that glycolytic reprogramming is critical to lung myofibroblast differentiation and pulmonary fibrosis. Using CRISPR-Cas9 tools, inhibition of glycolysis was achieved by gene disruption of *PFKFB3* (6-phosphofructo-2-kinase/fructose-2,6-biphosphatase 3, a critical glycolytic enzyme). This example raises our hope that gene editing can be used for individualised therapeutics.

A combination of holistic and traditional reductionist experimental approaches will thus be required for the understanding of this multifaceted disease process. Notably, there are far more omics-related studies investigating IPF than other ILDs. Thus, community efforts must be invested in comprehensively characterising all ILDs, to learn more precisely about their common and distinctive features, and translate this gain of knowledge into more refined treatment options and better patient care than currently practised.

Acknowledgements

We thank the Helmholtz Association for supporting this work, and Thomas M. Conlon (Comprehensive Pneumology Center, Ludwig-Maximilians-Universität, University Hospital Grosshadern and Helmholtz Zentrum München and Member of the German Center for Lung Research, Munich, Germany) for language editing and proofreading the manuscript.

References

1 Travis WD, Costabel U, Hansell DM, *et al.* An official American Thoracic Society/European Respiratory Society statement: update of the international multidisciplinary classification of the idiopathic interstitial pneumonias. *Am J Respir Crit Care Med* 2013; 188: 733–748.
2 Fernandez IE, Eickelberg O. New cellular and molecular mechanisms of lung injury and fibrosis in idiopathic pulmonary fibrosis. *Lancet* 2012; 380: 680–688.
3 Capobianco E. Ten challenges for systems medicine. *Front Genet* 2012; 3: 193.
4 Herazo-Maya JD, Kaminski N. Personalized medicine: applying 'omics' to lung fibrosis. *Biomark Med* 2012; 6: 529–540.
5 Raghu G, Collard HR, Egan JJ, *et al.* An official ATS/ERS/JRS/ALAT statement: idiopathic pulmonary fibrosis: evidence-based guidelines for diagnosis and management. *Am J Respir Crit Care Med* 2011; 183: 788–824.
6 Kass DJ, Kaminski N. Evolving genomic approaches to idiopathic pulmonary fibrosis: moving beyond genes. *Clin Transl Sci* 2011; 4: 372–379.
7 Peljto AL, Zhang Y, Fingerlin TE, *et al.* Association between the *MUC5B* promoter polymorphism and survival in patients with idiopathic pulmonary fibrosis. *JAMA* 2013; 309: 2232–2239.
8 Seibold MA, Wise AL, Speer MC, *et al.* A common *MUC5B* promoter polymorphism and pulmonary fibrosis. *N Engl J Med* 2011; 364: 1503–1512.
9 Noth I, Zhang Y, Ma SF, *et al.* Genetic variants associated with idiopathic pulmonary fibrosis susceptibility and mortality: a genome-wide association study. *Lancet Respir Med* 2013; 1: 309–317.
10 Oldham JM, Ma SF, Martinez FJ, *et al. TOLLIP*, *MUC5B*, and the response to *N*-acetylcysteine among individuals with idiopathic pulmonary fibrosis. *Am J Respir Crit Care Med* 2015; 192: 1475–1482.
11 Mathai SK, Pedersen BS, Smith K, *et al.* Desmoplakin variants are associated with idiopathic pulmonary fibrosis. *Am J Respir Crit Care Med* 2016; 193: 1151–1160.
12 Kropski JA, Young LR, Cogan JD, *et al.* Genetic evaluation and testing of patients and families with idiopathic pulmonary fibrosis. *Am J Respir Crit Care Med* 2017; 195: 1423–1428.
13 Stuart BD, Choi J, Zaidi S, *et al.* Exome sequencing links mutations in *PARN* and *RTEL1* with familial pulmonary fibrosis and telomere shortening. *Nat Genet* 2015; 47: 512–517.
14 Epaud R, Delestrain C, Louha M, *et al.* Combined pulmonary fibrosis and emphysema syndrome associated with *ABCA3* mutations. *Eur Respir J* 2014; 43: 638–641.
15 Pandit KV, Milosevic J, Kaminski N. MicroRNAs in idiopathic pulmonary fibrosis. *Transl Res* 2011; 157: 191–199.
16 Montgomery RL, Yu G, Latimer PA, *et al.* MicroRNA mimicry blocks pulmonary fibrosis. *EMBO Mol Med* 2014; 6: 1347–1356.
17 Kusko RL, Brothers JF II, Tedrow J, *et al.* Integrated genomics reveals convergent transcriptomic networks underlying chronic obstructive pulmonary disease and idiopathic pulmonary fibrosis. *Am J Respir Crit Care Med* 2016; 194: 948–960.
18 Xu Y, Mizuno T, Sridharan A, *et al.* Single-cell RNA sequencing identifies diverse roles of epithelial cells in idiopathic pulmonary fibrosis. *JCI Insight* 2016; 1: e90558.
19 Parker MW, Rossi D, Peterson M, *et al.* Fibrotic extracellular matrix activates a profibrotic positive feedback loop. *J Clin Invest* 2014; 124: 1622–1635.
20 Foster MW, Morrison LD, Todd JL, *et al.* Quantitative proteomics of bronchoalveolar lavage fluid in idiopathic pulmonary fibrosis. *J Proteome Res* 2015; 14: 1238–1249.
21 Carleo A, Bargagli E, Landi C, *et al.* Comparative proteomic analysis of bronchoalveolar lavage of familial and sporadic cases of idiopathic pulmonary fibrosis. *J Breath Res* 2016; 10: 026007.

22 Landi C, Bargagli E, Carleo A, *et al.* A system biology study of BALF from patients affected by idiopathic pulmonary fibrosis (IPF) and healthy controls. *Proteomics Clin Appl* 2014; 8: 932–950.
23 Heinzelmann K, Noskovicova N, Merl-Pham J, *et al.* Surface proteome analysis identifies platelet derived growth factor receptor-alpha as a critical mediator of transforming growth factor-beta-induced collagen secretion. *Int J Biochem Cell Biol* 2016; 74: 44–59.
24 Niu R, Liu Y, Zhang Y, *et al.* iTRAQ-based proteomics reveals novel biomarkers for idiopathic pulmonary fibrosis. *PLoS One* 2017; 12: e0170741.
25 Ashley SL, Xia M, Murray S, *et al.* Six-SOMAmer index relating to immune, protease and angiogenic functions predicts progression in IPF. *PLoS One* 2016; 11: e0159878.
26 Maplestone RA, Stone MJ, Williams DH. The evolutionary role of secondary metabolites – a review. *Gene* 1992; 115: 151–157.
27 Kang YP, Lee SB, Lee JM, *et al.* Metabolic profiling regarding pathogenesis of idiopathic pulmonary fibrosis. *J Proteome Res* 2016; 15: 1717–1724.
28 Kottmann RM, Kulkarni AA, Smolnycki KA, *et al.* Lactic acid is elevated in idiopathic pulmonary fibrosis and induces myofibroblast differentiation via pH-dependent activation of transforming growth factor-beta. *Am J Respir Crit Care Med* 2012; 186: 740–751.
29 Molyneaux PL, Cox MJ, Willis-Owen SA, *et al.* The role of bacteria in the pathogenesis and progression of idiopathic pulmonary fibrosis. *Am J Respir Crit Care Med* 2014; 190: 906–913.
30 Han MK, Zhou Y, Murray S, *et al.* Lung microbiome and disease progression in idiopathic pulmonary fibrosis: an analysis of the COMET study. *Lancet Respir Med* 2014; 2: 548–556.
31 Molyneaux PL, Willis Owen SA, Cox MJ, *et al.* Host–microbial interactions in idiopathic pulmonary fibrosis. *Am J Respir Crit Care Med* 2017; 195: 1640–1650.
32 Huang Y, Ma SF, Espindola MS, *et al.* Microbes associate with host innate immune response in idiopathic pulmonary fibrosis. *Am J Respir Crit Care Med* 2017; 196: 208–219.
33 Ley B, Collard HR, King TE Jr. Clinical course and prediction of survival in idiopathic pulmonary fibrosis. *Am J Respir Crit Care Med* 2011; 183: 431–440.
34 Herazo-Maya JD, Noth I, Duncan SR, *et al.* Peripheral blood mononuclear cell gene expression profiles predict poor outcome in idiopathic pulmonary fibrosis. *Sci Transl Med* 2013; 5: 205ra136.
35 Huang Y, Ma SF, Vij R, *et al.* A functional genomic model for predicting prognosis in idiopathic pulmonary fibrosis. *BMC Pulm Med* 2015; 15: 147.
36 Jenkins RG, Simpson JK, Saini G, *et al.* Longitudinal change in collagen degradation biomarkers in idiopathic pulmonary fibrosis: an analysis from the prospective, multicentre PROFILE study. *Lancet Respir Med* 2015; 3: 462–472.
37 Xue J, Kass DJ, Bon J, *et al.* Plasma B lymphocyte stimulator and B cell differentiation in idiopathic pulmonary fibrosis patients. *J Immunol* 2013; 191: 2089–2095.
38 Fernandez IE, Greiffo FR, Frankenberger M, *et al.* Peripheral blood myeloid-derived suppressor cells reflect disease status in idiopathic pulmonary fibrosis. *Eur Respir J* 2016; 48: 1171–1183.
39 du Bois RM. Strategies for treating idiopathic pulmonary fibrosis. *Nat Rev Drug Discov* 2010; 9: 129–140.
40 Hutchinson JP, Fogarty AW, McKeever TM, *et al.* In-hospital mortality following surgical lung biopsy for interstitial lung disease in the USA: 2000–2011. *Am J Respir Crit Care Med* 2016; 193: 1161–1167.
41 Kim S, Herazo-Maya JD, Kang DD, *et al.* Integrative phenotyping framework (iPF): integrative clustering of multiple omics data identifies novel lung disease subphenotypes. *BMC Genomics* 2015; 16: 924.
42 Kim SY, Diggans J, Pankratz D, *et al.* Classification of usual interstitial pneumonia in patients with interstitial lung disease: assessment of a machine learning approach using high-dimensional transcriptional data. *Lancet Respir Med* 2015; 3: 473–482.
43 Snetselaar R, van Moorsel CH, Kazemier KM, *et al.* Telomere length in interstitial lung diseases. *Chest* 2015; 148: 1011–1018.
44 Cogan JD, Kropski JA, Zhao M, *et al.* Rare variants in *RTEL1* are associated with familial interstitial pneumonia. *Am J Respir Crit Care Med* 2015; 191: 646–655.
45 Fingerlin TE, Murphy E, Zhang W, *et al.* Genome-wide association study identifies multiple susceptibility loci for pulmonary fibrosis. *Nat Genet* 2013; 45: 613–620.
46 Fingerlin TE, Zhang W, Yang IV, *et al.* Genome-wide imputation study identifies novel HLA locus for pulmonary fibrosis and potential role for auto-immunity in fibrotic idiopathic interstitial pneumonia. *BMC Genet* 2016; 17: 74.
47 Korfei M, von der Beck D, Henneke I, *et al.* Comparative proteome analysis of lung tissue from patients with idiopathic pulmonary fibrosis (IPF), non-specific interstitial pneumonia (NSIP) and organ donors. *J Proteomics* 2013; 85: 109–128.
48 Steele MP, Luna LG, Coldren CD, *et al.* Relationship between gene expression and lung function in idiopathic interstitial pneumonias. *BMC Genomics* 2015; 16: 869.
49 Doudna JA, Charpentier E. Genome editing. The new frontier of genome engineering with CRISPR-Cas9. *Science* 2014; 346: 1258096.
50 Sander JD, Joung JK. CRISPR-Cas systems for editing, regulating and targeting genomes. *Nat Biotechnol* 2014; 32: 347–355.
51 Xie N, Tan Z, Banerjee S, *et al.* Glycolytic reprogramming in myofibroblast differentiation and lung fibrosis. *Am J Respir Crit Care Med* 2015; 192: 1462–1474.

8. References

Alhamad, E. H., Lynch, J. P., 3rd, & Martinez, F. J. (2001). Pulmonary function tests in interstitial lung disease: what role do they have? *Clin Chest Med, 22*(4), 715-750, ix.

Allen, R. J., Porte, J., Braybrooke, R., Flores, C., Fingerlin, T. E., Oldham, J. M., . . . Jenkins, R. G. (2017). Genetic variants associated with susceptibility to idiopathic pulmonary fibrosis in people of European ancestry: a genome-wide association study. *Lancet Respir Med, 5*(11), 869-880. doi:10.1016/S2213-2600(17)30387-9

Arai, M., Ikawa, Y., Chujo, S., Hamaguchi, Y., Ishida, W., Shirasaki, F., . . . Takehara, K. (2013). Chemokine receptors CCR2 and CX3CR1 regulate skin fibrosis in the mouse model of cytokine-induced systemic sclerosis. *J Dermatol Sci, 69*(3), 250-258. doi:10.1016/j.jdermsci.2012.10.010

Aran, D., Looney, A. P., Liu, L., Wu, E., Fong, V., Hsu, A., . . . Bhattacharya, M. (2019). Reference-based analysis of lung single-cell sequencing reveals a transitional profibrotic macrophage. *Nat Immunol, 20*(2), 163-172. doi:10.1038/s41590-018-0276-y

Arkema, E. V., Grunewald, J., Kullberg, S., Eklund, A., & Askling, J. (2016). Sarcoidosis incidence and prevalence: a nationwide register-based assessment in Sweden. *Eur Respir J, 48*(6), 1690-1699. doi:10.1183/13993003.00477-2016

Armanios, M. Y., Chen, J. J., Cogan, J. D., Alder, J. K., Ingersoll, R. G., Markin, C., . . . Loyd, J. E. (2007). Telomerase mutations in families with idiopathic pulmonary fibrosis. *N Engl J Med, 356*(13), 1317-1326. doi:10.1056/NEJMoa066157

Auffray, C., Fogg, D., Garfa, M., Elain, G., Join-Lambert, O., Kayal, S., . . . Geissmann, F. (2007). Monitoring of blood vessels and tissues by a population of monocytes with patrolling behavior. *Science, 317*(5838), 666-670. doi:10.1126/science.1142883

Bagnato, G., & Harari, S. (2015). Cellular interactions in the pathogenesis of interstitial lung diseases. *Eur Respir Rev, 24*(135), 102-114. doi:10.1183/09059180.00003214

Barron, L., & Wynn, T. A. (2011). Fibrosis is regulated by Th2 and Th17 responses and by dynamic interactions between fibroblasts and macrophages. *Am J Physiol Gastrointest Liver Physiol, 300*(5), G723-728. doi:10.1152/ajpgi.00414.2010

Behr, J., Neuser, P., Prasse, A., Kreuter, M., Rabe, K., Schade-Brittinger, C., . . . Gunther, A. (2017). Exploring efficacy and safety of oral Pirfenidone for progressive, non-IPF lung fibrosis (RELIEF) - a randomized, double-blind, placebo-controlled, parallel group, multi-center, phase II trial. *BMC Pulm Med, 17*(1), 122. doi:10.1186/s12890-017-0462-y

Bonnans, C., Chou, J., & Werb, Z. (2014). Remodelling the extracellular matrix in development and disease. *Nat Rev Mol Cell Biol, 15*(12), 786-801. doi:10.1038/nrm3904

Booth, A. J., Hadley, R., Cornett, A. M., Dreffs, A. A., Matthes, S. A., Tsui, J. L., . . . White, E. S. (2012). Acellular normal and fibrotic human lung matrices as a culture system for in vitro investigation. *Am J Respir Crit Care Med, 186*(9), 866-876. doi:10.1164/rccm.201204-0754OC

Borie, R., Tabeze, L., Thabut, G., Nunes, H., Cottin, V., Marchand-Adam, S., . . . Crestani, B. (2016). Prevalence and characteristics of TERT and TERC mutations in suspected genetic pulmonary fibrosis. *Eur Respir J, 48*(6), 1721-1731. doi:10.1183/13993003.02115-2015

Bourke, S. J., Dalphin, J. C., Boyd, G., McSharry, C., Baldwin, C. I., & Calvert, J. E. (2001). Hypersensitivity pneumonitis: current concepts. *Eur Respir J Suppl, 32*, 81s-92s.

Boyette, L. B., Macedo, C., Hadi, K., Elinoff, B. D., Walters, J. T., Ramaswami, B., . . . Metes, D. M. (2017). Phenotype, function, and differentiation potential of human monocyte subsets. *PLoS One, 12*(4), e0176460. doi:10.1371/journal.pone.0176460

Brempelis, K. J., & Crispe, I. N. (2016). Infiltrating monocytes in liver injury and repair. *Clin Transl Immunology, 5*(11), e113. doi:10.1038/cti.2016.62

Camelo, A., Dunmore, R., Sleeman, M. A., & Clarke, D. L. (2014). The epithelium in idiopathic pulmonary fibrosis: breaking the barrier. *Front Pharmacol, 4*, 173. doi:10.3389/fphar.2013.00173

Canton, J., Neculai, D., & Grinstein, S. (2013). Scavenger receptors in homeostasis and immunity. *Nat Rev Immunol, 13*(9), 621-634. doi:10.1038/nri3515

Cardona, A. E., Sasse, M. E., Liu, L., Cardona, S. M., Mizutani, M., Savarin, C., . . . Ransohoff, R. M. (2008). Scavenging roles of chemokine receptors: chemokine receptor deficiency is associated with increased levels of ligand in circulation and tissues. *Blood, 112*(2), 256-263. doi:10.1182/blood-2007-10-118497

Chambers, D. C., Yusen, R. D., Cherikh, W. S., Goldfarb, S. B., Kucheryavaya, A. Y., Khusch, K., . . . Lung, T. (2017). The Registry of the International Society for Heart and Lung Transplantation: Thirty-fourth Adult Lung And Heart-Lung Transplantation Report-2017; Focus Theme: Allograft ischemic time. *J Heart Lung Transplant, 36*(10), 1047-1059. doi:10.1016/j.healun.2017.07.016

Clements, P. J., Roth, M. D., Elashoff, R., Tashkin, D. P., Goldin, J., Silver, R. M., . . . Scleroderma Lung Study, G. (2007). Scleroderma lung study (SLS): differences in the presentation and course of patients with limited versus diffuse systemic sclerosis. *Ann Rheum Dis, 66*(12), 1641-1647. doi:10.1136/ard.2007.069518

Corzo, C. A., Condamine, T., Lu, L., Cotter, M. J., Youn, J. I., Cheng, P., . . . Gabrilovich, D. I. (2010). HIF-1alpha regulates function and differentiation of myeloid-derived suppressor cells in the tumor microenvironment. *J Exp Med, 207*(11), 2439-2453. doi:10.1084/jem.20100587

Costabel, U., & Hunninghake, G. W. (1999). ATS/ERS/WASOG statement on sarcoidosis. Sarcoidosis Statement Committee. American Thoracic Society.

European Respiratory Society. World Association for Sarcoidosis and Other Granulomatous Disorders. *Eur Respir J, 14*(4), 735-737.

Cottin, V. (2016). Lung biopsy in interstitial lung disease: balancing the risk of surgery and diagnostic uncertainty. *Eur Respir J, 48*(5), 1274-1277. doi:10.1183/13993003.01633-2016

Cottin, V., Wollin, L., Fischer, A., Quaresma, M., Stowasser, S., & Harari, S. (2019). Fibrosing interstitial lung diseases: knowns and unknowns. *Eur Respir Rev, 28*(151). doi:10.1183/16000617.0100-2018

D'Haese, J. G., Demir, I. E., Friess, H., & Ceyhan, G. O. (2010). Fractalkine/CX3CR1: why a single chemokine-receptor duo bears a major and unique therapeutic potential. *Expert Opin Ther Targets, 14*(2), 207-219. doi:10.1517/14728220903540265

Damuzzo, V., Pinton, L., Desantis, G., Solito, S., Marigo, I., Bronte, V., & Mandruzzato, S. (2015). Complexity and challenges in defining myeloid-derived suppressor cells. *Cytometry B Clin Cytom, 88*(2), 77-91. doi:10.1002/cyto.b.21206

Das, A., Sinha, M., Datta, S., Abas, M., Chaffee, S., Sen, C. K., & Roy, S. (2015). Monocyte and macrophage plasticity in tissue repair and regeneration. *Am J Pathol, 185*(10), 2596-2606. doi:10.1016/j.ajpath.2015.06.001

Desai, O., Winkler, J., Minasyan, M., & Herzog, E. L. (2018). The Role of Immune and Inflammatory Cells in Idiopathic Pulmonary Fibrosis. *Front Med (Lausanne), 5*, 43. doi:10.3389/fmed.2018.00043

Dowman, L. M., McDonald, C. F., Hill, C. J., Lee, A. L., Barker, K., Boote, C., . . . Holland, A. E. (2017). The evidence of benefits of exercise training in interstitial lung disease: a randomised controlled trial. *Thorax, 72*(7), 610-619. doi:10.1136/thoraxjnl-2016-208638

du Plessis, N., Loebenberg, L., Kriel, M., von Groote-Bidlingmaier, F., Ribechini, E., Loxton, A. G., . . . Walzl, G. (2013). Increased frequency of myeloid-derived suppressor cells during active tuberculosis and after recent mycobacterium tuberculosis infection suppresses T-cell function. *Am J Respir Crit Care Med, 188*(6), 724-732. doi:10.1164/rccm.201302-0249OC

Ehrchen, J., Steinmuller, L., Barczyk, K., Tenbrock, K., Nacken, W., Eisenacher, M., . . . Roth, J. (2007). Glucocorticoids induce differentiation of a specifically activated, anti-inflammatory subtype of human monocytes. *Blood, 109*(3), 1265-1274. doi:10.1182/blood-2006-02-001115

Ellson, C. D., Dunmore, R., Hogaboam, C. M., Sleeman, M. A., & Murray, L. A. (2014). Danger-associated molecular patterns and danger signals in idiopathic pulmonary fibrosis. *Am J Respir Cell Mol Biol, 51*(2), 163-168. doi:10.1165/rcmb.2013-0366TR

Engblom, C., Pfirschke, C., & Pittet, M. J. (2016). The role of myeloid cells in cancer therapies. *Nat Rev Cancer, 16*(7), 447-462. doi:10.1038/nrc.2016.54

Espindola, M. S., Habiel, D. M., Narayanan, R., Jones, I., Coelho, A. L., Murray, L. A., . . . Hogaboam, C. M. (2018). Targeting of TAM Receptors Ameliorates Fibrotic Mechanisms in Idiopathic Pulmonary Fibrosis. *Am J Respir Crit Care Med*. doi:10.1164/rccm.201707-1519OC

Fabriek, B. O., van Bruggen, R., Deng, D. M., Ligtenberg, A. J., Nazmi, K., Schornagel, K., . . . van den Berg, T. K. (2009). The macrophage scavenger

receptor CD163 functions as an innate immune sensor for bacteria. *Blood, 113*(4), 887-892. doi:10.1182/blood-2008-07-167064

Feng, P. H., Lee, K. Y., Chang, Y. L., Chan, Y. F., Kuo, L. W., Lin, T. Y., . . . Kuo, H. P. (2012). CD14(+)S100A9(+) monocytic myeloid-derived suppressor cells and their clinical relevance in non-small cell lung cancer. *Am J Respir Crit Care Med, 186*(10), 1025-1036. doi:10.1164/rccm.201204-0636OC

Fernandez, I. E., Greiffo, F. R., Frankenberger, M., Bandres, J., Heinzelmann, K., Neurohr, C., . . . Eickelberg, O. (2016). Peripheral blood myeloid-derived suppressor cells reflect disease status in idiopathic pulmonary fibrosis. *Eur Respir J, 48*(4), 1171-1183. doi:10.1183/13993003.01826-2015

Fernandez Perez, E. R., Kong, A. M., Raimundo, K., Koelsch, T. L., Kulkarni, R., & Cole, A. L. (2018). Epidemiology of Hypersensitivity Pneumonitis among an Insured Population in the United States: A Claims-based Cohort Analysis. *Ann Am Thorac Soc, 15*(4), 460-469. doi:10.1513/AnnalsATS.201704-288OC

Fingerlin, T. E., Murphy, E., Zhang, W., Peljto, A. L., Brown, K. K., Steele, M. P., . . . Schwartz, D. A. (2013). Genome-wide association study identifies multiple susceptibility loci for pulmonary fibrosis. *Nat Genet, 45*(6), 613-620. doi:10.1038/ng.2609

Fischer, A., Antoniou, K. M., Brown, K. K., Cadranel, J., Corte, T. J., du Bois, R. M., . . . CTD-ILD, E. A. T. F. o. U. F. o. (2015). An official European Respiratory Society/American Thoracic Society research statement: interstitial pneumonia with autoimmune features. *Eur Respir J, 46*(4), 976-987. doi:10.1183/13993003.00150-2015

Fischer, A., & du Bois, R. (2012). Interstitial lung disease in connective tissue disorders. *Lancet, 380*(9842), 689-698. doi:10.1016/S0140-6736(12)61079-4

Flament, T., Bigot, A., Chaigne, B., Henique, H., Diot, E., & Marchand-Adam, S. (2016). Pulmonary manifestations of Sjogren's syndrome. *Eur Respir Rev, 25*(140), 110-123. doi:10.1183/16000617.0011-2016

Florez-Sampedro, L., Song, S., & Melgert, B. N. (2018). The diversity of myeloid immune cells shaping wound repair and fibrosis in the lung. *Regeneration (Oxf), 5*(1), 3-25. doi:10.1002/reg2.97

Frankenberger, M., Haussinger, K., & Ziegler-Heitbrock, L. (2005). Liposomal methylprednisolone differentially regulates the expression of TNF and IL-10 in human alveolar macrophages. *Int Immunopharmacol, 5*(2), 289-299. doi:10.1016/j.intimp.2004.09.033

Franklin, R. A., Liao, W., Sarkar, A., Kim, M. V., Bivona, M. R., Liu, K., . . . Li, M. O. (2014). The cellular and molecular origin of tumor-associated macrophages. *Science, 344*(6186), 921-925. doi:10.1126/science.1252510

Fujino, N., Kubo, H., & Maciewicz, R. A. (2017). Phenotypic screening identifies Axl kinase as a negative regulator of an alveolar epithelial cell phenotype. *Lab Invest, 97*(9), 1047-1062. doi:10.1038/labinvest.2017.52

Gabrilovich, D. I., & Nagaraj, S. (2009). Myeloid-derived suppressor cells as regulators of the immune system. *Nat Rev Immunol, 9*(3), 162-174. doi:10.1038/nri2506

Gamrekelashvili, J., Giagnorio, R., Jussofie, J., Soehnlein, O., Duchene, J., Briseno, C. G., . . . Limbourg, F. P. (2016). Regulation of monocyte cell fate by blood

vessels mediated by Notch signalling. *Nat Commun, 7*, 12597. doi:10.1038/ncomms12597

Ge, X. Y., Fang, S. P., Zhou, M., Luo, J., Wei, J., Wen, X. P., . . . Zou, Z. (2016). TLR4-dependent internalization of CX3CR1 aggravates sepsis-induced immunoparalysis. *Am J Transl Res, 8*(12), 5696-5705.

Geissmann, F., Jung, S., & Littman, D. R. (2003). Blood monocytes consist of two principal subsets with distinct migratory properties. *Immunity, 19*(1), 71-82.

Gilani, S. R., Vuga, L. J., Lindell, K. O., Gibson, K. F., Xue, J., Kaminski, N., . . . Duncan, S. R. (2010). CD28 down-regulation on circulating CD4 T-cells is associated with poor prognoses of patients with idiopathic pulmonary fibrosis. *PLoS One, 5*(1), e8959. doi:10.1371/journal.pone.0008959

Ginhoux, F., & Jung, S. (2014). Monocytes and macrophages: developmental pathways and tissue homeostasis. *Nat Rev Immunol, 14*(6), 392-404. doi:10.1038/nri3671

Greiffo, F. R., Eickelberg, O., & Fernandez, I. E. (2017). Systems medicine advances in interstitial lung disease. *Eur Respir Rev, 26*(145). doi:10.1183/16000617.0021-2017

Gross, T. J., & Hunninghake, G. W. (2001). Idiopathic pulmonary fibrosis. *N Engl J Med, 345*(7), 517-525. doi:10.1056/NEJMra003200

Guiot, J., Moermans, C., Henket, M., Corhay, J. L., & Louis, R. (2017). Blood Biomarkers in Idiopathic Pulmonary Fibrosis. *Lung, 195*(3), 273-280. doi:10.1007/s00408-017-9993-5

Heinzelmann, K., Noskovicova, N., Merl-Pham, J., Preissler, G., Winter, H., Lindner, M., . . . Eickelberg, O. (2016). Surface proteome analysis identifies platelet derived growth factor receptor-alpha as a critical mediator of transforming growth factor-beta-induced collagen secretion. *Int J Biochem Cell Biol, 74*, 44-59. doi:10.1016/j.biocel.2016.02.013

Herazo-Maya, J. D., Noth, I., Duncan, S. R., Kim, S., Ma, S. F., Tseng, G. C., . . . Kaminski, N. (2013). Peripheral blood mononuclear cell gene expression profiles predict poor outcome in idiopathic pulmonary fibrosis. *Sci Transl Med, 5*(205), 205ra136. doi:10.1126/scitranslmed.3005964

Hochheiser, K., Heuser, C., Krause, T. A., Teteris, S., Ilias, A., Weisheit, C., . . . Kurts, C. (2013). Exclusive CX3CR1 dependence of kidney DCs impacts glomerulonephritis progression. *J Clin Invest, 123*(10), 4242-4254. doi:10.1172/JCI70143

Hoffmann-Vold, A. M., Weigt, S. S., Palchevskiy, V., Volkmann, E., Saggar, R., Li, N., . . . Belperio, J. A. (2018). Augmented concentrations of CX3CL1 are associated with interstitial lung disease in systemic sclerosis. *PLoS One, 13*(11), e0206545. doi:10.1371/journal.pone.0206545

Horan, G. S., Wood, S., Ona, V., Li, D. J., Lukashev, M. E., Weinreb, P. H., . . . Violette, S. M. (2008). Partial inhibition of integrin alpha(v)beta6 prevents pulmonary fibrosis without exacerbating inflammation. *Am J Respir Crit Care Med, 177*(1), 56-65. doi:10.1164/rccm.200706-805OC

Hundhausen, C., Misztela, D., Berkhout, T. A., Broadway, N., Saftig, P., Reiss, K., . . . Ludwig, A. (2003). The disintegrin-like metalloproteinase ADAM10 is involved in constitutive cleavage of CX3CL1 (fractalkine) and regulates CX3CL1-

mediated cell-cell adhesion. *Blood, 102*(4), 1186-1195. doi:10.1182/blood-2002-12-3775

Hutchinson, J., Fogarty, A., Hubbard, R., & McKeever, T. (2015). Global incidence and mortality of idiopathic pulmonary fibrosis: a systematic review. *Eur Respir J, 46*(3), 795-806. doi:10.1183/09031936.00185114

Iannuzzi, M. C., Rybicki, B. A., & Teirstein, A. S. (2007). Sarcoidosis. *N Engl J Med, 357*(21), 2153-2165. doi:10.1056/NEJMra071714

Ikezoe, K., Handa, T., Mori, K., Watanabe, K., Tanizawa, K., Aihara, K., . . . Mishima, M. (2014). Neutrophil gelatinase-associated lipocalin in idiopathic pulmonary fibrosis. *Eur Respir J, 43*(6), 1807-1809. doi:10.1183/09031936.00192613

Ishida, Y., Gao, J. L., & Murphy, P. M. (2008). Chemokine receptor CX3CR1 mediates skin wound healing by promoting macrophage and fibroblast accumulation and function. *J Immunol, 180*(1), 569-579.

Ishida, Y., Kimura, A., Nosaka, M., Kuninaka, Y., Hemmi, H., Sasaki, I., . . . Kondo, T. (2017). Essential involvement of the CX3CL1-CX3CR1 axis in bleomycin-induced pulmonary fibrosis via regulation of fibrocyte and M2 macrophage migration. *Sci Rep, 7*(1), 16833. doi:10.1038/s41598-017-17007-8

Jegal, Y., Kim, D. S., Shim, T. S., Lim, C. M., Do Lee, S., Koh, Y., . . . Colby, T. V. (2005). Physiology is a stronger predictor of survival than pathology in fibrotic interstitial pneumonia. *Am J Respir Crit Care Med, 171*(6), 639-644. doi:10.1164/rccm.200403-331OC

Jung, S. (2018). Macrophages and monocytes in 2017: Macrophages and monocytes: of tortoises and hares. *Nat Rev Immunol, 18*(2), 85-86. doi:10.1038/nri.2017.158

Kalathil, S. G., Lugade, A. A., Pradhan, V., Miller, A., Parameswaran, G. I., Sethi, S., & Thanavala, Y. (2014). T-regulatory cells and programmed death 1+ T cells contribute to effector T-cell dysfunction in patients with chronic obstructive pulmonary disease. *Am J Respir Crit Care Med, 190*(1), 40-50. doi:10.1164/rccm.201312-2293OC

Kawanaka, N., Yamamura, M., Aita, T., Morita, Y., Okamoto, A., Kawashima, M., . . . Makino, H. (2002). CD14+,CD16+ blood monocytes and joint inflammation in rheumatoid arthritis. *Arthritis Rheum, 46*(10), 2578-2586. doi:10.1002/art.10545

King, T. E., Jr., Bradford, W. Z., Castro-Bernardini, S., Fagan, E. A., Glaspole, I., Glassberg, M. K., . . . Group, A. S. (2014). A phase 3 trial of pirfenidone in patients with idiopathic pulmonary fibrosis. *N Engl J Med, 370*(22), 2083-2092. doi:10.1056/NEJMoa1402582

Kocheril, S. V., Appleton, B. E., Somers, E. C., Kazerooni, E. A., Flaherty, K. R., Martinez, F. J., . . . Crofford, L. J. (2005). Comparison of disease progression and mortality of connective tissue disease-related interstitial lung disease and idiopathic interstitial pneumonia. *Arthritis Rheum, 53*(4), 549-557. doi:10.1002/art.21322

Kolahian, S., Fernandez, I. E., Eickelberg, O., & Hartl, D. (2016). Immune Mechanisms in Pulmonary Fibrosis. *Am J Respir Cell Mol Biol, 55*(3), 309-322. doi:10.1165/rcmb.2016-0121TR

Kostlin, N., Kugel, H., Spring, B., Leiber, A., Marme, A., Henes, M., . . . Gille, C. (2014). Granulocytic myeloid derived suppressor cells expand in human

pregnancy and modulate T-cell responses. *Eur J Immunol, 44*(9), 2582-2591. doi:10.1002/eji.201344200

Kotsianidis, I., Nakou, E., Bouchliou, I., Tzouvelekis, A., Spanoudakis, E., Steiropoulos, P., . . . Bouros, D. (2009). Global impairment of CD4+CD25+FOXP3+ regulatory T cells in idiopathic pulmonary fibrosis. *Am J Respir Crit Care Med, 179*(12), 1121-1130. doi:10.1164/rccm.200812-1936OC

Landsman, L., Bar-On, L., Zernecke, A., Kim, K. W., Krauthgamer, R., Shagdarsuren, E., . . . Jung, S. (2009). CX3CR1 is required for monocyte homeostasis and atherogenesis by promoting cell survival. *Blood, 113*(4), 963-972. doi:10.1182/blood-2008-07-170787

Lechner, A. J., Driver, I. H., Lee, J., Conroy, C. M., Nagle, A., Locksley, R. M., & Rock, J. R. (2017). Recruited Monocytes and Type 2 Immunity Promote Lung Regeneration following Pneumonectomy. *Cell Stem Cell, 21*(1), 120-134 e127. doi:10.1016/j.stem.2017.03.024

Lederer, D. J., & Martinez, F. J. (2018). Idiopathic Pulmonary Fibrosis. *N Engl J Med, 379*(8), 797-798. doi:10.1056/NEJMc1807508

Lee, M., Lee, Y., Song, J., Lee, J., & Chang, S. Y. (2018). Tissue-specific Role of CX3CR1 Expressing Immune Cells and Their Relationships with Human Disease. *Immune Netw, 18*(1), e5. doi:10.4110/in.2018.18.e5

Leslie, K. O. (2009). My approach to interstitial lung disease using clinical, radiological and histopathological patterns. *J Clin Pathol, 62*(5), 387-401. doi:10.1136/jcp.2008.059782

Ley, B., Brown, K. K., & Collard, H. R. (2014). Molecular biomarkers in idiopathic pulmonary fibrosis. *Am J Physiol Lung Cell Mol Physiol, 307*(9), L681-691. doi:10.1152/ajplung.00014.2014

Ley, B., & Collard, H. R. (2013). Epidemiology of idiopathic pulmonary fibrosis. *Clin Epidemiol, 5*, 483-492. doi:10.2147/CLEP.S54815

Ley, B., Ryerson, C. J., Vittinghoff, E., Ryu, J. H., Tomassetti, S., Lee, J. S., . . . Collard, H. R. (2012). A multidimensional index and staging system for idiopathic pulmonary fibrosis. *Ann Intern Med, 156*(10), 684-691. doi:10.7326/0003-4819-156-10-201205150-00004

Li, W. (2012). Eat-me signals: keys to molecular phagocyte biology and "appetite" control. *J Cell Physiol, 227*(4), 1291-1297. doi:10.1002/jcp.22815

Liu, B., Dhanda, A., Hirani, S., Williams, E. L., Sen, H. N., Martinez Estrada, F., . . . Nussenblatt, R. B. (2015). CD14++CD16+ Monocytes Are Enriched by Glucocorticoid Treatment and Are Functionally Attenuated in Driving Effector T Cell Responses. *J Immunol, 194*(11), 5150-5160. doi:10.4049/jimmunol.1402409

Lo Buono, N., Parrotta, R., Morone, S., Bovino, P., Nacci, G., Ortolan, E., . . . Funaro, A. (2011). The CD157-integrin partnership controls transendothelial migration and adhesion of human monocytes. *J Biol Chem, 286*(21), 18681-18691. doi:10.1074/jbc.M111.227876

Lo Re, S., Lison, D., & Huaux, F. (2013). CD4+ T lymphocytes in lung fibrosis: diverse subsets, diverse functions. *J Leukoc Biol, 93*(4), 499-510. doi:10.1189/jlb.0512261

Marchal-Somme, J., Uzunhan, Y., Marchand-Adam, S., Valeyre, D., Soumelis, V., Crestani, B., & Soler, P. (2006). Cutting edge: nonproliferating mature immune

cells form a novel type of organized lymphoid structure in idiopathic pulmonary fibrosis. *J Immunol, 176*(10), 5735-5739.
Martinez, F. J., Collard, H. R., Pardo, A., Raghu, G., Richeldi, L., Selman, M., . . . Wells, A. U. (2017). Idiopathic pulmonary fibrosis. *Nat Rev Dis Primers, 3*, 17074. doi:10.1038/nrdp.2017.74
Marvel, D., & Gabrilovich, D. I. (2015). Myeloid-derived suppressor cells in the tumor microenvironment: expect the unexpected. *J Clin Invest*, 1-9. doi:10.1172/JCI80005
Mathai, S. C., & Danoff, S. K. (2016). Management of interstitial lung disease associated with connective tissue disease. *BMJ, 352*, h6819. doi:10.1136/bmj.h6819
Mathai, S. K., Gulati, M., Peng, X., Russell, T. R., Shaw, A. C., Rubinowitz, A. N., . . . Herzog, E. L. (2010). Circulating monocytes from systemic sclerosis patients with interstitial lung disease show an enhanced profibrotic phenotype. *Lab Invest, 90*(6), 812-823. doi:10.1038/labinvest.2010.73
Mionnet, C., Buatois, V., Kanda, A., Milcent, V., Fleury, S., Lair, D., . . . Julia, V. (2010). CX3CR1 is required for airway inflammation by promoting T helper cell survival and maintenance in inflamed lung. *Nat Med, 16*(11), 1305-1312. doi:10.1038/nm.2253
Misharin, A. V., Cuda, C. M., Saber, R., Turner, J. D., Gierut, A. K., Haines, G. K., 3rd, . . . Perlman, H. (2014). Nonclassical Ly6C(-) monocytes drive the development of inflammatory arthritis in mice. *Cell Rep, 9*(2), 591-604. doi:10.1016/j.celrep.2014.09.032
Misharin, A. V., Morales-Nebreda, L., Reyfman, P. A., Cuda, C. M., Walter, J. M., McQuattie-Pimentel, A. C., . . . Perlman, H. (2017). Monocyte-derived alveolar macrophages drive lung fibrosis and persist in the lung over the life span. *J Exp Med, 214*(8), 2387-2404. doi:10.1084/jem.20162152
Moore, B., Lawson, W. E., Oury, T. D., Sisson, T. H., Raghavendran, K., & Hogaboam, C. M. (2013). Animal models of fibrotic lung disease. *Am J Respir Cell Mol Biol, 49*(2), 167-179. doi:10.1165/rcmb.2013-0094TR
Narasimhan, P. B., Marcovecchio, P., Hamers, A. A. J., & Hedrick, C. C. (2019). Nonclassical Monocytes in Health and Disease. *Annu Rev Immunol, 37*, 439-456. doi:10.1146/annurev-immunol-042617-053119
Nogee, L. M., Dunbar, A. E., 3rd, Wert, S. E., Askin, F., Hamvas, A., & Whitsett, J. A. (2001). A mutation in the surfactant protein C gene associated with familial interstitial lung disease. *N Engl J Med, 344*(8), 573-579. doi:10.1056/NEJM200102223440805
Nomiyama, H., Osada, N., & Yoshie, O. (2013). Systematic classification of vertebrate chemokines based on conserved synteny and evolutionary history. *Genes Cells, 18*(1), 1-16. doi:10.1111/gtc.12013
Nowarski, R., Jackson, R., & Flavell, R. A. (2017). The Stromal Intervention: Regulation of Immunity and Inflammation at the Epithelial-Mesenchymal Barrier. *Cell, 168*(3), 362-375. doi:10.1016/j.cell.2016.11.040
Osafo-Addo, A. D., & Herzog, E. L. (2017). CCL2 and T cells in pulmonary fibrosis: an old player gets a new role. *Thorax, 72*(11), 967-968. doi:10.1136/thoraxjnl-2017-210517

Parker, M. W., Rossi, D., Peterson, M., Smith, K., Sikstrom, K., White, E. S., . . . Bitterman, P. B. (2014). Fibrotic extracellular matrix activates a profibrotic positive feedback loop. *J Clin Invest, 124*(4), 1622-1635. doi:10.1172/JCI71386

Passlick, B., Flieger, D., & Ziegler-Heitbrock, H. W. (1989). Identification and characterization of a novel monocyte subpopulation in human peripheral blood. *Blood, 74*(7), 2527-2534.

Patel, A. A., Zhang, Y., Fullerton, J. N., Boelen, L., Rongvaux, A., Maini, A. A., . . . Yona, S. (2017). The fate and lifespan of human monocyte subsets in steady state and systemic inflammation. *J Exp Med, 214*(7), 1913-1923. doi:10.1084/jem.20170355

Peljto, A. L., Zhang, Y., Fingerlin, T. E., Ma, S. F., Garcia, J. G., Richards, T. J., . . . Schwartz, D. A. (2013). Association between the MUC5B promoter polymorphism and survival in patients with idiopathic pulmonary fibrosis. *JAMA, 309*(21), 2232-2239. doi:10.1001/jama.2013.5827

Pilling, D., Fan, T., Huang, D., Kaul, B., & Gomer, R. H. (2009). Identification of markers that distinguish monocyte-derived fibrocytes from monocytes, macrophages, and fibroblasts. *PLoS One, 4*(10), e7475. doi:10.1371/journal.pone.0007475

Podolanczuk et.al. (2018). *Innate and adaptive immunity in subclinical ILD in the Multi-Ethnic Study of Atherosclerosi*. Paper presented at the International Colloquium on Lung and Airway Fibrosis (ICLAF), Pacific Grove, CA.

Prasse, A., Pechkovsky, D. V., Toews, G. B., Jungraithmayr, W., Kollert, F., Goldmann, T., . . . Zissel, G. (2006). A vicious circle of alveolar macrophages and fibroblasts perpetuates pulmonary fibrosis via CCL18. *Am J Respir Crit Care Med, 173*(7), 781-792. doi:10.1164/rccm.200509-1518OC

Raghu, G., Anstrom, K. J., King, T. E., Jr., Lasky, J. A., & Martinez, F. J. (2012). Prednisone, azathioprine, and N-acetylcysteine for pulmonary fibrosis. *N Engl J Med, 366*(21), 1968-1977. doi:10.1056/NEJMoa1113354

Raghu, G., Collard, H. R., Egan, J. J., Martinez, F. J., Behr, J., Brown, K. K., . . . Fibrosis, A. E. J. A. C. o. I. P. (2011). An official ATS/ERS/JRS/ALAT statement: idiopathic pulmonary fibrosis: evidence-based guidelines for diagnosis and management. *Am J Respir Crit Care Med, 183*(6), 788-824. doi:10.1164/rccm.2009-040GL

Raghu, G., Remy-Jardin, M., Myers, J. L., Richeldi, L., Ryerson, C. J., Lederer, D. J., . . . Latin American Thoracic, S. (2018). Diagnosis of Idiopathic Pulmonary Fibrosis. An Official ATS/ERS/JRS/ALAT Clinical Practice Guideline. *Am J Respir Crit Care Med, 198*(5), e44-e68. doi:10.1164/rccm.201807-1255ST

Raghu, G., Rochwerg, B., Zhang, Y., Garcia, C. A., Azuma, A., Behr, J., . . . Latin American Thoracic, A. (2015). An Official ATS/ERS/JRS/ALAT Clinical Practice Guideline: Treatment of Idiopathic Pulmonary Fibrosis. An Update of the 2011 Clinical Practice Guideline. *Am J Respir Crit Care Med, 192*(2), e3-19. doi:10.1164/rccm.201506-1063ST

Reyfman, P. A., Walter, J. M., Joshi, N., Anekalla, K. R., McQuattie-Pimentel, A. C., Chiu, S., . . . Misharin, A. V. (2018). Single-Cell Transcriptomic Analysis of Human Lung Provides Insights into the Pathobiology of Pulmonary Fibrosis. *Am J Respir Crit Care Med*. doi:10.1164/rccm.201712-2410OC

Riario Sforza, G. G., & Marinou, A. (2017). Hypersensitivity pneumonitis: a complex lung disease. *Clin Mol Allergy, 15*, 6. doi:10.1186/s12948-017-0062-7

Richeldi, L., du Bois, R. M., Raghu, G., Azuma, A., Brown, K. K., Costabel, U., . . . Investigators, I. T. (2014). Efficacy and safety of nintedanib in idiopathic pulmonary fibrosis. *N Engl J Med, 370*(22), 2071-2082. doi:10.1056/NEJMoa1402584

Rieber, N., Brand, A., Hector, A., Graepler-Mainka, U., Ost, M., Schafer, I., . . . Hartl, D. (2013). Flagellin induces myeloid-derived suppressor cells: implications for Pseudomonas aeruginosa infection in cystic fibrosis lung disease. *J Immunol, 190*(3), 1276-1284. doi:10.4049/jimmunol.1202144

Rock, J. R., Barkauskas, C. E., Cronce, M. J., Xue, Y., Harris, J. R., Liang, J., . . . Hogan, B. L. (2011). Multiple stromal populations contribute to pulmonary fibrosis without evidence for epithelial to mesenchymal transition. *Proc Natl Acad Sci U S A, 108*(52), E1475-1483. doi:10.1073/pnas.1117988108

Rosen, Y. (2007). Pathology of sarcoidosis. *Semin Respir Crit Care Med, 28*(1), 36-52. doi:10.1055/s-2007-970332

Salisbury, M. L., Myers, J. L., Belloli, E. A., Kazerooni, E. A., Martinez, F. J., & Flaherty, K. R. (2017). Diagnosis and Treatment of Fibrotic Hypersensitivity Pneumonia. Where We Stand and Where We Need to Go. *Am J Respir Crit Care Med, 196*(6), 690-699. doi:10.1164/rccm.201608-1675PP

Salvaggio, J. E., & deShazo, R. D. (1986). Pathogenesis of hypersensitivity pneumonitis. *Chest, 89*(3 Suppl), 190S-193S.

Seibold, M. A., Wise, A. L., Speer, M. C., Steele, M. P., Brown, K. K., Loyd, J. E., . . . Schwartz, D. A. (2011). A common MUC5B promoter polymorphism and pulmonary fibrosis. *N Engl J Med, 364*(16), 1503-1512. doi:10.1056/NEJMoa1013660

Sellares, J., Veraldi, K. L., Thiel, K. J., Cardenes, N., Alvarez, D., Schneider, F., . . . Feghali-Bostwick, C. A. (2018). Intracellular Heat Shock Protein 70 Deficiency in Pulmonary Fibrosis. *Am J Respir Cell Mol Biol*. doi:10.1165/rcmb.2017-0268OC

Selman, M., Pardo, A., & King, T. E., Jr. (2012). Hypersensitivity pneumonitis: insights in diagnosis and pathobiology. *Am J Respir Crit Care Med, 186*(4), 314-324. doi:10.1164/rccm.201203-0513CI

Shaw, M., Collins, B. F., Ho, L. A., & Raghu, G. (2015). Rheumatoid arthritis-associated lung disease. *Eur Respir Rev, 24*(135), 1-16. doi:10.1183/09059180.00008014

Shi, C., & Pamer, E. G. (2011). Monocyte recruitment during infection and inflammation. *Nat Rev Immunol, 11*(11), 762-774. doi:10.1038/nri3070

Shimizu, K., Furuichi, K., Sakai, N., Kitagawa, K., Matsushima, K., Mukaida, N., . . . Wada, T. (2011). Fractalkine and its receptor, CX3CR1, promote hypertensive interstitial fibrosis in the kidney. *Hypertens Res, 34*(6), 747-752. doi:10.1038/hr.2011.23

Sinha, M., Sen, C. K., Singh, K., Das, A., Ghatak, S., Rhea, B., . . . Roy, S. (2018). Direct conversion of injury-site myeloid cells to fibroblast-like cells of granulation tissue. *Nat Commun, 9*(1), 936. doi:10.1038/s41467-018-03208-w

Smith, M. L. (2016). Update on Pulmonary Fibrosis: Not All Fibrosis Is Created Equally. *Arch Pathol Lab Med, 140*(3), 221-229. doi:10.5858/arpa.2015-0288-SA

Soehnlein, O., Zernecke, A., Eriksson, E. E., Rothfuchs, A. G., Pham, C. T., Herwald, H., . . . Lindbom, L. (2008). Neutrophil secretion products pave the way for inflammatory monocytes. *Blood, 112*(4), 1461-1471. doi:10.1182/blood-2008-02-139634

Springer, T. A. (1994). Traffic signals for lymphocyte recirculation and leukocyte emigration: the multistep paradigm. *Cell, 76*(2), 301-314.

Srivastava, M. K., Bosch, J. J., Thompson, J. A., Ksander, B. R., Edelman, M. J., & Ostrand-Rosenberg, S. (2008). Lung cancer patients' CD4(+) T cells are activated in vitro by MHC II cell-based vaccines despite the presence of myeloid-derived suppressor cells. *Cancer Immunol Immunother, 57*(10), 1493-1504. doi:10.1007/s00262-008-0490-9

Talmadge, J. E., & Gabrilovich, D. I. (2013). History of myeloid-derived suppressor cells. *Nat Rev Cancer, 13*(10), 739-752. doi:10.1038/nrc3581

Thannickal, V. J., Zhou, Y., Gaggar, A., & Duncan, S. R. (2014). Fibrosis: ultimate and proximate causes. *J Clin Invest, 124*(11), 4673-4677. doi:10.1172/JCI74368

Thomeer, M. J., Costabe, U., Rizzato, G., Poletti, V., & Demedts, M. (2001). Comparison of registries of interstitial lung diseases in three European countries. *Eur Respir J Suppl, 32*, 114s-118s.

Tosh, D., & Slack, J. M. (2002). How cells change their phenotype. *Nat Rev Mol Cell Biol, 3*(3), 187-194. doi:10.1038/nrm761

Travis, W. D., Costabel, U., Hansell, D. M., King, T. E., Jr., Lynch, D. A., Nicholson, A. G., . . . Pneumonias, A. E. C. o. I. I. (2013). An official American Thoracic Society/European Respiratory Society statement: Update of the international multidisciplinary classification of the idiopathic interstitial pneumonias. *Am J Respir Crit Care Med, 188*(6), 733-748. doi:10.1164/rccm.201308-1483ST

Travis, W. D., Hunninghake, G., King, T. E., Jr., Lynch, D. A., Colby, T. V., Galvin, J. R., . . . Wells, A. (2008). Idiopathic nonspecific interstitial pneumonia: report of an American Thoracic Society project. *Am J Respir Crit Care Med, 177*(12), 1338-1347. doi:10.1164/rccm.200611-1685OC

Ugel, S., De Sanctis, F., Mandruzzato, S., & Bronte, V. (2015). Tumor-induced myeloid deviation: when myeloid-derived suppressor cells meet tumor-associated macrophages. *J Clin Invest, 125*(9), 3365-3376. doi:10.1172/JCI80006

Varga, G., Ehrchen, J., Tsianakas, A., Tenbrock, K., Rattenholl, A., Seeliger, S., . . . Sunderkoetter, C. (2008). Glucocorticoids induce an activated, anti-inflammatory monocyte subset in mice that resembles myeloid-derived suppressor cells. *J Leukoc Biol, 84*(3), 644-650. doi:10.1189/jlb.1107768

Vasquez-Dunddel, D., Pan, F., Zeng, Q., Gorbounov, M., Albesiano, E., Fu, J., . . . Kim, Y. (2013). STAT3 regulates arginase-I in myeloid-derived suppressor cells from cancer patients. *J Clin Invest, 123*(4), 1580-1589. doi:10.1172/JCI60083

Verschoor, C. P., Johnstone, J., Millar, J., Dorrington, M. G., Habibagahi, M., Lelic, A., . . . Bowdish, D. M. (2013). Blood CD33(+)HLA-DR(-) myeloid-derived

suppressor cells are increased with age and a history of cancer. *J Leukoc Biol, 93*(4), 633-637. doi:10.1189/jlb.0912461

Vij, R., & Strek, M. E. (2013). Diagnosis and treatment of connective tissue disease-associated interstitial lung disease. *Chest, 143*(3), 814-824. doi:10.1378/chest.12-0741

Vuga, L. J., Tedrow, J. R., Pandit, K. V., Tan, J., Kass, D. J., Xue, J., . . . Duncan, S. R. (2014). C-X-C motif chemokine 13 (CXCL13) is a prognostic biomarker of idiopathic pulmonary fibrosis. *Am J Respir Crit Care Med, 189*(8), 966-974. doi:10.1164/rccm.201309-1592OC

Walter, S., Weinschenk, T., Stenzl, A., Zdrojowy, R., Pluzanska, A., Szczylik, C., . . . Singh-Jasuja, H. (2012). Multipeptide immune response to cancer vaccine IMA901 after single-dose cyclophosphamide associates with longer patient survival. *Nat Med, 18*(8), 1254-1261. doi:10.1038/nm.2883

Wang, Zhang, Y., Liu, Y., Wang, L., Zhao, L., Yang, T., . . . Gao, Q. (2014). Association of myeloid-derived suppressor cells and efficacy of cytokine-induced killer cell immunotherapy in metastatic renal cell carcinoma patients. *J Immunother, 37*(1), 43-50. doi:10.1097/CJI.0000000000000005

Wells, A. U., Brown, K. K., Flaherty, K. R., Kolb, M., Thannickal, V. J., & Group, I. P. F. C. W. (2018). What's in a name? That which we call IPF, by any other name would act the same. *Eur Respir J, 51*(5). doi:10.1183/13993003.00692-2018

White, E. S. (2015). Lung extracellular matrix and fibroblast function. *Ann Am Thorac Soc, 12 Suppl 1*, S30-33. doi:10.1513/AnnalsATS.201406-240MG

Wuyts, W. A., Agostini, C., Antoniou, K. M., Bouros, D., Chambers, R. C., Cottin, V., . . . Verleden, G. M. (2013). The pathogenesis of pulmonary fibrosis: a moving target. *Eur Respir J, 41*(5), 1207-1218. doi:10.1183/09031936.00073012

Wynn, T. A. (2008). Cellular and molecular mechanisms of fibrosis. *J Pathol, 214*(2), 199-210. doi:10.1002/path.2277

Wynn, T. A. (2011). Integrating mechanisms of pulmonary fibrosis. *J Exp Med, 208*(7), 1339-1350. doi:10.1084/jem.20110551

Xu, Q., Norman, J. T., Shrivastav, S., Lucio-Cazana, J., & Kopp, J. B. (2007). In vitro models of TGF-beta-induced fibrosis suitable for high-throughput screening of antifibrotic agents. *Am J Physiol Renal Physiol, 293*(2), F631-640. doi:10.1152/ajprenal.00379.2006

Xu, W., Xiao, Y., Liu, H., Qin, M., Zheng, W., & Shi, J. (2014). Nonspecific interstitial pneumonia: clinical associations and outcomes. *BMC Pulm Med, 14*, 175. doi:10.1186/1471-2466-14-175

Xue, J., Kass, D. J., Bon, J., Vuga, L., Tan, J., Csizmadia, E., . . . Duncan, S. R. (2013). Plasma B lymphocyte stimulator and B cell differentiation in idiopathic pulmonary fibrosis patients. *J Immunol, 191*(5), 2089-2095. doi:10.4049/jimmunol.1203476

Yang, Luna, L. G., Cotter, J., Talbert, J., Leach, S. M., Kidd, R., . . . Steele, M. P. (2012). The peripheral blood transcriptome identifies the presence and extent of disease in idiopathic pulmonary fibrosis. *PLoS One, 7*(6), e37708. doi:10.1371/journal.pone.0037708

Yang, J., Zhang, L., Yu, C., Yang, X. F., & Wang, H. (2014). Monocyte and macrophage differentiation: circulation inflammatory monocyte as biomarker for inflammatory diseases. *Biomark Res, 2*(1), 1. doi:10.1186/2050-7771-2-1

Yeager, M. E., Nguyen, C. M., Belchenko, D. D., Colvin, K. L., Takatsuki, S., Ivy, D. D., & Stenmark, K. R. (2012). Circulating myeloid-derived suppressor cells are increased and activated in pulmonary hypertension. *Chest, 141*(4), 944-952. doi:10.1378/chest.11-0205

Yona, S., Kim, K. W., Wolf, Y., Mildner, A., Varol, D., Breker, M., . . . Jung, S. (2013). Fate mapping reveals origins and dynamics of monocytes and tissue macrophages under homeostasis. *Immunity, 38*(1), 79-91. doi:10.1016/j.immuni.2012.12.001

Yoon, B. R., Yoo, S. J., Choi, Y., Chung, Y. H., Kim, J., Yoo, I. S., . . . Lee, W. W. (2014). Functional phenotype of synovial monocytes modulating inflammatory T-cell responses in rheumatoid arthritis (RA). *PLoS One, 9*(10), e109775. doi:10.1371/journal.pone.0109775

Yu, G., Kovkarova-Naumovski, E., Jara, P., Parwani, A., Kass, D., Ruiz, V., . . . Pardo, A. (2012). Matrix metalloproteinase-19 is a key regulator of lung fibrosis in mice and humans. *Am J Respir Crit Care Med, 186*(8), 752-762. doi:10.1164/rccm.201202-0302OC

Zhang, Y., Liu, Q., Zhang, M., Yu, Y., Liu, X., & Cao, X. (2009). Fas signal promotes lung cancer growth by recruiting myeloid-derived suppressor cells via cancer cell-derived PGE2. *J Immunol, 182*(6), 3801-3808. doi:10.4049/jimmunol.0801548

Zhong, H., Gutkin, D. W., Han, B., Ma, Y., Keskinov, A. A., Shurin, M. R., & Shurin, G. V. (2014). Origin and pharmacological modulation of tumor-associated regulatory dendritic cells. *Int J Cancer, 134*(11), 2633-2645. doi:10.1002/ijc.28590

Ziegler-Heitbrock, L. (2007). The CD14+ CD16+ blood monocytes: their role in infection and inflammation. *J Leukoc Biol, 81*(3), 584-592. doi:10.1189/jlb.0806510

Ziegler-Heitbrock, L. (2015). Blood Monocytes and Their Subsets: Established Features and Open Questions. *Front Immunol, 6*, 423. doi:10.3389/fimmu.2015.00423

Zuo, F., Kaminski, N., Eugui, E., Allard, J., Yakhini, Z., Ben-Dor, A., . . . Heller, R. A. (2002). Gene expression analysis reveals matrilysin as a key regulator of pulmonary fibrosis in mice and humans. *Proc Natl Acad Sci U S A, 99*(9), 6292-6297. doi:10.1073/pnas.092134099

9. Acknowledgements

“Talent wins games, but team work and intelligence win championships” (Michael Jordan). It was only possible to complete this journey with the support of many people. I have learnt so much and all these achievements are accomplished through an incredible team work.

To my mentors Prof. Dr. Oliver Eickelberg and especially to Dr. Isis Fernandez for the guidence and suppport in my career. To PD. Dr. Anne Hilgendorf for the support and LMU supervision.

To Prof. Dr Oliver Söhnlein, member of my thesis commitee, for scientific discussions and support in my career. To the CPC Research School, Dr. Dr. Melanie Königshoff, PD Dr. Claudia Staab-Weijnitz, Dr. Hoeke Baarsma and Dr. Doreen Franke for an outstanting scientific training.

To the Eickelberg lab and to the immunophenotyping core unit for all the help and fruitful discussions. To Daniela Dietel for her support and help during experiments and blood process. To Dr. Marion Frankenberg for all the effort recruiting patients, collectig blood samples and clinical data. To Prof. Dr. Jürgen Behr for sending us blood samples. To all the colaborators that helped and contributed to these studies.

To Aina, Carolina, Martina, Nina and Rita for all the moments shared during these years. It was a lot of fun when your were around. To the CPC Research School Class of 2014/2015. To Mareike, Laura, and again to Rita and Carolina for the support and friendship.

To the CPC and Helmholtz Zentrum München for the structure and finantial support. To ERS short term fellowship and Dr. David Lagares for the opportunity to go to Boston at the MGH/Harvard and increase my scientific experience.

And finally to my family for being so close even from so far. And to Jacob for supporting my career and always being by my side.